The Application of Microtephrochronology to Archaeology:

A Critical Assessment with Reference to Maya Archaeology

Sarah M. P. Jack

Dissertation

M.Sc. Archaeological Science

Oxford University

September 2005

Abstract

This study assesses the applicability of microtephrochronology—or the correlation of isochrononous microscopic tephra horizons—to the study of archaeological sequences. Samples from Lamanai Lake (New River Lagoon) and three lowland Maya archaeological sites in Belize (Lamanai, Medicinal Trail and Yalbac) are analysed using current microtephra extraction, identification and characterisation protocols. Bulk tephra samples from Lake Amatitlan in highland Guatemala are also characterised geochemically using wavelength dispersive electron microprobe analysis.

This study highlights the main limitations of microtephrochronology and suggests possible improvements. These include: a) tailoring laboratory extraction and identification protocols to suit archaeological soil sequences rather than palaeoenvironmental deposits; b) collaborating with micromorphologists to identify reworked microtephra deposits; and c) exploring alternative methods of geochemical characterisation, including laser-ablation inductively coupled mass spectrometry (LA-ICP-MS) and secondary ion mass spectrometry (SIMS).

In its current state, microtephrochronology cannot be considered a reliable geoarchaeological dating technique. Although there is some room for improvement, fundamental limitations remain (e.g. the reliance on timely eruptions occurring in the past; geochemical indistinctness of many eruptions; chemical alteration of tephra in the post-depositional environment; and the unsuitability of many reworked soil deposits). Consequently, attention should be focused on alternative archaeological applications for microtephra analysis. These include refining ceramic typologies and, more

significantly, the use of microtephra as a tool for assessing site formation processes and the integrity of archaeological sequences. It is this latter application that holds most potential for microtephra as a useful archaeological tool.

Contents

Figures

Glossary

Basaltic tephra:	**tephra** of basic composition; usually dark in colour; lower silica content than **rhyolitic tephra**
Cryptotephra:	hidden **tephra** invisible to the naked eye; usu. refers to glass fraction only (see also **microtephra**)
Distal site:	site situated some distance from volcanic centres (*cf.* **proximal site**)
Felsic eruption:	explosive volcanic eruption resulting in abundant aerosols and widespread dispersal of **tephra** (*cf.* **mafic eruption**)
Mafic eruption:	less explosive volcanic eruption with local **tephra** dispersal (*cf.* **felsic** eruption)
Microtephra:	microscopic **tephra** invisible to the naked eye; usu. refers to glass fraction only (see also **cryptotephra**)
Microtephrochronology:	use of **microtephra** to correlate stratigraphic sequences; usually undertaken at distal sites
Palaeoenvironmental site:	lake, peat deposit or natural outcrop
Plinian eruption:	sheet-forming eruption (*cf.* **Strombolian eruption**)
Proximal Site:	site situated close to volcanic centres (*cf.* **distal site**)
Pyroclastic material:	volcanic ejecta
Rhyolitic tephra:	**tephra** of granitic composition; high silica content (see also **silicic tephra**)
Silicic tephra:	**tephra** with high silica content (see also **ryholitic tephra**)
Strombolian eruption:	cone-forming eruption (*cf.* **Plinian eruption**)
Tephra:	air-fall component of **volcanic ejecta**, including glass and crystalline material from the magma and broken volcanic cone rock carried into the atmosphere; often used in tephrochronological studies to refer to glass fraction only
Tephrochronology:	use of **tephra** beds to correlate stratigraphic sequences

Abbreviations

WDA:	Wavelength Dispersive Microscopy
EDA:	Energy Dispersive Microscopy
XRF:	X-Ray Fluorescence
NAA:	Neutron Activation Analysis
LA-ICP-MS:	Laser-Ablation Inductively Coupled Plasma Mass Spectrometry
SIMS:	Secondary Ion Mass Spectrometry
AMS:	Accelerator Mass Spectrometry

SG:	Standard Gravity
SPT:	Sodium Polytungstate
RI:	Refractive Index

MAT:	Middle American Trench
CAVA:	Central American Volcanic Arc: Guatemala and El Salvador
CVA:	Chiapanecan Volcanic Arc: incl. El Chichon
TVC:	Los Tuxtlas Volcanic Field, Mexico
TVB:	Transmexican Volcanic Belt: crosses Central Mexico

PrC:	Preclassic (1800BC-AD250)
EC:	Early Classic (AD250-600)
LC:	Late Classic (AD600-800)
TC:	Terminal Classic (AD800-925)
PC:	Postclassic (AD925-1530)
Hist:	Historical (AD1530-present)

Acknowledgments

Firstly, I would like to thank Jaime Awe and the Belize Institute of Archaeology for supporting this research and facilitating the export process. I would also like to thank members of the Valley of Peace Archaeology Project, the Lamanai Archaeological Project, the Programme for Belize Archaeology Project and the Blue Creek Archaeological Project for welcoming me onto their projects to sample their study sites. In particular, I would like to thank Lisa Lucero, Scott Simmons, David Hyde, Fred Valdez, Tim Beach and John Lohse for their help and hospitality. I am also indebted to Sarah Metcalfe, Anabel Ford and their respective collaborators for access to samples from Lamanai Lake and Lake Amatitlan respectively.

In Oxford, many thanks go to Simon Blockley, Mark Pollard, Christine Lane, Chris Doherty, Judy Watson, Robert Hedges and many others at the Research Laboratory for Archaeology and the History of Art (RLAHA).

Finally, I owe many thanks to my family and friends for all their love and support.

Fieldwork for this dissertation was funded by the Arts and Humanities Research Board (Overseas Study Grant), the Oxford University School of Archaeology (Meyerstein Research Award) and Hertford College (Standard and Special Graduate Travel Grants).

1. INTRODUCTION

Approximately one billion cubic metres (1km^3) of volcanic glass are produced each year as a result of rapid cooling of magma on the Earth (Morgan and Spera 2001). This glass makes up approximately 12% of the average exposed continental crust surface, exceeded in abundance only by plagioclase and quartz (which make up approximately 35% and 20% respectively; Nesbitt and Young 1984 in Wolff-Boenisch *et al*. 2004:4843). These glass particles, together with other forms of tephra (volcanic ejecta), have increasingly played a role as critical time-stratigraphic markers for the correlation of marine, ice-core and terrestrial sequences for palaeoclimatic, palaeoenvironmental and archaeological studies (Lowe *et al*. 2001). This correlation of isochronous volcanic tephra horizons is commonly known as tephrochronology.

The identification of widespread time-parallel marker horizons offers the potential to a) apply age brackets to sediment sequences, b) compare independent chronologies and c) test conventional dating techniques such as radiocarbon dating, biostratigraphic analyses and archaeological artefact typologies. Recent advances in laboratory protocols have enabled the detection and extraction of microtephras (also known as cryptotephras or microscopic glass shards invisible to the naked eye) from distal palaeoenvironmental deposits thousands of kilometres away from source volcanoes. The ability to trace tephras over much wider geographical areas has radically extended the scope of tephrochronology in palaeoenvironmental studies (Turney *et al*. 2004).

There has been some suggestion that microtephrochronology could profitably enhance the study of archaeological sites (e.g. Blockley pers. comm.). However, no such

applications appear to have been published. In response, this dissertation addresses the applicability of microtephrochronology to archaeology with special reference to the Maya area. The initial aim of this study was to construct a tephrochronology for the lowland Maya area to assess the usefulness of tephrostratigraphy as a tool for archaeological site correlation. However, recognition of several fundamental limitations necessitated a shift in direction. Although this dissertation begins conventionally with an introduction (chapter 1), an overview of the principles of volcanism and tephrochronology (chapter 2) and background on volcanism and archaeology in the Maya area (chapter 3), the bulk of this dissertation is structured around three problem areas. These include laboratory extraction and identification protocols (chapter 4), dispersal, deposition and reworking of tephra (chapter 5), and the use of major element geochemistry as the only identification and correlation criterion (chapter 6). These are followed by a discussion (chapter 7) and conclusion (chapter 8), in which suggestions for improvement and possible alternative archaeological uses of microtephra are provided. The latter include refining ceramic typologies and, more significantly, the use of microtephra as a tool for assessing site formation processes and the integrity of archaeological sequences.

2. PRINCIPLES OF VOLCANISM AND TEPHROCHRONOLOGY

Tephrochronology uses volcanic air-fall deposits (tephra) to correlate stratigraphic sequences. Recently, it has seen an expansion from the use of visible volcanic ash layers to the location and identification of small numbers of individual glass shards invisible to the naked eye (microtephra; e.g. Turney *et al*. 1997). This has enabled correlation and dating of deposits at extreme distances from volcanism, and has proved particularly useful for palaeoenvironmental studies. This chapter provides an introduction to volcanism, tephrochronology and microtephrochronology.

2.1. INTRODUCTION TO VOLCANISM:

Tephra refers to unconsolidated, fine-grained pyroclastic material commonly known as volcanic ash (<2mm). It is the air-fall component of volcanic ejecta, and includes both glass and crystalline material from the magma as well as broken volcanic cone rock carried into the atmosphere (Pilcher 2002:1). In many studies, the term tephra is used to refer to the glass component only. This glassy component is liquid magma that cools rapidly as it projects into the atmosphere and forms without crystallising (*ibid.*). Large quantities of glass can be produced and projected many kilometres into the atmosphere, consequently dispersing many thousands of kilometres away as distal microtephras (e.g. Wastegård *et al*. 2000; see glossary on p.ix. for terminology)

2.1.1. Eruption mechanics:

The products of volcanic eruptions are lavas and pyroclastic rocks (Hall 1996:24). Major groups of volcanic rocks are shown in fig. 2.1.1-2. Magmas with low viscosity and a low content of dissolved gas (e.g. basaltic magmas) are generally erupted quietly as lava flows, whilst magmas with high viscosity or a high content of dissolved gas (e.g. felsic magmas such as rhyolite and phonolite) are erupted explosively, resulting in a high proportion of pyroclastic products and very little lava (Hall 1996:24; see fig. 2.1.1-2.). In the latter case, the decrease in pressure as the magma approaches the surface of the volcano causes rapid exsolution of the dissolved gas and an expansion in the volume of vesiculating magma (Hall 1996:46). The magma is rapidly forced to the surface, producing very high eruption plumes that disperse tephra over a wide geographical area. Consequently, most distal microtephras are rhyolitic rather than basaltic. There are, however, some

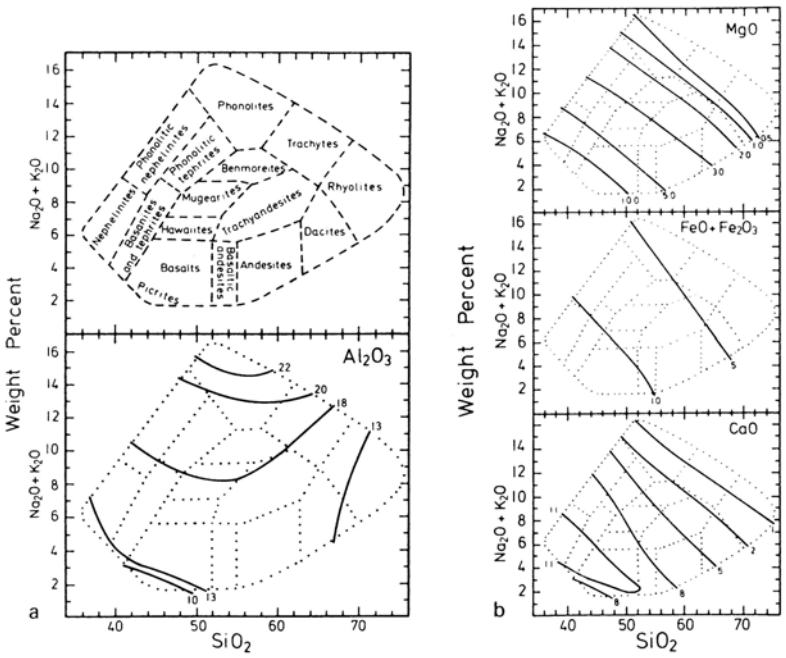

Figure 2.1.1-1. Classification of major groups of volcanic rocks in alkali-silica variation diagrams showing weight percent concentrations of the oxides Al_2O3, MgO, CaO and $FeO+Fe_2O_3$ (Fisher and Schminke 1984:16)

exceptions, such as when basaltic magma forces its way to the surface and initiates new explosive eruptions, or when water or ice come into contact with hot volcanic rock or basaltic magma (Hall 1996:45). Volcanoes can also change character throughout development or in the midst of an eruption; for example the historic eruptions of Hekla, Iceland, first projected acid or intermediate ash and pumice followed by basalt (Hall 1996:46).

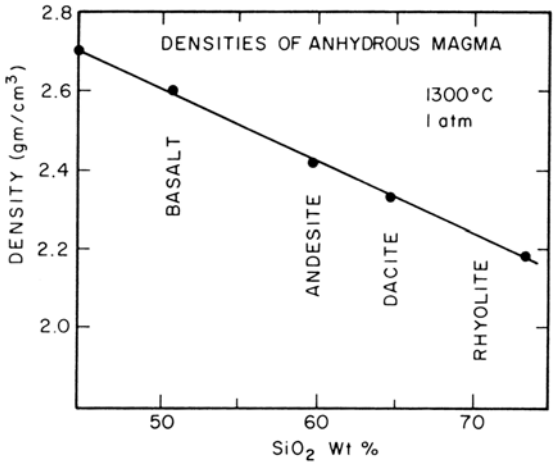

Figure 2.1.1-2. Densities of typical basalt, andesite and ryholite magmas (Hess 1989:65)

2.1.2. Tephra distribution:

Pyroclastic material is either discharged in fragmental form, resulting in scoria cones and ash fall deposits, or released more coherently as ash flow deposits (Hall 1996:46). Following an explosive eruption, fine-grained pyroclastic materials rise high into the air and eventually fall to the ground to give a layer of ash (Hall 1996:47). In some cases, these ash sheets cover thousands of kilometres in distance. The dust cloud from the 1783 Laki fissure eruption in Iceland, for example, spread over Europe and North America, lasting several months (Hall 1996:48). Likewise, the 1883 explosions of Krakatoa threw ash so high into the atmosphere that the finer dust spread over much of the Earth, taking 14 days to make its first complete circuit of the globe (*ibid.*). The extent of ash fall depends on a number of factors, including a) how high ash is projected into the air, and b) the effects of wind, rain and other climatic processes (see chapter 5).

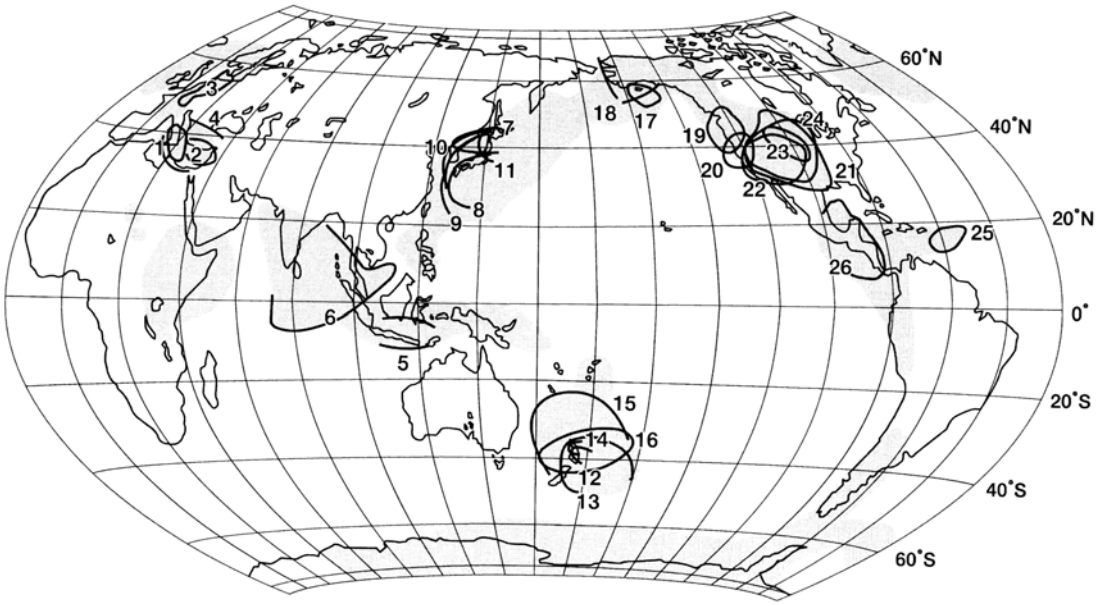

Figure 2.1.2-1. Atlas showing approximate outer limits of identified widespread tephras:
1. Avellino (Z-1, Vesuvius); 2. Minoan (Santorini); 3. Laacher See; 4. Campanian (Campi Fregrei); 5. Tambora 1815; 6. Youngest Toba; 7. Baegudusan-Tm; 8. Kikai-Akakoya; 9. Aira-Tn; 10. Aso-4; 11. Toya; 12. Taupo; 13. Kawakawa (Taupo); 14. Rotoiti (Haroharo/Okataina); 15. Rangitawa (Wakamaru); 16. Potaka (?); 17. Katmai (Novarupta); 18. Old Crow (Emmons Lake?); 19. Mazama (Crater Lake); 20. Rockland (Brokeoff?); 21. Lava Creek (Yellowstone); 22. Bishop (Long Valley); 23. Mesa Falls (Yellowstone); 24. Huckleberry Ridge (Yellowstone); 25. Roseau; 26. Los Chocoyos (Atitlan). (Machida 2003:6)

2.2. PRINCIPLES OF TEPHROCHRONOLOGY:

Tephrochronology has a wide variety of applications and is considered an important tool in a number of disciplines. It is frequently used by palaeoecologists to measure rates of sedimentation or climate change (e.g. Björck and Wastegård. 1999; Reheis *et al.* 1996) and has been used as a chronological dating technique at archaeological and palaeoenvironmental sites (e.g. Lowe *et al.* 2000). Tephra is frequently extracted for analysis from sites in northwest Europe, New Zealand and northern USA for stratigraphic studies, but is also increasingly extracted from sites in Mexico, the Antarctic peninsula, and Kamchatka (Pilcher 2002:1). The presence of tephra at various palaeoenvironmental sites has also provided an opportunity to independently test existing correlation schemes based on the more traditional approaches of radiocarbon dating and biostratigraphy (Turney 1998:199).

Tephrochronology relies on the presence of distinctive tephra layers. Since a typical eruption lasts for just days or months and is shortly followed by tephra dispersal, each tephra deposit forms a highly defined time marker. The stratigraphic value of a tephra layer is, however, only realised when a) its distinguishing criteria have been recognised and b) its age has been determined (Westgate and Gorton 1981:76).

Various methods have been used to provide dates for tephra sequences, including radiocarbon dating of associated organic matter, potassium-argon dating and argon-argon dating for older deposits, oxygen isotopes and biostratigraphic analysis in deep sea sequences, fission-track dating, qualitative hydration dating, magnetic polarity, and the use of annually laminated varved lake sediments. Since many of these dating techniques are problematic, it is generally considered preferable, where possible, to use historically dated eruptions to provide tephra timescales.

Efforts have also been made to find a rapid, single parameter method for tephra identification and correlation (e.g. Czamanske and Porter 1965), but most tephrochronologists consider a multiple criteria approach necessary (Westgate and Gorton 1981:76). Westgate and Gorton (1981:76) suggest that equivalence of samples should only be considered firmly established if a) their stratigraphic, palaeontologic, palaeomagnetic, and radiometric age relations are compatible, b) the geochemical and physical properties of glass shards and phenocrysts agree, and c) the combination of these characteristics is distinctive from that of other tephra beds in the area. Since the last requirement assumes a comprehensive knowledge of local geological records, it is not always achieved.

2.3. THE EXPANSION OF TEPHROCHRONOLOGY TO MICROTEPHROCHRONOLOGY:

A study in the 1970s highlighted the existence of tephra in deep-sea sediments at distances as great as 3000km from their source (Huang *et al*. 1973 in Westgate and Gorton 1981:74). Even in terrestrial deposits, where the potential for degradation is higher, discrete but discontinuous beds were persistently identified at distances exceeding 1500km (Westgate and Gorton 1981:74). Although it was realised that widespread tephra layers could be used to correlate stratigraphic sequences over long distances, the application of distal tephrochronology was limited by the insubstantial nature of distal deposits. Due to aeolian sorting, the size and quantity of tephra particles decreases with distance from source.

The recent extension of tephrochronology from the use of visible tephra layers to the location and identification of small numbers of individual microtephras (invisible to the naked eye) has entailed the development of new extraction and identification techniques centring on density separation, light microscopy and electron microprobe analysis (Hall and Pilcher 2002:224). The ability to correlate invisible layers illustrates the widespread value of tephrochronology as a tool for correlating and dating deposits at extreme distances from volcanism. Recent palaeoenvironmental studies (e.g. Dugmore *et al*. 1995; Hall and Pilcher 2002; Hall *et al*. 1994) suggest that microtephrochronology may potentially revolutionise timeframe construction in problematic deposits. However, very few studies have attempted to apply microtephrochronology to terrestrial archaeological deposits. This study therefore assesses the extension of tephrochronology to microtephrochronology and the potential

shift in application from palaeoenvironmental to archaeological studies.

3. REGIONAL BACKGROUND

This chapter provides a brief overview of Central American and Mexican volcanism and tephrochronology, followed by an introduction to Maya archaeology and sample sites. Although this study assesses more generally the applicability of microtephrochronology to archaeology, the Maya area will feature throughout this dissertation as a case study.

3.1. CENTRAL AMERICAN AND MEXICAN VOLCANISM AND TEPHROCHRONOLOGY:

There are four principal areas of volcanic activity in Central America and Mexico:

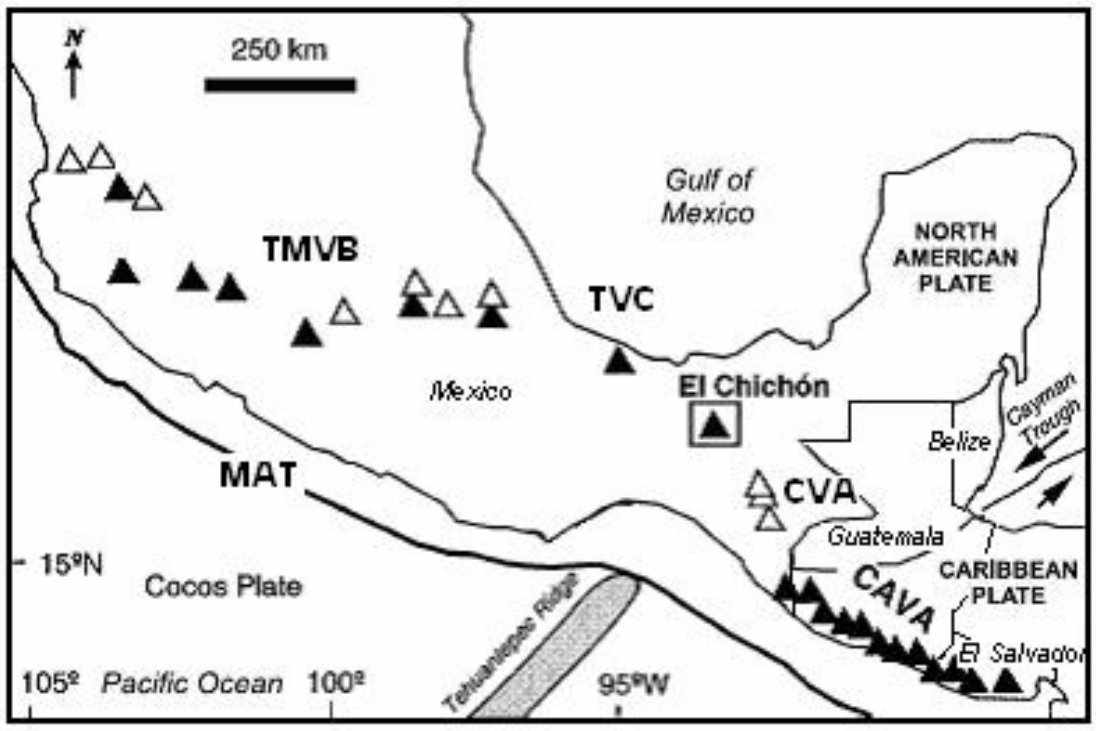

Figure 3.1-1. Map showing four principal areas of volcanic activity in Central America and Mexico: Trans-Mexican Volcanic Belt (TMVB); Los Tuxtlas Volcanic Field (TVC); Chiapanecan Volcanic Arc (CVA); and Central American Volcanic Arc (CAVA). The CAVA lies parallel to the Middle American Trench (MAT). (modified from Taran *et al.* 1998:437 and Macías *et al.* 2003)

3.1.1. Central America:

The basaltic and andesitic cones of the CAVA parallel the offshore MAT and the active underthrust zone (Rose *et al*. 1981:193). In addition, silicic Plinian tephra units representing more than 30 Quaternary eruptions blanket Guatemala and El Salvador, mainly erupted from five principal sources (Rose *et al*. 1981:193). These five calderas form a west-northwest trending line which parallels both the CAVA and the MAT (*ibid.*):

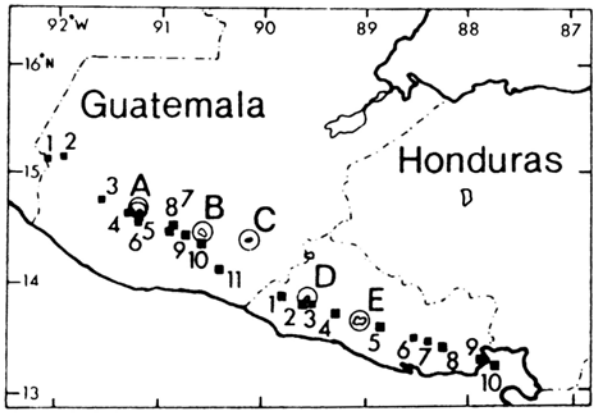

Figure 3.1.1-1. Location map for the volcanic front volcanoes of northern Central America (■) and the five Quaternary calderas: A. Atitlán; B. Amatitlan; C. Ayarza; D. Coatepeque; E. Ilopango (Rose *et al.* 1981:195)

The interfingering of caldera ashes from multiple eruptions has enabled the construction of a network of relative ages (*ibid.*). Most units are typical Plinian airfall deposits, but several have associated non-welded ashflows (ibid:198). Tephrochronological studies in the area include characterising and correlating ash-flow deposits (e.g. Hahn *et al*. 1981 and Rose *et al*. 1979; both in Rose *et al*. 1981:194), as well as the correlation of deep sea tephra with Guatemalan tephra layers (e.g. Drexler *et al*. 1980 and Peterson 1980 in Rose *et al*. 1981:195).

Most caldera eruptions in the area are, however, tens of thousands of years old and precede human colonisation of the Americas. One exception is the Tierra Blanca Joven (TBJ) eruption of the Ilopango caldera, which took place in the early first millennium

AD (see Mehringer *et al*. 2005 for controversies regarding the date of the eruption). The TBJ tephra and associated ashflows appear to be dacite and rhyodacite in composition and have been described in detail by Hart and Steen-McIntyre (1980).

Steen McIntyre (1981:359) states that, although we do not know how far downwind the TBJ tephra extends, it is likely that tephra fall covers most of Central America and Mexico, since abundant glass-coated phenocrysts and glass shards of fresh appearance have been recovered from lake-core sediments from the Peten, Guatemala (Deevy *et al*. 1979).

Figure 3.1.1-2. Map showing possible extent of the TBJ tephra (Steen-McIntyre 1981:360)

3.1.2. Mexico:

Tephras of the TVB have been extensively studied and geochemically characterised (e.g. Ortega-Guerrero and Newton 1998; Tephrabase). However, the TVB is located a considerable distance away from archaeological and palaeoenvironmental sites analysed in this study (see below) and is therefore likely to be of limited relevance. The CVA, on the other hand, is of interest. Recent analyses show that El Chichón erupted explosively at least twelve times in the past 8000 years, occurring in 1982 and approximately 550, 900, 1250, 1500, 1600, 1900, 2000, 2500, 3100, 3700 and 7700 years BP (Espíndola *et al*. 2000). The 1982 eruption also illustrated that visible deposits of airfall ash could cover a considerable geographic extent (e.g. reaching Belize; Ford, Graham and Pyburn pers. comm.).

3.2. INTRODUCTION TO MAYA ARCHAEOLOGY:

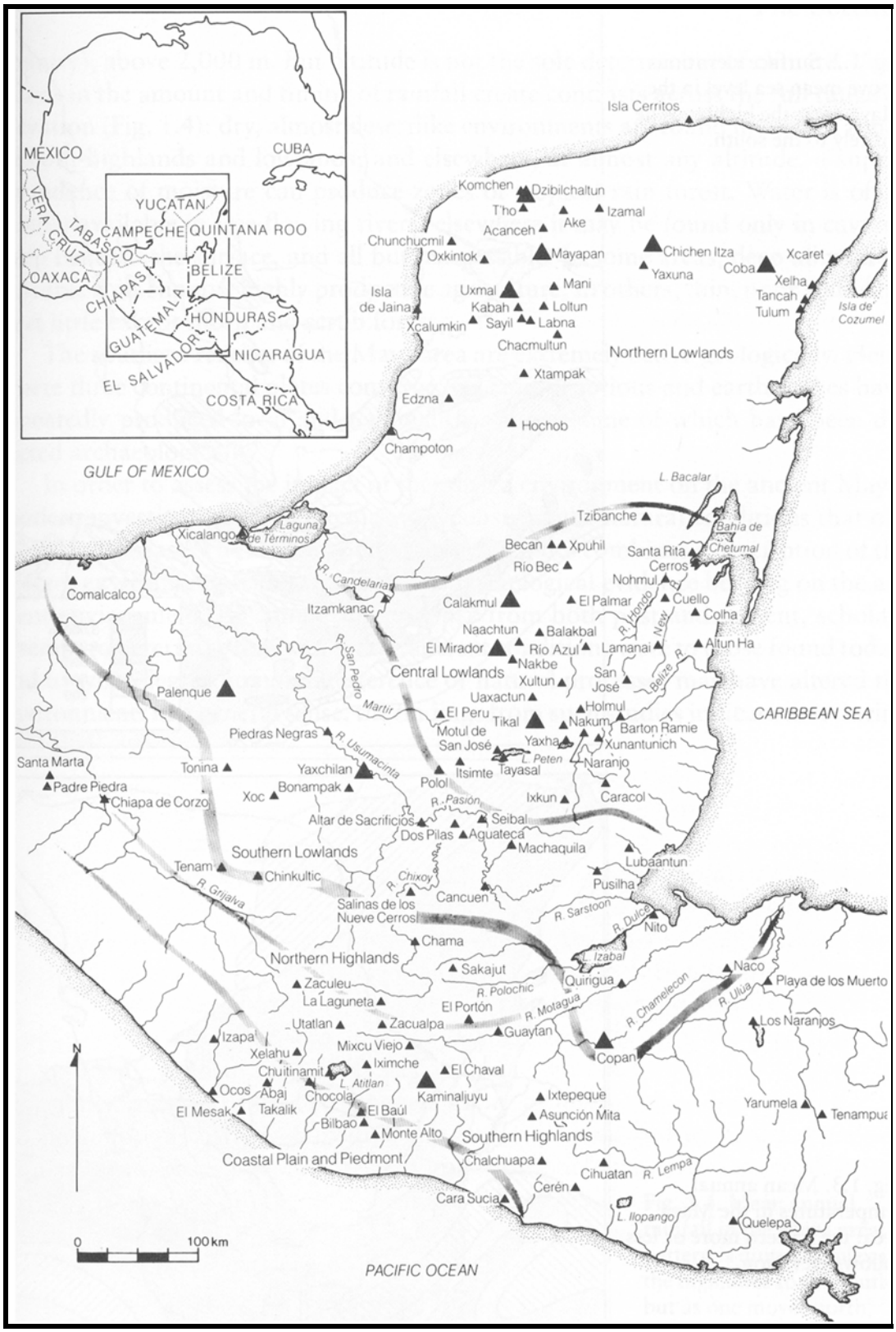

Figure 3.2-1. Map of the Maya area showing principle archaeological features (Sharer 1994:21)

The Maya area is defined by the distribution of both ancient Maya ruins and modern peoples speaking Mayan languages (Sharer 1994). It encompasses an area of 324 000km^2 covering the southeastern extremity of Mexico and the modern nations of Belize, Guatemala, Honduras and El Salvador (*ibid.*). The Maya area is traditionally viewed as comprising two broad zones: the ecologically diverse highlands and the inhospitable but densely occupied lowlands. Although there is increasing recognition that the Maya area consists of diverse environments with various trajectories of cultural development, the lowland-highland dichotomy remains largely intact.

In the first half of the second millennium BC, early villages emerged along the Pacific coast of highland Guatemala (e.g. see Sharer 1994). By 1000 BC, settlement had expanded along rivers to the central lowlands, shortly followed by settlement in non-riverine areas. By the mid-first millennium BC, complex societies were emerging in the highlands and central and southern lowlands, characterised by monumental architecture and elaborate sculptures (*ibid.*). This development continued through the Late Preclassic period (400 BC–AD 250) and Early Classic (AD 250–600), culminating in large ceremonial centres with monumental architecture, temple structures adorned with elaborate masonry and plaster masks of gods and ancestors, carved stelae monuments glorifying rulers, the associated notion of kingship and the 'elite', an elaborate calendar system, writing, religion and art (*ibid.*).

Although both the highlands and lowlands saw continuous cultural development and population growth during the Early Classic period, growth appears to have halted in the highlands during the Late Classic (600–900 AD), despite accelerating in the central, southern and northern lowlands (Ford and Rose 1995). During the final years of the

Late Classic and the start of the Postclassic (beginning AD 925), settlements in highland Guatemala appear to have experienced renewed growth and competition (*ibid.*). By contrast, settlements in the lowlands experienced the Classic Maya "collapse", with an end to monumental construction, widespread site abandonment, and a considerable decrease in population (e.g. Culbert 1973).

Some attempts have been made to explain these differences with reference to volcanic activity. Ford and Rose (1995) interpret the widespread inclusion of tephra in lowland ceramics during the Late Classic (see fig. 3.2-2.) as indicative of regular and consistent volcanic activity and tephra dispersal. They suggest that a period of intense volcanism would render proximal highland settlements unsuitable for occupation, whilst distal settlements on the lowland limestone shelf would prosper as a result of enhanced soil fertility (Ford and Rose 1995:158). Conversely, a cessation in volcanism during the Postclassic could explain the renewed growth of highland sites, and may account, at least in part, for the collapse of lowland sites (*ibid.*:160). The authors readily acknowledge, however, that these statements are sweeping and parsimonious (*ibid.*). If the sequence of eruptions in the Maya area was more fully understood, the relationship between volcanism and cultural activity could be better addressed. Furthermore, microtephrochronology, if successful, would allow correlation of sites throughout the Maya area, thus providing a more refined chronological reference with which to explore changes in cultural development and population dynamics in both lowland and highland areas.

Figure 3.2-2. Areas with ash-tempered ceramics during a) the Early Classic, b) the Late Classic, c) the Terminal Classic and d) the Postclassic (Simmons and Brem 1979:80)

3.3. ENVIRONMENTAL AND ARCHAEOLOGICAL SITES ANALYSED IN THIS STUDY:

In highland Maya areas, large numbers of distinct tephra layers are readily visible in stratigraphic sections of soils (e.g. resulting from Ilopango TBJ, El Salvador and Los Chocoyos, Guatemala). In the lowland Maya area, hundreds of kilometres from the highlands, almost all these layers appear to be represented at microscopic level only. Thus, sites in lowland Belize provide an opportunity to assess the applicability of microtephrochronology to the study of distal palaeoenvironmental and archaeological sites. Samples from five sites were analysed for this study. These included two lake sites (from highland Guatemala and lowland northern Belize) and three archaeological sites (from lowland central and northern Belize). It was hoped that microtephra from the three archaeological sites could be correlated with microtephra in the Belizean lake core and perhaps have comparable geochemistries to tephras from the highland Guatemalan lake core.

3.3.1. Lake sites:

Two lake sites were chosen to provide reference chronologies against which tephra sequences from archaeological sites could be compared.

Lake Amatitlan, located in the Maya highlands just south of the Valley of Guatemala, was known to have received considerable quantities of proximal airfall tephra (e.g. Rose *et al*. 1981). Cores were taken in 2000 by a team from the University of Florida at Gainesville for palaeoclimatic studies (Popenoe de Hatch *et al*. 2002:111). Station 3

(Site 15-III-2000) was located in the northwestern area of the lake (northern basin; see figure 3.3.1-1.) and yielded samples down to a depth of 701cm. After magnetic susceptibility profiles were established, 1cm sub-samples were sent to the author (via the University of California Santa Barbara) for electron microprobe analysis. It was believed that the Station 3 core could potentially act as a reference chronology representing highland Guatemalan eruptions if the geochemical compositions of tephra deposits could be successfully characterised. Although six calibrated radiocarbon dates (ranging from approximately 620 BC to AD 1290; see fig. 6.2.4.1-1.) were produced for the Station 3 core, the reliability of the dates is unclear and considered provisional for purposes of this study.

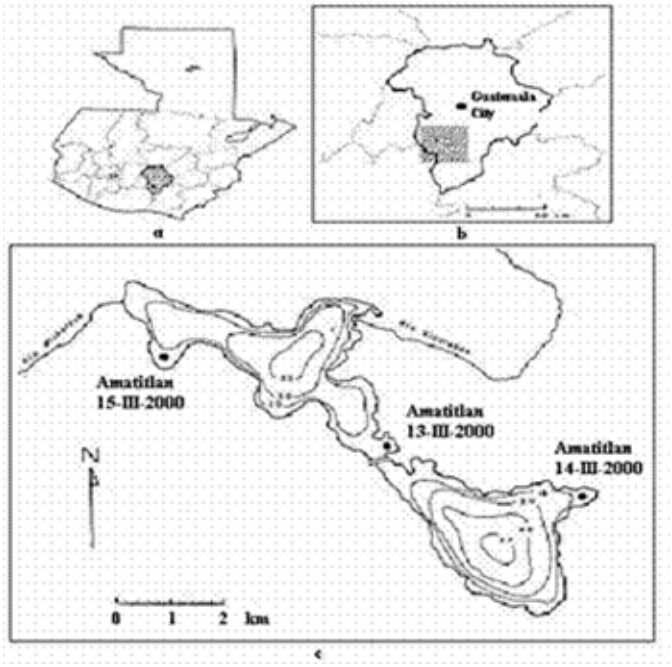

Figure 3.3.1-1. Map of Guatemala and Lake Amatitlan: a. location of the Valley of Guatemala and Lake Amatitlan; b. location of Guatemala City and Lake Amatitlan (hatched area); c. plan view of Lake Amatitlan showing Site 15-III-2000 (modified from Popenoe de Hatch *et al*. 2002:112)

Lamanai Lake (also known as Lamanai Lagoon and New River Lagoon) is a large, freshwater system which flows into the Caribbean Sea through the New River. On its north-west bank sits the archaeological site of Lamanai (discussed below; see fig. 3.3.2-1.). Lake cores were taken by a University of Edinburgh team to study Late Holocene climatic variability in the Maya lowlands (Breen 2002). This involved analysis using a range of proxies (e.g. $\delta^{18}O$, $\delta^{13}C$ and diatoms) and dating control provided by ^{14}C and ^{210}Pb. X-ray analysis failed to reveal the presence of tephra concentrations, so no tephra

extraction procedures were carried out by the Edinburgh team.

3.3.2. Archaeological sites:

Three archaeological sites in central and northern Belize were sampled for microtephra analysis. It was hoped that different aspects of site occupation or abandonment could be addressed at each of the sites, enabling a more thorough assessment of the limitations and potential for microtephrochronological analysis at archaeological sites.

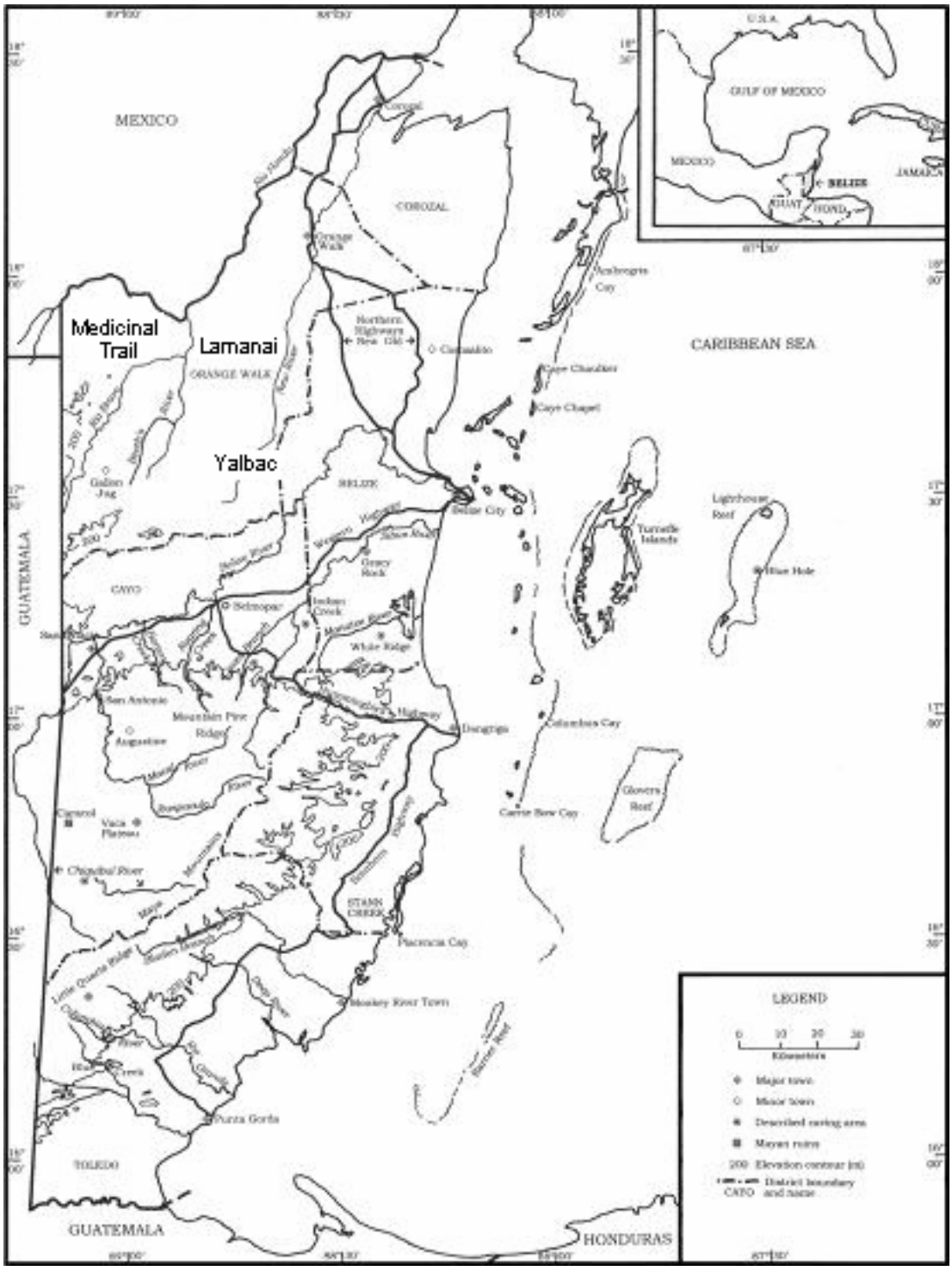

Figure 3.3.2-1. Map of Belize showing approximate locations of sites sampled for this study (Medicinal Trail, Lamanai and Yalbac). (modified from Veni 1996 in Owen 2002:3)

The **Medicinal Trail** site is located in the Rio Bravo Conservation Area in northern Belize (fig. 3.3.2-1). Architecturally, it consists of a single outlying structure and structures associated with three contiguous north-south trending courtyards (Hyde

2005). Excavations in 2004-2005 suggest that the Northern and Middle courtyards were constructed and occupied from the Preclassic era, whilst the southern courtyard was constructed during Classic times. Ceramics dating to the Late or Terminal Classic periods from SUBOP F, Northern Courtyard, suggest that human occupation or activity persisted till this period. Samples analysed in this study were taken from soil that had accumulated above an ancient structure in the northern courtyard (excavation unit OP7-SUBOPCC). Consequently, it was thought that microtephrochronology in this instance could provide a means of establishing a *terminus ante quem* for site abandonment, but would provide little information on cultural activity during occupation. The precision of the *terminus ante quem* date does, of course, depend on whether explosive eruptions (with widespread tephra dispersal) occurred shortly after abandonment or many decades later.

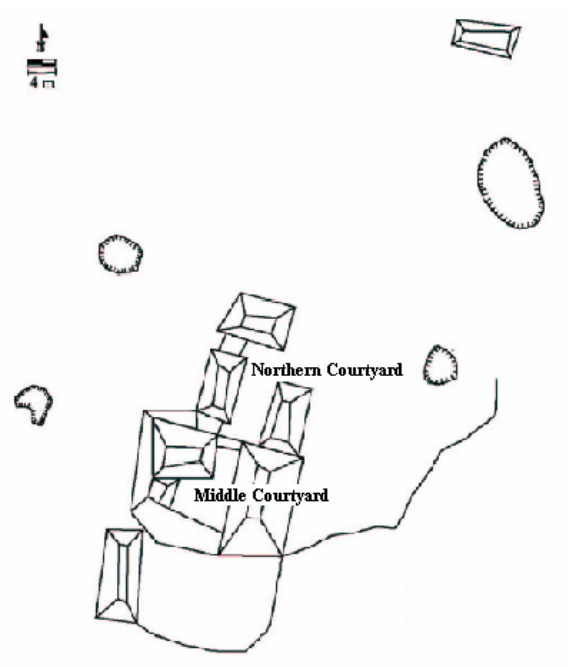

Figure 3.3.2-2. Tape and compass map of RB62 Operation 7, Medicinal Trail site (modified from Hyde 2005:12)

The site of **Lamanai** is located along the shores of Lamanai lake in northern Belize. Archaeological research has revealed a long, unbroken sequence of occupation spanning the Preclassic through Postclassic times, suggesting the site survived the demographic and socio-political collapse experienced by other southern lowland sites in the ninth and tenth centuries AD (Pendergast 1981; 1986). Eye-witness reports

indicate that large ash falls covered the site after the 1982 eruption of El Chichon, Mexico (Graham, pers. comm.). Samples for this study were taken from the 'uptown' extramural area north of Structure N11-3 (excavation units N15.5 W7 and N18.5 W10). This area was referred to informally as an 'off-platform' area and lacked obstructive architectural structures (Simmons and Howard 2003:14). Since it is located less than 200m east of the lake, it was thought possible to correlate tephra layers at the archaeological site with those from the lake core. This would enable us to address the potential of microtephrochronology to date Maya 'off-platform' areas, which are thought to have been locales for extramural household activity and possibly craft workshops (Simmons and Howard 2003:16).

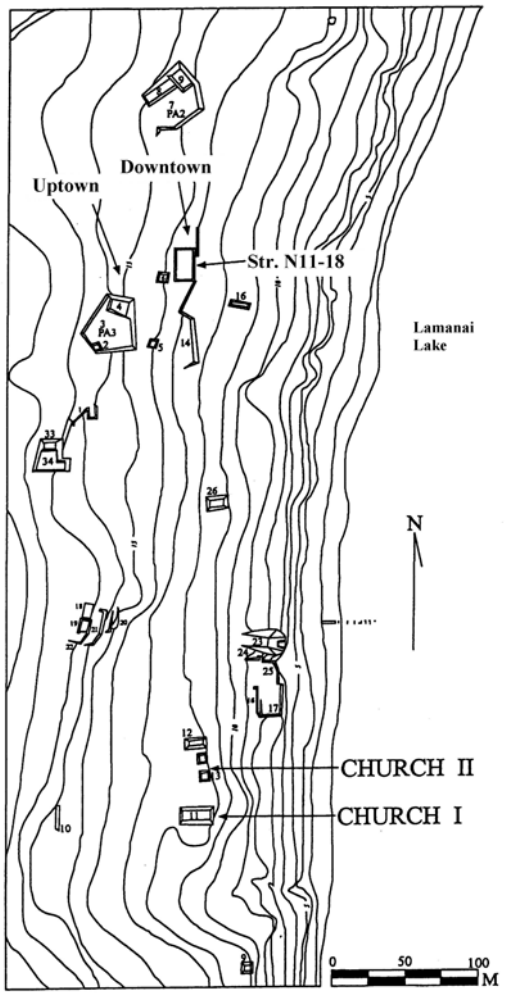

Figure 3.3.2-3. Lamanai site plan (modified from Simmons and Howard 2003:11)

The site of **Yalbac** is located in the Valley of Peace area in central Belize (see fig. 3.3.2-1.), with temple construction spanning the early Preclassic through Late Classic, and some evidence of human activity persisting into the Postclassic (Andrade 2005:48). As is typically found at Maya sites, new floors and buildings appear to have been constructed in such as way as to incorporate entire existing structures, as well as

typologically datable ceramics as construction fill and/or offerings. Thus, a record of construction is preserved within each building or below each floor. An excavation unit in Plaza 1 (which exposed a sequence of plaster floors) was sampled to assess the potential of microtephrochronology at ancient urban centres with monumental constructions and extensively plastered floors and walls. If microtephra was inadvertently or purposefully incorporated within or between plaster layers during construction, it should be possible to provide *terminus post quem* dates for construction. Depending on the reliability of techniques used to date eruptions, it was thought that the presence of tephra may provide greater precision than Maya ceramic types, which often span several hundreds of years (Gifford 1976).

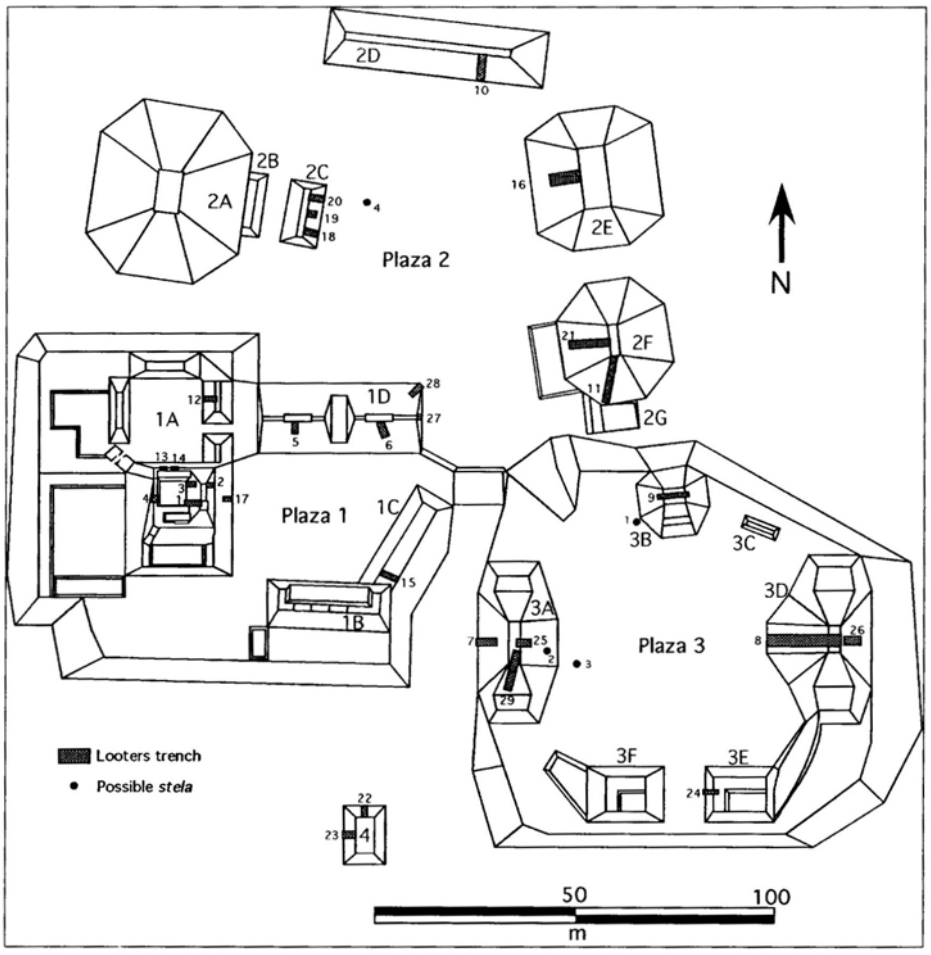

Figure 3.3.2-4. Yalbac site plan; samples taken from excavation unit in Plaza 1 (Lucero 2005:2)

4. METHODOLOGY

4.1. FIELD SAMPLING:

4.1.1. Standard procedures of field sampling:

Field sampling for palaeoenvironmental studies usually involves the use of a piston-corer or auger to remove complete sediment sequences from lake bottoms or peat deposits. In some cases sediment monoliths are abstracted from exposed geological outcroppings or excavation units.

4.1.2. Procedures of field sampling employed in this study:

At the archaeological sites of Lamanai and Medicinal Trail in Belize, 25 and 50cm contiguous sediment monoliths were obtained by the author from the sides of exposed excavation units using plastic half-drainpipes. Where a sequence exceeded 50cm (e.g. at Medicinal Trail), two or more overlapping drainpipes were used (fig. 4.3.2-1). At the site of Yalbac, samples were collected and bagged directly from the excavation profile due to extremely dry weather which rendered it impossible to obtain a contiguous sediment monolith that did not collapse during sampling. In all cases, basic lithological logging was undertaken and depths below ground surface recorded.

The Lamanai Lake core was sampled by a team from Edinburgh University. 10cm sub-samples were abstracted by the author during a visit to the Geography Department at Nottingham University, where the core is currently stored. Lithological logging had

previously been undertaken by the Edinburgh team during a research study on climate change in Northern Belize.

A proximal lake core was sampled from Amatitlan in highland Guatemala by a University of Florida team. Vials containing pre-extracted tephra (including mineral fractions and other materials greater than 250μm in size) were sent to the author by a research group at the University of California Santa Barbara. Unfortunately no lithological information was available, and no microtephras were present due to small size fractions being discarded during extraction.

4.1.3. Limitations:

Ideally, a consideration of lake basin basymetries and tephra fallout patterns would be considered prior to sampling, and multiple cores would be taken. However, this is seldom achievable. At archaeological sites, we are restricted by the location of excavation units and the depth to which units have been excavated. Samples from archaeological sites analysed for this study were far from ideal. Yalbac samples consisted predominantly of compact, man-made plaster floors from the centre of an ancient plaza; samples from Lamanai were taken from shallow units that had been excavated some decades earlier; and samples from Medicinal Trail were taken from soil that had accumulated on top of an ancient construction (i.e. on a slope).

4.2. TEPHRA EXTRACTION:

Tephrochronology relies on the extraction of tephra shards from sediments for visual

identification and high-precision geochemical comparison (Blockley *et al*. 2005). In general, extraction procedures involve the removal of unwanted organic material using ashing (Pilcher and Hall 1992) and acid digestion (Rose *et al*. 1996), or the concentration and extraction of tephra from minerogenic sediments using density separation (Turney 1998; Blockley *et al*. 2005) and in some cases magnetic separation (Froggatt and Gossan 1982 in Lane 2004). Most extraction procedures involve a combination of these techniques. However, recent studies (Blockley *et al*. 2005; Dugmore *et al*. 1992) suggest that certain methods employed for the removal of unwanted material should be avoided because they can affect tephra geochemistry; for example acid digestion and alkali washes should be avoided altogether, whilst ashing should not take place prior to microprobe analysis. Here I outline standard procedures of microtephra extraction, the methodology employed in this study, and the implications and problems of the various extraction techniques.

4.2.1. Principles and standard procedures of microtephra extraction:

Tephra extraction procedures vary between laboratories. Most laboratories generally employ the density separation technique outlined by Turney (1998 described below) combined with 'purification' techniques to remove organic material, carbonates and diatoms. This normally involves an acid digestion phase, where samples are immersed in concentrated sulphuric and nitric acid for approximately 2 hours (sometimes up to two days) at 90°C to remove the organic component (Dugmore *et al*. 1992). A further purification step to remove diatoms, sponge spicules and other biogenic silicates is often applied to distal microtephra from lake sediments; this involves a 4 hour wash in 0.3M sodium hydroxide (Rose *et al*. 1996).

4.2.2. Procedures of microtephra extraction employed in this study:

Most of the procedures employed in this study are also routinely used at other laboratories. The main difference between the extraction methodology of this study and most other protocols is that this study excludes acid and alkali cleaning and instead relies solely on density separation.

Contiguous samples of 10cm vertical thickness (in approximately equal volumes) were sampled from each sediment sequence. This was repeated using contiguous samples of 4cm vertical interval for the top 20cm of Medicinal Trail in order to resolve peaks in shard concentration (see fig. 4.3.2-1.). Following Pilcher and Hall (1992), samples from the Medicinal Trail site were ashed in a furnace at 550°C for two hours. The quick burning procedure was not conducted on samples from the remaining sites due to the tendency for samples of high clay content to fire into bricks. Recovered material was transferred to round-bottomed, 15ml centrifuge tubes to which 1M HCl was added to disaggregate the sediment and dissolve soluble inorganics (i.e. mainly carbonates). The length of time samples remained in HCl depended on sediment type and degree of fizzing, but was usually an hour or two and never more than 24 hours. The sediment (with HCl) was then sieved using mesh sieve sizes of 80 and 25μm to separate out the sediment size fraction believed to contain most microtephra particles (25-80μm). The larger fraction (>80μm) was also retained, but the smaller fraction containing fine clay and silt particles (<25μm) was discarded.

This was followed by a non-hazardous stepped flotation density-separation technique which is attributed to Turney (1998) and Blockley *et al*. (2005) but is known to have

been employed many decades earlier (e.g. Pilcher and Hall 1992; Smith and Westgate 1969). This technique involves the use of sodium polytungstate (SPT; $Na_6(H_2W_{12}O_{40}).H_2O$) as a flotation medium. Round-bottomed tubes containing the 25-80μm residue were centrifuged twice in 4ml SPT of a relative density of 1.95g cm^{-3} at a speed of 2500 rpm for fifteen minutes and decanted to remove the lighter (mostly biogenic) compounds. This was repeated. The remaining material (>1.95g cm^{-3}) was then floated off twice (firstly 2ml and then 4ml) using 6ml SPT to a pre-determined standard gravity (SG) of 2.55g cm^{-3}. After each centrifuge treatment, the 'float' was decanted into conical centrifuge tubes. All flotants were retained but attention was focused on material of 1.95-2.55g cm^{-3} SG, which was considered to be the optimum density for recovering rhyolitic (silicic) glass shards (Blockley pers. comm.; adapted from Turney 1998 and Blockley *et al*. 2005). Distilled water was added to all tubes and centrifuged at 2500 rpm for 5 minutes (with brake) and poured off. This was repeated an additional four times per sample to enable the supernatant (diluted SPT) to be collected and filtered for reuse.

The extraction procedure was also undertaken on the >80μm sieve fraction of select samples in case tephras reaching Belize were greater than 25-80μm (see Ford and Rose 1995; see fig. 4.3.2-6.).

4.2.3. Limitations:

There are a number of problems associated with standard microtephra extraction procedures. Knowledge of glass dissolution mechanisms suggests fine-grained tephra samples are prone to chemical alteration and dissolution in a range of environments,

including acidic and basic conditions (Blockley *et al*. 2005). Indeed, the susceptibility of glass to chemical alteration depends on a number of factors, including the molecular structure of the glass, reaction kinetics, the ratio between surface area and volume of the shards, solution pH, and temperature (Pollard *et al*. 2003). Accordingly, it is likely that the acid and alkali 'cleaning' phases at some laboratories cause alteration of the geochemical signature of the shards (Blockley *et al*. 2005).

Since microtephrochronology relies almost solely on high-precision geochemical analysis to correlate tephra layers, the possibility that glass shards have been chemically altered undermines the technique. If alteration has occurred, it calls into question the reliability of the current database of tephra chemical signatures and the resulting conclusions that are made. Although traditional tephrochronology on visible tephra layers follows the same principles, the problems are more extreme for microtephrochronology because a) the large surface area to volume ratio of microtephras make them more susceptible to glass alteration, and b) there is often a complete reliance on glass geochemistry in microtephra studies, whereas there is the possibility of using other means (e.g. mineralogical and stratigraphic information) to correlate tephra layers that are visible.

To overcome these problems, Blockley *et al*. (2005) suggest a 'new' extraction method that avoids the use of destructive acid and alkali pre-treatments. Nevertheless, there are problems with the 'new' technique. Although the emphasis on stepped flotation reduces the potential for chemical alteration in the laboratory, it does not prevent degradation in the post-depositional environment (Blockley *et al*. 2005). Even in the laboratory, some degree of chemical alteration is inevitable; no liquid medium is chemically inert, and

glass tephra shards alter when solely in contact with demineralised water (*ibid.*). Another problem with the technique is that a proportion of shards are likely to be discarded when material of optimum specific gravity is rinsed in distilled water and poured off. Thus, there will still be some degree of sample loss.

There are also considerable problems in applying a universal protocol with pre-determined SGs for recovering tephra. Principally, tephra densities vary with type of volcanic material, particle size and vesicularity, such that trial-and-error is required to establish the optimum specific gravity for each new tephra type being studied (Turney 1998). Even within a single tephra horizon, tephra densities can vary because a) not all glasses are vesicular, b) not all glasses display the same level of vesicularity, and c) not all vesicles are of the same size (Westgate and Gorton 1981). Furthermore, it appears that tephra densities can be altered under natural sedimentary conditions, such as through the formation of hydration layers on the surface of shards (Blockley *et al*. 2005). Consequently, the optimal relative densities for recovering tephra can vary depending on post-depositional environment and degree of chemical alteration, even if tephras originated from the same eruption. Finally, Turney (1998:204-205) warns that ashing samples in a furnace may alter the relative density of tephra shards. Although ashing is not undertaken on samples prior to microprobe analysis, it often forms an integral part of initial core scanning and tephra extraction.

Despite these problems, attempts have been made to establish a universal density separation protocol. After experimentation on Vedde ash from Nordfjord (Norway), Turney (1998) suggested a relative density of 2.4-2.5g cm^{-3} as a useful starting point for concentrating tephra. This was then modified by Blockley *et al*. (2005), who

suggest floats of 1.98 and 2.5g cm^{-3}. The optimal relative density used at the Oxford tephra laboratory has been modified further to 1.95-2.55g cm^{-3}.

Blockley *et al*. (2005) claim that a series of experiments were conducted to establish a) the typical range of SGs for common constituents of sediments and b) the optimal SG for concentrating known tephras. According to their studies, it was found that little detrital material was removed at densities of 1.5 and 1.75g cm^{-3}, whereas different detrital components were progressively removed at liquid medium densities of between 2 and 2.25g cm^{-3} (*ibid.*). As demonstrated by previous researchers, sponge spicules float off at a liquid density of 2g cm^{-3}, whilst diatoms float off at densities of up to 2.25g cm^{-3}. If this is the case, none of the cleaning float densities suggested by Blockley *et al*. (2.0 or 1.98 g cm^{-3}) or used at the Oxford laboratory based on Blockley's suggestions (1.95g cm^{-3}) seems appropriate for removing detrital material, sponge spicules and diatoms. Although this does not necessarily affect tephra recovery success, it complicates identification of tephra.

More significantly, Blockley *et al*. (2005) note that 'even very subtle changes in liquid density (of ca 0.1g cm^{-3}) can have dramatic effects on recovery success'. In other words, it is vital that the SGs used during flotation are appropriate and robust. However, during extraction of samples for this study, it became increasingly apparent that the protocol outlined by Blockley *et al*. (2005) leads to inadvertent dilution of SPT to unknown SGs. This is because test-tubes with material undergoing the 2.55g cm^{-3} SPT flotation contain small amounts of 1.95g cm^{-3} SPT prior to the 2.55g cm^{-3} flotation. This dilutes the 2.55g cm^{-3} SPT, causing the SPT to be of unknown SG lighter than 2.55g cm^{-3}; the extent of dilution depends on the amount of liquid in any given test-

tube prior to the addition of 2.55g cm^{-3} SPT. With such small quantities of SPT in use, the presence of any 1.95g cm^{-3} SPT will severely reduce the SG of the 2.55g cm^{-3} SPT. Consequently, it seems imperative that samples are washed and dried prior to each SPT centrifugation if this problem is to be avoided. Alternatively, the 2.55g cm^{-3} SG flotation process could be repeated using fresh 2.55g cm^{-3} SPT for each float. The SG of SPT will be closer to 2.55g cm^{-3} for the repeat float, since it would be diluted with SPT that is slightly lighter than 2.55g cm^{-3} SG rather than SPT that is 1.95g cm^{-3} SG. Both these suggested protocols would, however, severely add to laboratory time.

It should also be emphasised that the discussed density separation technique is only efficient at isolating the rhyolitic component of tephra and is inefficient at concentrating remaining constituents such as basaltic shards. In other words, we are innately limiting our dataset with this protocol. To overcome this, work is in progress on the separation of basaltic glass (Davies *et al*. 2001), though suggested protocols are not widely undertaken at microtephra laboratories.

4.3. TEPHRA IDENTIFICATION:

4.3.1. Principles and standard procedures of microtephra identification:

Microtephra shards are generally identified on the basis of morphology and optical characteristics. Some tephrochronologists have stressed the physical properties of glass shards, documenting morphology, transparency, vesicularity, microphenocryst content, hydration, and refractive index as means of distinguishing between different tephra types, because glass shards can vary in appearance depending on the properties of the

magma and the eruptive mechanism (Westgate and Gorton 1981:77-78). In most microtephra studies, however, tephra identification is undertaken to produce a quantitative tephra count as a means of determining which samples should be remounted for microprobe analysis, rather than as a way of distinguishing between eruptions.

There are three main criteria for distinguishing glass tephra shards from other particles. The first centres on the visual characteristics of materials under plane and cross-polarised light (Pyne-O'Donnell *et al*. 2004). Samples are secured on glass slides using a mounting medium such as Canada Balsam, Glycerol or Euparol, and viewed under a polarised light microscope. Under cross-polarised light, translucent minerals of crystalline structure rotate light and therefore appear bright against a black background. This birefringence (or display of interference patterns) results from some minerals having two different indices of refraction. A key feature of volcanic glass is that it is amorphous (i.e. lacks a well-defined crystalline structure). Consequently glass tephra lacks interference patterns when viewed under cross-polarised light, and can therefore be distinguished from translucent minerals that exhibit birefringence.

The second main criterion for identifying tephra exploits differences in the refractive indices of tephra, the mounting medium and other materials. The refractive index (RI) of a given material is expressed as a number (e.g. 1.500) and is determined by the speed of light waves in a vacuum and within a medium. This speed varies because of the dielectric (insulating) polarisability of charged particles, which act as harmonic oscillators (Pyne-O'Donnell *et al*. 2004). RIs increase with electron density, and therefore with mass and atomic number. The Becke line is a bright halo of light that

appears around the edge of an object when there is a difference in the RIs of the particle and surrounding medium. The Becke line will move towards the region with the higher index of refraction, such that light will concentrate either inside or outside an object. The standard mounting media for microtephra on glass shards is Canada Balsam, which has a RI of 1.523. Pyne-O'Donnell *et al*. (2004) state that glass tephra shards consist predominantly of silica (atomic number 14; maximum content 75%wt) with small amounts of heavy minerals, such that they tend to have a minimum RI of approximately 1.490. The Becke line is therefore assumed to move away from tephra shards (and biogenic silicates) when in Canada Balsam. This difference in RI also leads to a pinkish hue in tephras under transmitted light, which again aids identification (*ibid.*).

Alternative mounting media include Glycerol (RI of 1.475) and Euparol (RI of 1.483). Since biogenic silicates can mimic tephra in Canada Balsam, the mounting media of Glycerol and Euparol are more appropriate for samples abundant in biogenic silicates. This is because the maximum RI of biogenic silica is 1.470, whilst the minimum RI of tephra is 1.490. Consequently Glycerol and Euparol can be used to distinguish between biogenic silica and tephra, as the Becke line will move towards tephra shards and away from biogenic silica. Furthermore, tephra can be distinguished from biogenic silica because the latter retains a pinkish hue whereas the former takes on a greenish colour under transmitted light (Pyne-O'Donnell *et al*. 2004).

Finally, the physical appearance of shards plays a major role in microtephra identification. Training in tephra identification usually involves the use of reference slides to familiarise oneself with 'typical' tephra appearances. Glass tephra shards are generally assumed to lack internal structure, have concoidal fractures around the edges,

and frequently contain vesicles that may or may not be elongated (Lane and Blockley pers. comm.).

4.3.2. Procedures of microtephra identification employed in this study:

Flotants of 1.95-2.55g cm^{-3} were mounted on glass slides in Euparol and examined for the presence of glass microshards using polarised (transmitted) light microscopes at x10 to x40 magnification. Euparol was chosen over Canada Balsam because of the presumed abundance of biogenic silica in some samples. Coordinates of each tephra shard on slides were recorded using a microscope with a horizontal moving stage. The resulting tephra counts were expressed graphically (as histograms) alongside other stratigraphic information (see figs. 4.3.2-1. to 4.3.2-5.). 10cm tephra scans revealed variable low shard counts between 0 and 37, and for the most part only silicic (rhyolitic) shards were identified. 4cm tephra scans of Medicinal Trail samples did, however, reveal considerably higher shard counts.

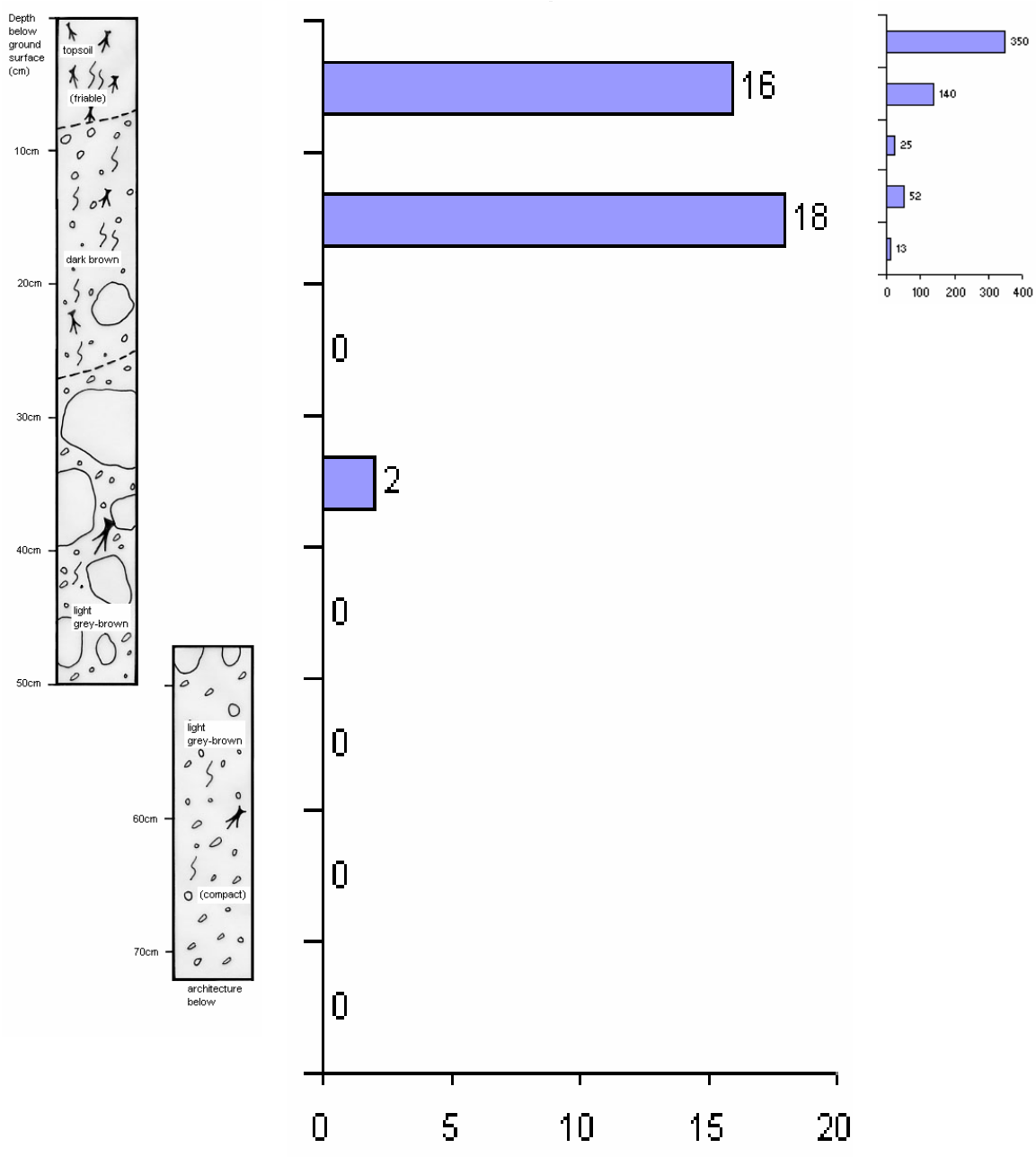

Figure 4.3.2-1. Medicinal Trail cores with histogram showing tephra counts (at 10cm and 4cm resolution)

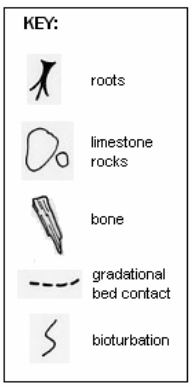

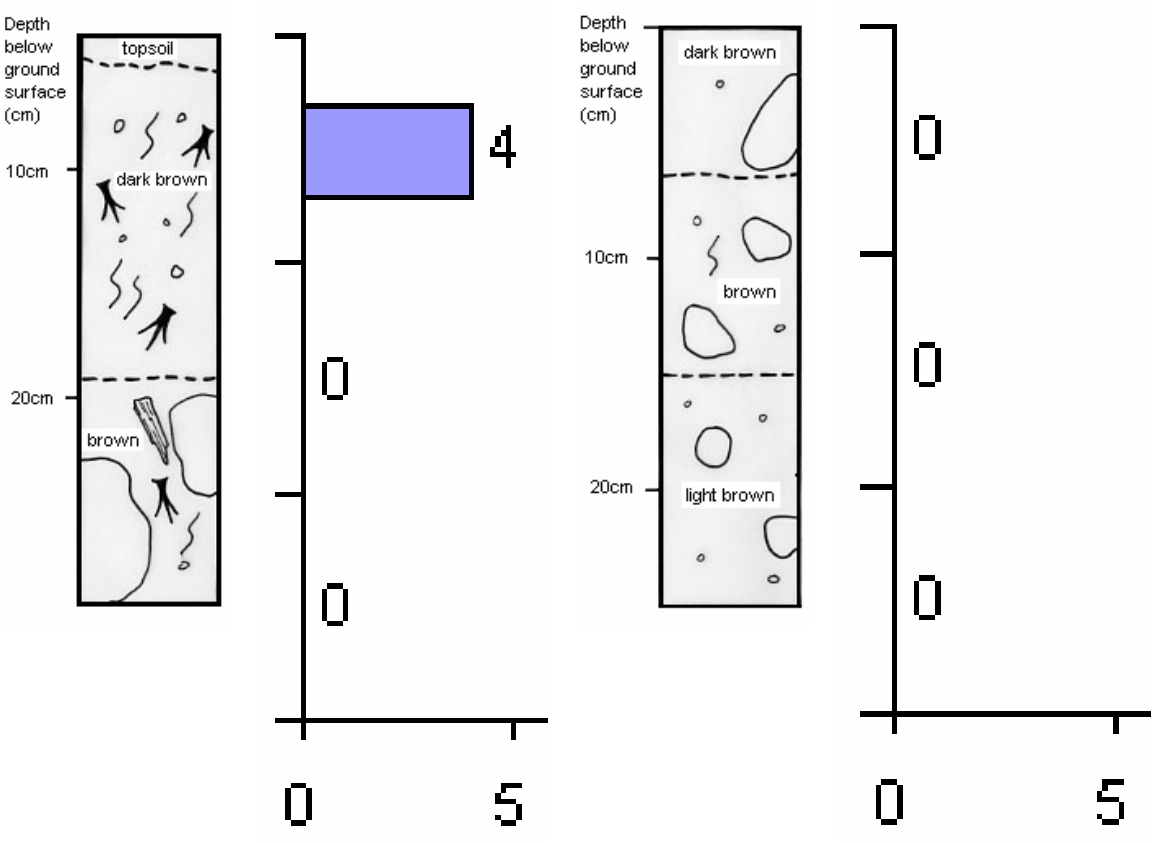

Figure 4.3.2-2. Lamanai Unit 1 (L) and Unit 2 (R) cores with histograms showing tephra counts (at 10cm resolution)

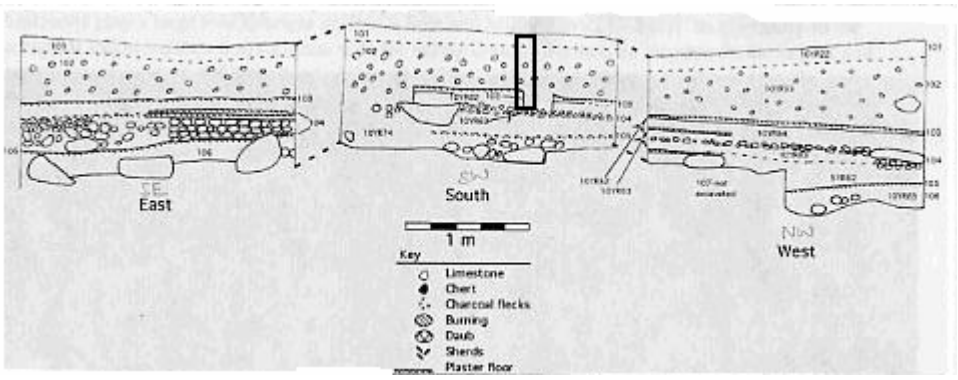

Figure 4.3.2-3. Yalbac Plaza 1 unit with sample area indicated

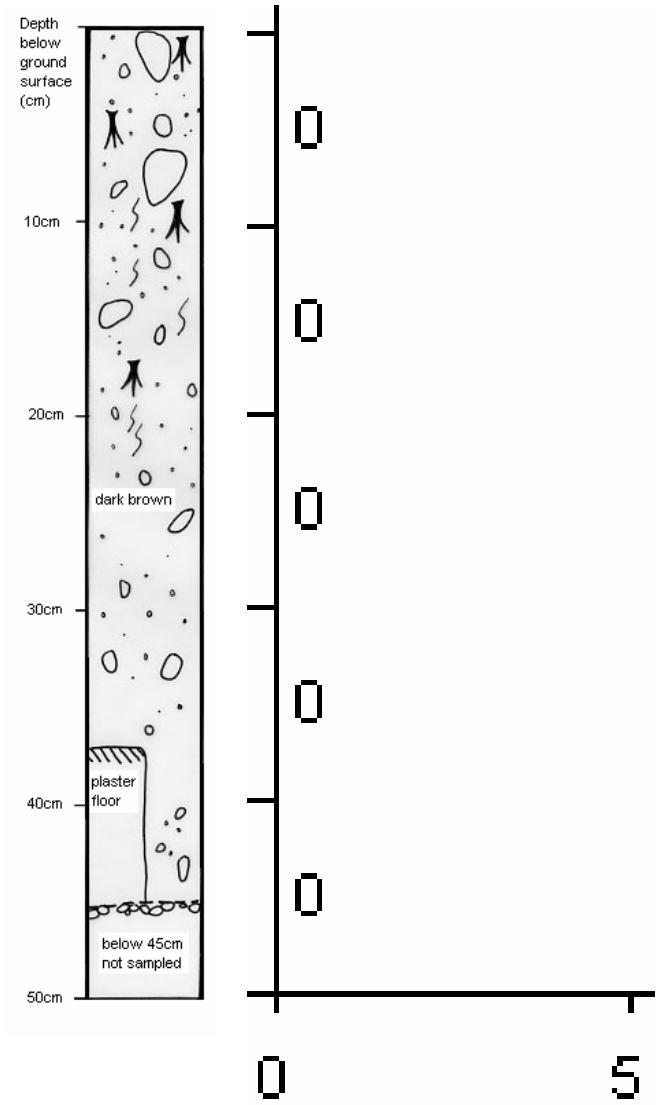

Figure 4.3.2-4. Yalbac Plaza 1 core with histogram showing tephra counts (at 10cm resolution)

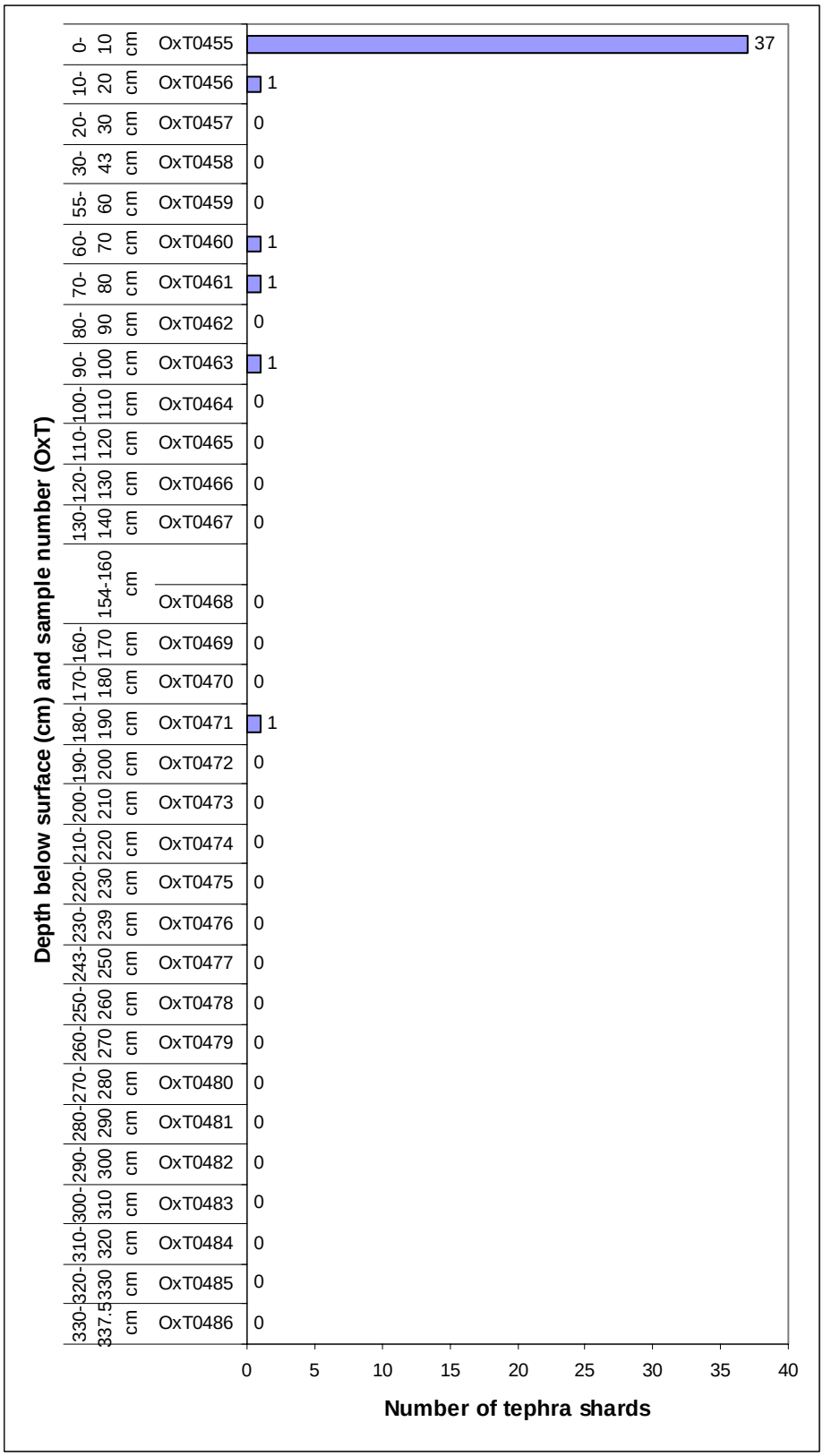

Figure 4.3.2-5. Histogram showing Lamanai Lake tephra counts (at 10cm resolution)

Cleaning floats (<1.95g cm^{-3}; >2.55g cm^{-3}) of a selection of samples were also mounted on slides and scanned in case tephra from Belizean samples were particularly vesicular (and consequently of low density), basaltic (and consequently of greater density), or inadvertently poured off due to problems with the flotation technique (see p. 28-32.). The >80µm sieve fraction of a selection of samples was also mounted and scanned in case distal tephra in Central and Northern Belize was greater than 25-80µm in size:

				25-80µm			> 80µm
Project	Site	Depth	Sample	< 1.95g cm-3	1.95-2.55g cm-3	> 2.55g cm-3	1.95-2.55g cm-3
P020	Lamanai Unit 1	4-14cm	OxT0437	mounted	standard mount	mounted	mounted
P020	Lamanai Unit 1	14-24cm	OxT0438	mounted	standard mount	mounted	mounted
P023	Lamanai Lake	0-10cm	OxT0455	mounted	standard mount	mounted	mounted
P023	Lamanai Lake	70-80cm	OxT0461	mounted	standard mount	mounted	mounted
P023	Lamanai Lake	180-190cm	OxT0471	mounted	standard mount	mounted	mounted
P021	Yalbac	0-10cm	OxT0495	mounted	standard mount	mounted	mounted
P019	Medicinal Trail	0-10cm	OxT0855	mounted	standard mount	mounted	mounted
P019	Medicinal Trail	10-20cm	OxT0856	mounted	standard mount	mounted	mounted

Figure 4.3.2-6. Size and density fractions of select samples mounted and scanned for microtephras; no additional microtephras identified

4.3.3. Limitations:

At first site, the identification of microtephra seems relatively straightforward. However, problems arise with each of the three main criteria. Mineral inclusions in glass or glass aggregates may cause some microtephra to show a degree of interference (i.e. birefringence) that complicates identification according to the first criterion. This can be overcome with careful microscopy and attention to detail but are not fully resolvable. Problems also arise with the use of certain mounting media and the behaviour of the Becke Line. As previously mentioned, diatom fragments and higher-plant silica bodies such as phytoliths can have optical properties similar to those of the volcanic glass when mounted in Canada Balsam. Furthermore, many tephra shards

have a lower silica content than the maximum 75%wt, contain larger quantities of iron (atomic number 26), and therefore have RIs that are >1.523 and Becke Lines that move inwards in Canada Balsam. Consequently, it is quite possible that a considerable number of tephra shards have Becke Lines that act in precisely the opposite way from that which is considered diagnostic of tephra.

The use of Euparol is also problematic, particularly because its RI appears to change with time; the RI is 1.483 as a liquid but varies from 1.478 at 20ºC to 1.535 when solid (Woods 2003). Accordingly, an effort must be made to scan all slides under the microscope within a short space of time, since the change in RI of the mounting medium alters the behaviour of the Becke Line. Furthermore, the use of Euparol in this study has alerted us to the possibility that microtephra may deteriorate as a result of contact with this medium; microtephra was identified on one slide (OxT0455; see fig. 4.3.3-1. and 4.3.3-3. a-j. for further micrographs) during initial scanning but had 'disappeared' when the slide was rescanned. This phenomenon also appears to have occurred with samples from Europe and North America (Lane and Watson pers. comm.). If this is the case, Euparol should be abandoned as a mounting medium in future microtephra studies.

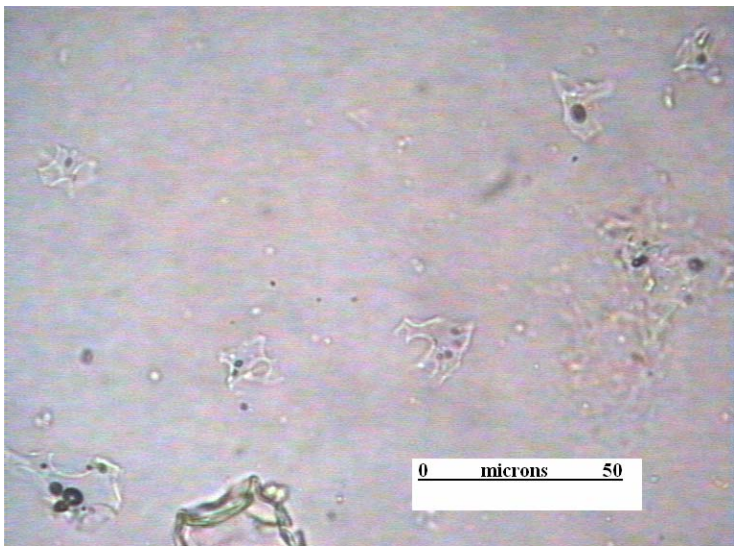

Figure 4.3.3-1. Micrograph of OxT0455 (slide coordinates: 12.5, 51.5) showing microtephras; these and other shards could not be relocated on the slide after initial scanning and photography

It is worth noting that the range and value of the RI of volcanic glass (as measured with RI oils) was previously used as a way of distinguishing between different tephra types (Westgate and Gorton 1981:79). Although the success of this technique was limited, it reminds us that there are some—albeit small—differences in the RIs of volcanic glasses from different sources, such that it may not be entirely appropriate to assume that all microtephra can be identified using the assumed behaviour of the Becke Line as a criterion.

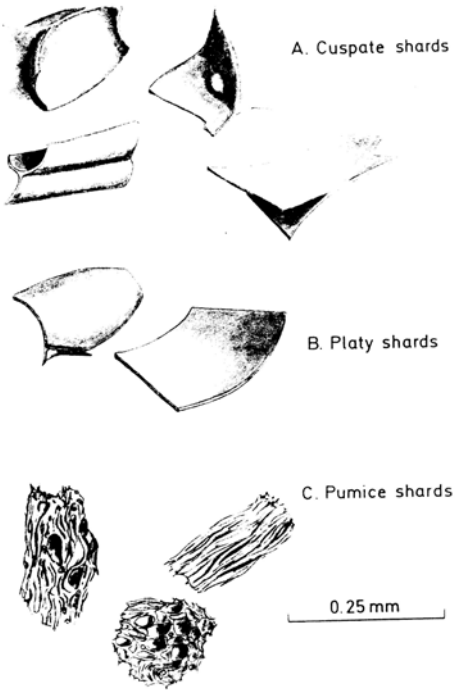

Figure 4.3.3-2. Diagrammatic representation and terms for common glass shards (Fisher and Schminke 1984:101)

Perhaps the most problematic criterion of microtephra identification is physical appearance. It should be noted that there is a wide range of tephra morphologies and colours, such that the physical 'traits' of microtephra cannot be simplified to a few commonly occurring forms. Although vitreous microtephra shards should behave as other glasses, some may appear to have internal structure because of high vesicularity or alteration (see fig. 4.3.3-2. and 4.3.3-3.). Not all tephra particles will have a "fresh appearance" of concoidal or sharp edges that appear to have been fractured in the immediate past. Indeed, many microtephra particles from archaeological and palaeoenvironmental sites are likely to be eroded, worn and rounded. Within the

Oxford tephra group, there was some dispute about the identity of particles in some samples analysed for this study; initially some were considered to be phytoliths but were later identified as tephras (esp. OxT0855 samples; see 4.3.3-3. c-f). If we are to have full confidence in our ability to identify all microtephras in a given sample, efforts ***must*** be made to familiarise ourselves with the ***full*** range of known tephra morphologies.

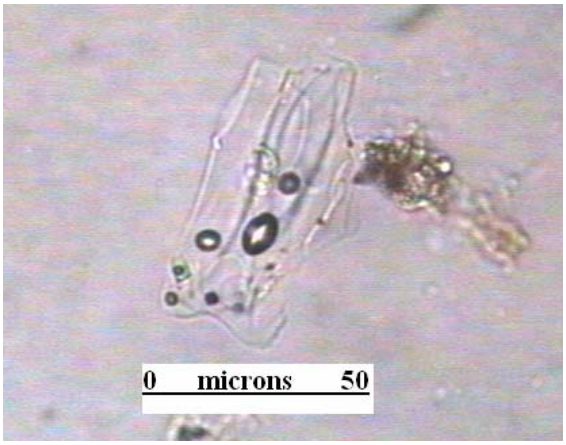

a. Lamanai Lake: OxT0455 (slide coordinates: 10, 60) Microtephra in Euparol

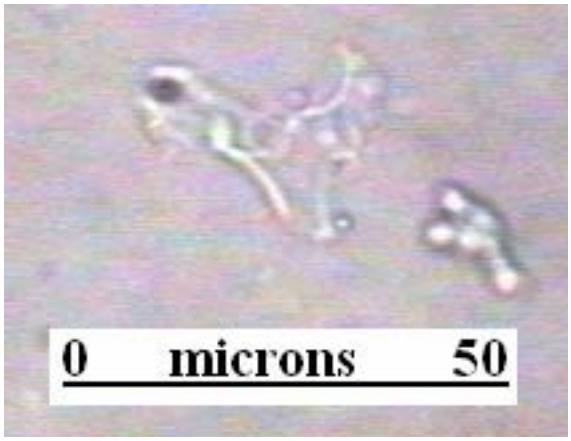

b. Lamanai Lake: OxT0 (slide coordinates:) Microtephra in Euparol

c. Medicinal Trail: OxT0855 (slide coordinates: 2, 56) Controversial microtephra in Euparol

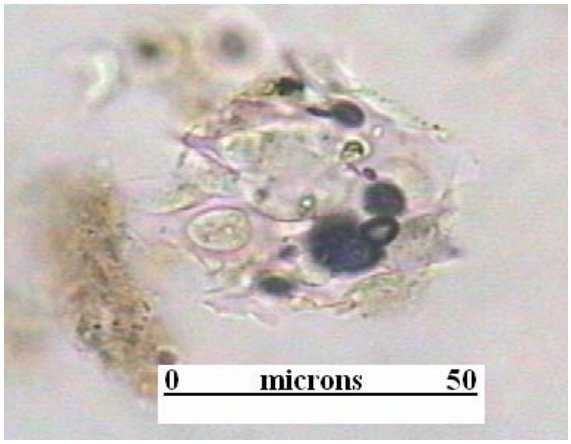

d. Medicinal Trail (slide coordinates: 2.5, 51.2) Controversial microtephra in Euparol

e. Medicinal Trail: OxT0855 (slide coordinates: 3, 52) Controversial microtephra in Euparol

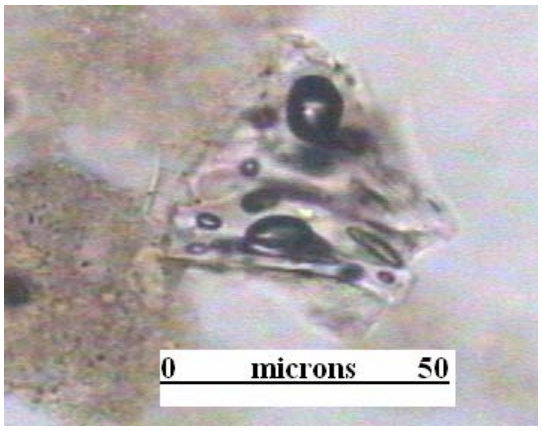

f. Medicinal Trail: OxT0855 (slide coordinates: 12, 46.9) Microtephra in Euparol

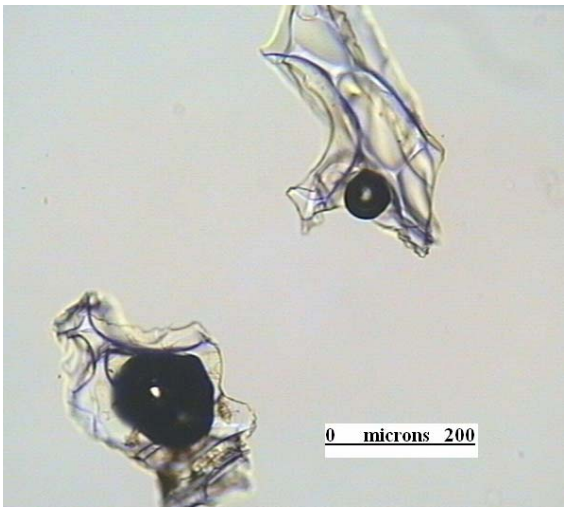

g. Lake Amatitlan: OxT0540 (slide coordinates: 15, 51) Tephras in Resin

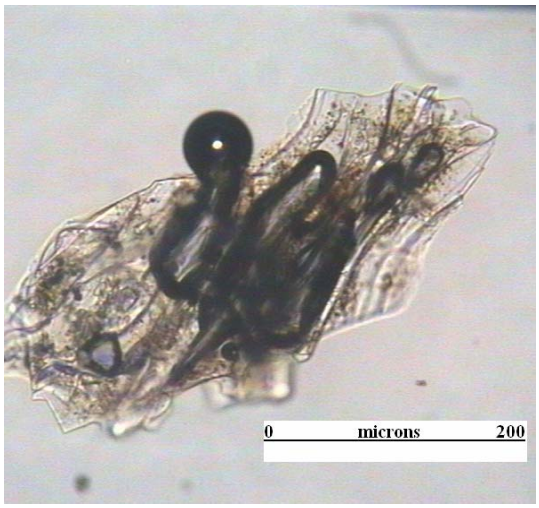

h. Lake Amatitlan: OxT0538 (stage coordinates: 11.6, 52.2) Tephra in Resin

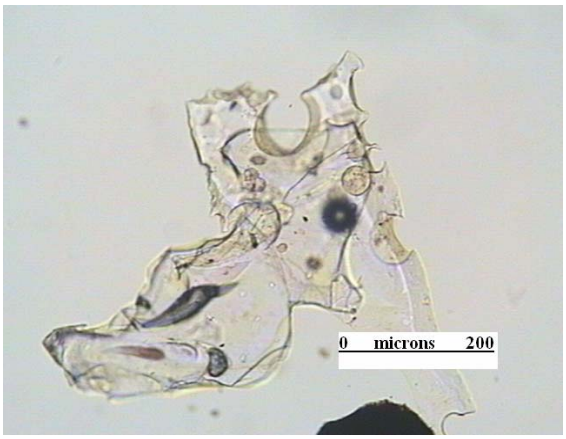

i. Lake Amatitlan: OxT0544 (slide coordinates: 20, 51) Tephra in Resin

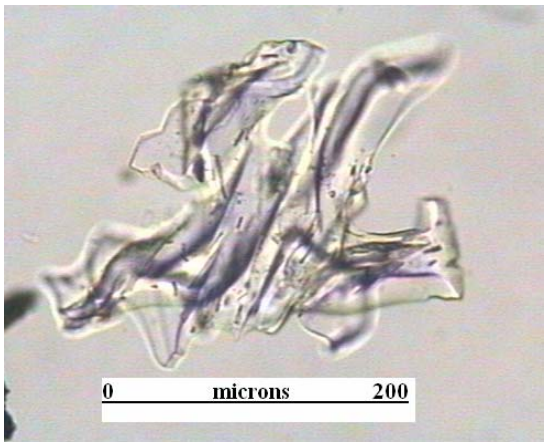

j. Lake Amatitlan: OxT0546 (slide coordinates: 17, 52) Tephra in Resin

Figure 4.3.3-3. a-j. Micrographs showing range of microtephra and tephra morphologies in samples analysed for this study; includes microtephras initially believed to be phytoliths (b-e)

Finally, a recent study by Lane (2004:41) has drawn attention to the fact that microtephras could be present in cores (identified in 1cm scans) even when no shards were identified in 10cm scans. This was also illustrated during scans of 10cm and 4cm vertical sub-samples from the Medicinal Trail site analysed for this study (fig. 4.3.2-1.). 10cm depth scans revealed the presence of just 16 and 18 shards in the top 0-10cm and 10-20cm respectively, but 4cm scans revealed as many as 350, 140 and 25 shards in the top 0-4cm, 4-8cm and 8-12cm respectively. This difference is staggering. In Lane's study, the presence of greater numbers of shards in 1cm scans was attributed to inconsistent lateral deposition of microtephra within a single core or sediment sequence. Although this could also account for the inconsistency between 10cm and 4cm scans in samples analysed for this study, there are several other potential causes. Firstly, approximately $1cm^3$ of soil or sediment is sampled prior to each extraction, whether the sample represents 10cm, 4cm or 1cm vertical depth. In other words, 1cm vertical depth is represented by just $1mm^3$ of soil or sediment for 10cm depth sub-samples, whereas 1cm vertical depth is represented by 2.5 mm^3 for 4cm depth sub-samples and $1cm^3$ for 1cm depth sub-samples. Clearly 1cm or 4cm depth sub-samples are likely to contain greater quantities of shards per centimetre than 10cm depth sub-samples. Secondly, not all floated material of 1.95-2.55g cm^{-3} SG per sample was mounted onto slides; it was deemed adequate to mount one slide per sub-sample, rather than using as many slides as necessary until all material of 1.95-2.55g cm^{-3} SG was mounted. The obvious consequence of this protocol is that tephra counts are not comparable between samples, and only provide an indication of whether tephra is or is not present. In the case of 4cm depth sub-samples, all material of 1.95-2.55g cm^{-3} SG was mounted for each sub-sample, whereas this was not the case for 10cm depth sub-samples. Consequently, the quantity of tephra is under-represented for the latter. Thirdly, tephra recovery is likely

to vary unpredictably with factors such as SPT dilution (discussed above). In all cases, the under-representation of tephra in 10cm depth sub-samples raises considerable questions about the reliability of our current extraction and identification procedures, and implies the need for processing multiple samples to test repeatability of results.

5. TEPHRA DISPERSAL AND SITE FORMATION PROCESSES

The absence of tephra at archaeological and palaeoenvironmental sites can be attributed to natural and cultural site formation processes. Two principle issues are of concern: 1) factors affecting distribution and deposition of tephra at sites (i.e. whether or not tephra reached certain sites and areas within each site) and 2) the possibility of reworking (i.e. whether tephra arriving at sites and incorporated into sediment sequences was subsequently reworked by natural and/or cultural processes). The problems of distribution, deposition and reworking are widespread at both archaeological and palaeoenvironmental sites, but the former suffer from the added possibility of cultural modification with human activity.

5.1. MICROTEPHRA DISPERSAL AND DEPOSITION:

5.1.1. Principles of tephra dispersal and deposition:

As discussed in chapter 2, the dynamics of volcanic eruptions depend on magma viscosity and the content of dissolved gas. The dispersal of airborne volcanic glass tephra follows explosive volcanic eruptions where magma is primarily of high silicic composition (Wolff-Boenisch 2004:4843). The extent of ash falls depends largely on the height to which fine grains are thrown into the air (Hall 1996:47). Most eruptions are Strombolian in nature, meaning ash clouds are projected less than a kilometre in height and consequently fall back onto the volcano to build up a cone. Less frequent Plinian eruptions consist of powerful blasts and ash columns of 10km or more in height. The ash from Plinian eruptions form sheet deposits over wide areas and can be

identified as microtephras in distal locations. In principle, glass shards fall on land or in water within hours or days after an explosive eruption (Carey 1997) and can therefore be used as time-parallel markers. Although pyroclastic surge deposits are concentrated in valleys and depressions, it appears that airfall tephra is likely to cover the ground more uniformly, irrespective of depressions (inferred from Hall 1996:51).

5.1.2. Limitations:

There are a number of limitations associated with tephra dispersal and deposition. Firstly, ash fall does not always take place immediately after eruption. If highly vesicular pumice is produced, it can float for days or even years (Wolff-Boenisch 2004:4843). Some tephra (e.g. the Mazama ash in the Columbia Basin) is thought to have blown around for thousands of years before final deposition (Davis 2005). Although short time lags are often insignificant when considering archaeological and palaeoenvironmental timescales, greater lags can have severe implications for the use of tephra as a chronological marker.

Another limitation results from the fact that tephra is rarely distributed evenly. This occurs on both an inter- and intra-site level and can complicate or prevent tephra recovery and correlation. Volcanic deposition patterns appear to be affected by eruption mechanics, transport and depositional mechanisms (Cas and Wright 1987:478). Although deposition in proximal areas is influenced largely by eruption mechanics, deposition at distal sites may be influenced by local effects such as strong aeolian activity or snow cover (Bergman *et al*. 2004). Langdon and Barber (2004) hypothesise that deposition in distal areas is predominantly controlled by precipitation patterns. In

their view, deposition only occurs with wet fall-out, even though ash cloud distribution is controlled by other atmospheric dynamics. This has implications for tephra deposition in areas with strong seasonal differences in rainfall patterns (e.g. tropical areas with marked wet and dry seasons).

Hall and Pilcher (2002:225) emphasise the need for in-depth studies on the processes which carry tephra to distal sites. The confirmation of Icelandic Hekla 4 tephra in British deposits, for instance, indicates a pattern of ash dispersal that is much more complex than is shown on most isopach maps (*ibid.*). The recent nuclear fall-out resulting from the Chernobyl disaster also illustrates the patchiness of aerosol fall-out (Pilcher 2002:3), and our poor understanding of the mechanisms of aeolian tephra distribution and deposition. Furthermore, the number of ash layers and the abundance of volcanic ash at proximal and distal sites do not appear to be in simple relationships (Hall and Pilcher 2002:225). At proximal sites where volcanoes exist in close proximity, volcanic deposits will often overlap, complicating identification of single eruptions (Cas and Wright 1987:478). At distal sites with very few microtephras, not all areas receive tephra. Accordingly, distal sites must be chosen carefully to avoid misunderstandings regarding the extent of tephra dispersal and their potential for microtephrochronology.

The uneven distribution of tephra also occurs on an intra-site basis. Principally, tephra deposition rates are likely to be lowest in forested land and highest in open areas (cf.

Tauber 1967 re: pollen). The uneven distribution of tephra is exacerbated at archaeological sites, where ancient architectural constructions are present. Figure 5.1.2-1. is a schematic representation of wind flow streamlines around buildings:

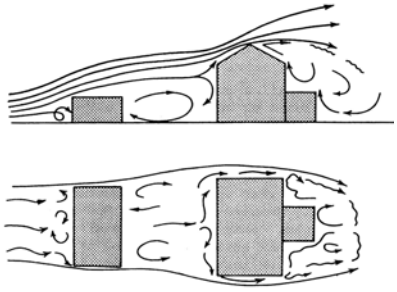

Figure 5.1.2-1. Schematic windflow streamlines around buildings (Blong 1981:412)

Blong (1981:413) suggests that tephra would drop out of the wind flow in turbulent wakes with no strong flow in any one direction, whereas surfaces will be swept clear if wind flow streamlines are adjacent to the ground or roof. Tephra drifts should be minimal on hill-tops and abundant on the sheltered sides of hills, depressions and cuts and within courtyards (*ibid.*). Although Blong's work centres on contemporary proximal sites and large ash falls, it is useful to consider these patterns of wind movement when studying distal archaeological sites containing microtephra. Figure 5.1.2-2. (left) also represents proximal sites receiving large ash falls, but is of some use for our understanding of how tephra may be distributed at distal archaeological sites, and therefore what areas should be chosen for sampling.

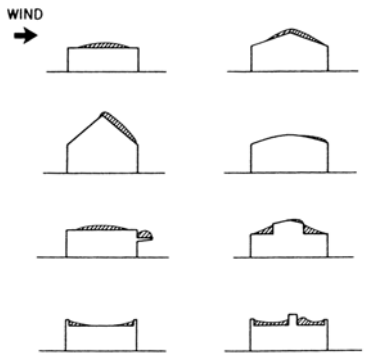

Figure 5.1.2-2. Distribution of tephra loads on a variety of roof styles (Blong 1981:415)

Lake cores are often analysed to provide master chronological sequences of volcanic eruptions and tephra fall-outs against which other sequences can be compared (e.g. two Central American lake cores were analysed in this study to provide points of comparison for archaeological samples). However, the deposition of tephra is also inconsistent in lakes. Boygle (1999) identified incomplete blanketing of tephra in a

proximal Icelandic lake, whilst Pyne-O'Donnell identified similar intra-basin variability in a distal Scottish lake (Blockley pers. comm.).

In other words, local depositional mechanisms, site locations and stratigraphic contexts must be considered in greater detail if we are to maximise tephra recovery and increase our chances of developing successful microtephrochronology. At terrestrial archaeological sites, this means a consideration for the location of buildings and past vegetation, whilst in lake contexts a greater effort must be made to understand basin basymetry and catchment dynamics (see Lane 2004:38-39;50).

5.2. THE PROBLEM OF REWORKING:

Following deposition, various mixing processes act on tephra unless it is rapidly buried by younger sediment (Westgate and Gorton 1981:91). At terrestrial (sub-aerial) sites, important processes include soil-forming processes, creep, frost activity, bioturbation, and reworking by wind and running water (*ibid.*). In sub-aqueous depositional environments, mixing processes include bioturbation, erosion, and resedimentation due to lake level changes, inflow variations, slumping and associated turbidity flows (*ibid.*).

It seems appropriate to consider pollen reworking as a proxy for microtephra in terrestrial soil contexts. A poor understanding of the ways in which pollen is incorporated into soils has resulted in considerable debate concerning the interpretation of soil pollen assemblages and the relationship between depth and time (Keatinge 1983:1). The principal mode of incorporation is thought to be earthworm mixing (Darwin 1881; Havinga 1968), whilst downwashing of pollen grains through the soil

has been suggested as a secondary mechanism of minor importance (Keatinge 1983). Earthworms mix soil by ingesting soil during feeding and ejecting it elsewhere during burrowing activities (*ibid.*:8). Pierce (1978) notes that the largest mineral particle found in the crop and gizzard of selected earthworm species in Wales was c.1mm. Accordingly, both pollen and microtephra could be ingested by earthworms (unless the texture of glass shards affects the ability of earthworms to ingest and transport them), whilst larger particles such as stones and artefacts would settle down through a soil containing active burrowing earthworms and concentrate at a depth where earthworm activity declined (Keatinge 1983).

Earthworm species differ in the depth of soil they occupy and hence the depth to which pollen, microtephra, stones and artefacts are moved. Edwards and Lofty (1977 in *ibid.*:8-9) and Nordström and Rundgren (1973 in *ibid.*) suggest three main groupings of earthworms based on depth of burrowing activity. These include surface feeding, intermediate, and deep-burrowing species. An important consequence of activity by different types of earthworm is that the depth of pollen or tephra in a soil profile is related to earthworm ecology and not necessarily to time (as would be the case in pollen diagrams from lake sediments and peat bogs). Consequently it may be inappropriate to use microtephra particles from archaeological soil profiles as reliable chronological markers.

In contrast to earthworm activity, which leads to mixing of small particles within a certain depth range and movement of larger particles to greater depths, glacio-tectonic processes can act to expose ancient strata and relocate tephra to a stratigraphic position much younger than the intrinsic age of the tephra (e.g. tephra-bearing sediments in the

western Canadian plains, see Westgate and Gorton 1981:91). Although there is no threat of glacial activity in tropical Central America, the Canadian example serves to illustrate that local stratigraphic controls must be carefully examined to safeguard against serious errors in interpretation (Westgate and Gorton 1981:91).

In addition to natural site formation processes, cultural formation processes (ancient and modern human activity) are likely to accelerate the reworking of tephra at archaeological sites. It is likely, for example, that the ancient Maya swept away tephra (or swept it aside to use as ceramic temper) after it had fallen on plastered buildings or plaza floors. Rain would then complete this process by washing away any remaining tephra. Loose dry material can rest on steep slopes, but loose water-saturated material is likely to wash away (Hall 1996:52), in which case redeposited tephra would accumulate in low-lying depressions only. This raises some important questions. Can tephrochronology really be applied to occupied urban centres, or can it only be applied to abandoned sites and those in which human modification of the landscape is minimal? What locations are most suitable for sampling? And how can we ever be sure that microtephra accumulations represent primary deposits?

Identification and correlation of tephra deposits is obviously hindered by this reworking. When analysing visible tephra layers, reworking can be detected by a) the presence of non-volcanic sediment and mineral assemblage, b) the separation of phenocrysts from the vitric component, c) abnormal bed thickness or grain-size given distance from source, and d) diffuse boundaries to the bed (Westgate and Gorton 1981:91). Unfortunately, reworked distal microtephra layers cannot be identified using these criteria. Proximal tephra beds may in some cases escape full reworking because of their

thickness, but thin distal beds are likely to be lost as discrete units (*ibid.*). The susceptibility of microtephra to reworking suggests the need for multiple stratigraphic controls and a greater understanding of depositional context.

5.3. DEPOSITION OF TEPHRA AT SITES ANALYSED FOR THIS STUDY:

The highland Guatemalan ash samples from Lake Amatitlan were intended to provide a reference chronology and geochemical database for Guatemalan eruptions. Proximal tephra from nearby volcanoes was known to have accumulated in the lake and was identified in samples analysed for this study.

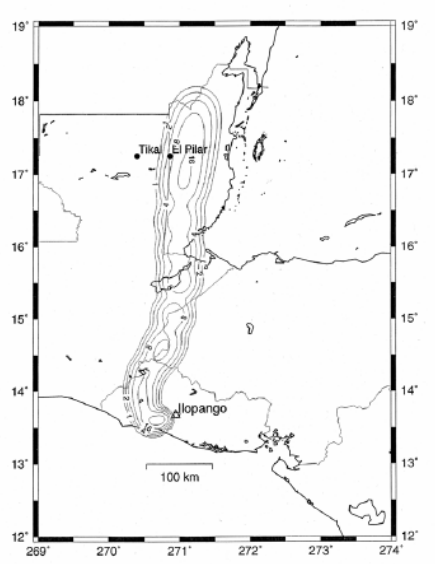

Figure 5.3-1. Hypothetical distribution of ash fall for the Maya lowlands using eruption parameters for the 1st millennium AD eruption of Ilopango, El Salvador (from Ford; generated by Hurst)

The distal lowland Belizean core from Lamanai Lake was intended to act as a reference chronology against which archaeological samples from the same region could be compared. Based on windflow diagrams (fig. 5.3-1.) and distance from source volcanoes in Guatemala, El Salvador and Mexico, it was assumed that ash fall would have covered the lake at various points in the past. Patterns of high level winds compiled from radiosonde records indicate that ash from Guatemala will travel in a northeasterly to easterly direction (towards the lowlands) in the dry season between December to April, but will travel in a westerly direction for eruptions during the wet season between May to November (see fig. 5.3-2.; Ford and Rose 1995:154).

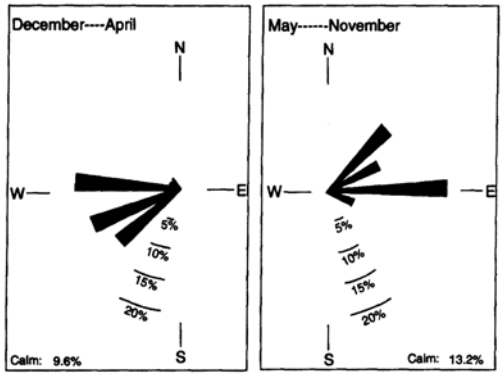

Figure 5.3-2. Wind rose diagram showing predominant winds aloft at altitudes between 10000 and 50000 ft at Guatemala City (Ford and Rose 1995:155)

The distal lowland Belizean archaeological sites (Lamanai, Medicinal Trail and Yalbac) were expected to have microtephra, not only because of their location but also because eyewitness reports indicate that ash fall covered towns, villages and archaeological sites in the area (including Lamanai) following the 1982 eruption of El Chichon, Mexico (e.g. Graham pers. comm.). As shown in chapter 4, microtephras were identified at Lamanai and Medicinal Trail but not in the plaster layers of Yalbac.

5.3.1. Problems of reworking at sites chosen for this study:

As expected, tephra was identified throughout the Guatemalan sequence but very few microtephras were identified in the Belizean samples. Furthermore, tephra was concentrated in the top 0-20cm of sequences and were generally absent below this. This absence of tephra can be attributed to a number of factors, including lack of eruptions, depositional mechanisms, chemical disintegration, and reworking. The likelihood of reworking and soil erosion is extremely high in tropical soils, which are continually leached and suffer the continual loss of soluble elements (Eden 1964:7-8).

In tropical areas, many of the soil formations are of great antiquity (Eden 1964:97). The processes of tropical weathering which result in the widely distributed kaolinoid soils also produce a relatively water-stable residual soil (*ibid.*:102). However, the partial percolation of silt-laden run-off through a fertile soil clogs the pore spaces, and causes

the fine particles to filter out and form a layer which impedes normal percolation (*ibid.*:105). Consequently the top inch or two of soil rapidly becomes saturated and will continually be lost as run-off (*ibid.*). This phenomenon appears to be the most serious cause of soil erosion and tropical regions and is likely to account for the loss of small particles such as tephra.

6. GEOCHEMISTRY

Major element geochemical analysis of individual glass shards is usually the only means by which microtephra layers can be characterised and correlated. Glass shards are formed during the rapid cooling of magma and are seldom products of crystal accumulation or contamination, and are consequently thought to best represent magma composition (Barker 1983; Hall 1996:120-121). Unfortunately there are a number of limitations associated with geochemical analysis of tephra. These limitations primarily hinder on: a) the chemical variation of tephra with each eruption, b) methods of geochemical analysis (principally electron microprobe analysis) and c) the chemical alteration and stability of tephra.

6.1. CHEMICAL VARIATION OF TEPHRA WITH EACH ERUPTION:

6.1.1. Principles:

Chemical 'fingerprinting' of tephra in many parts of the world is based on the premise that volcanic activity occurs along distinct volcanic fissure systems and on central volcanoes (collectively termed volcanic systems), and that each system has chemical characteristics which can be exploited to identify its products (Larsen 1981:96). In most cases, the products of each system are chemically distinct from those of other systems (*ibid.*), whilst some volcanoes (e.g. Hekla in Iceland) produce distinct products from different eruptions (Hall and Pilcher 2002:228).

6.1.2. Chemical variation of tephras in Central America:

Since the formation of the soma crater around 0.3 million years ago, El Chichón volcano (in the CVA) has erupted juvenile trachyandesitic products of essentially the same major element chemical composition (Rose *et al*. 1984 in Espíndola *et al*. 2000:99). Consequently, it is likely to be near-impossible to assign dates to tephra layers that have been identified as originating from El Chichón, unless stratigraphical controls are in place.

In Guatemala and El Salvador, a variety of techniques have been used to characterise volcanic deposits. These include standard field and petrographic observations (stratigraphic data, thickness, grain size, lithic content, mineralogy), geochemical analysis (particularly trace elements in bulk samples), and quantitative mineralogical analysis of hornblende and Fe-Ti oxides (Rose *et al*. 1981:19304). Rose *et al*. (1981:209) indicate that glass compositions, as determined by microprobe, are insufficiently distinct when dealing with so many similar units. Although volcanic deposits from highland Guatemala and El Salvador can be readily distinguished from those of other provinces, considerable effort is required to distinguish among local units (Rose *et al*. 1981:193).

6.1.3. Limitations:

It is important to emphasise that not all tephra layers are separable using precise major element geochemistry. For example, the Icelandic Hekla AD 1947 and AD 1510 tephras are very similar to one another but distinct from Hekla 1 (2310 BC) and Hekla

5 (5990 BC), which are again very similar to one another (Hall and Pilcher 2002: 228). Likewise, many South American eruptions share the same chemistry and cannot be distinguished on the basis of their geochemical signatures (Pilcher 2002:2). Even when there are differences in chemical composition of eruptions from the same volcanic system, the differences are often so small that they are easily obscured unless samples are subjected to identical preparation protocols and analysed in the same batch (Larsen 1981:101). To resolve these issues, proximal tephra layers with similar geochemistries are often separated on stratigraphic grounds (Hall and Pilcher 2002:228), but this is inherently more complicated for distal samples where very few shards represent each eruption.

Another problem arises with glass layers of variable composition or multiple origin (e.g. the OMH-185 layer from three Irish sites studied by Hall and Pilcher 2002). Since some deposits contain variable shard geochemistries, large numbers of single shard analyses are necessary to provide adequate identification (Hall and Pilcher 2002:228).

6.2. METHODS OF GEOCHEMICAL ANALYSIS:

Geochemical analysis of tephra can be broadly divided into two types: the analysis of individual grains and the analysis of bulk separates. Electron microprobes can be used to establish major element geochemistry of individual glass shards, whilst X-ray fluorescence (XRF) and neutron activation analysis (NAA) have been used to establish minor and trace element geochemistry of bulk tephra (Westgate and Gorton 1981:73). Grain-discrete methods of analysis have the advantage of being sensitive to contamination effects and inhomogeneities, and generally take priority over methods

that require use of bulk separates (*ibid.*). Bulk tephra analysis often suffers from the presence of inclusions, microlites, foreign particles, weathering products, and in some cases the occurrence of detrital glass reworked from older tephra (Westgate and Gorton 1981:77). Bulk tephra is also subject to fractionation during transport and deposition (e.g. composition varies with distance from source) and can therefore be unsuitable for geochemical correlation (*ibid.*). In microtephra studies, samples collected are often too small for bulk chemical analysis and focus is therefore placed on single-grain analysis of glass shards.

6.2.1. Principles of electron microprobe analysis:

The electron microprobe has greatly facilitated the use of chemical composition of tephras as a tool in tephrochronology (Larsen 1981:96). Scanning electron microscopy (SEM) can be used to determine chemical composition for small sample masses relatively quickly and efficiently. Volcanic glass and minerals can be analysed separately, and shard size can be as small as a few microns in diameter (*ibid.*). Microprobes generate and accelerate electrons before focusing an intense electron beam (usually 10μm diameter) onto a small sample in an evacuated chamber. Interactions of the incident beam with the nucleus of the component atoms of the sample results in backscattered electrons (Goodhew *et al*. 2001; Potts *et al*. 1995). The number of backscattered electrons varies with atomic number of the sample atoms (*ibid.*). Thus, elements with heavier atomic mass scatter more electrons and appear brightest in the SEM backscatter electron image (BSE).

Depending on the model, electron microprobes can carry out two forms of analysis:

wavelength dispersive analysis (WDA) and energy dispersive analysis (EDA). WDA can differentiate between x-rays of similar energy more accurately than EDA (Goodhew *et al*. 2001; Potts *et al*. 1995). A series of crystals are used to sequentially diffract x-rays characteristic of individual elements towards the detector, thus providing geochemical information (*ibid.*). EDA uses a solid state Si-Li detector; the x-rays generated by the interaction of the incidental electrons with the sample produces a current proportional to the energy of the x-rays (*ibid.*). Unfortunately x-rays of similar energies produce similar peaks which are difficult to resolve. Some attempts have been made to characterise volcanic glass by EDA (e.g. Dwyer 1995 in Hall and Pilcher 2002), but generally acceptable precision is not achieved. Consequently WDA is preferable over EDA for geochemical analysis of tephra (Hall and Pilcher 2002). The advantage of EDA, however, is that it is more commonly available, simpler, and the spectrum containing information on the elements can be obtained very quickly (*ibid.*).

6.2.2. Standard procedures of electron microprobe analysis:

Once tephra has been identified in sediment cores, levels containing peak glass shard concentrations are extracted again (as outlined in chapter 4) for geochemical analysis. Samples are mounted in resin on glass slides, metal stubs or resin blocks and ground to expose tephra shards. Exposed shards are then polished to provide a flat surface for WDA analysis.

Hall and Pilcher (2002:224) comment that "finding sparse glass shards under optical microscope conditions is demanding but finding those same glass shards when attempting single shard electron microprobe analysis seems, initially, almost

impossible". They suggest using stage coordinates of the light microscope to record the position of individual shards selected for geochemical analyses and then find these same shards using the stage coordinates of the electron microprobe, saving expensive machine time. However, this is not routinely carried out at all laboratories.

Normally nine major element oxides are measured sequentially using WDA analysis. Since sodium (and to a lesser extent potassium) in the glass is often driven out by the heat from the electron beam, sodium measurements are generally undertaken as the first and last in each series to detect sodium mobilisation. This is critical because sodium is an important diagnostic element in volcanic glass. Some researchers (e.g. Pilcher 2002:2) also suggest de-focusing the beam to about 8μm to reduce heating and hence sodium mobilisation.

6.2.3. Procedures of electron microprobe analysis employed in this study:

In this study, EDA was carried out on material extracted from the top 10cm of the Lamanai Unit 1 core to resolve a dispute concerning the morphology of Central American microtephra (see chapter 4). Although EDA cannot provide precise quantitative data to distinguish between different tephras, it is possible to achieve sufficient resolution to determine the general identity of beamed particles. This also provided an opportunity to scan the sample for other pyroclastic material (see appendix C). Extracted samples were mounted on small adhesive stubs and coated with a thin layer of carbon before EDA.

All other microprobe analyses involved WDA on single glass shards. The top 20cm of

the Medicinal Trail core was sub-sampled again at 4cm resolution and extracted. Dried samples from the top 0-4 cm and 4-8cm were sprinkled onto 25mm diameter resin blocks and covered in a layer of SPECIFEX epoxy resin. When the resin had set, the preparation was ground using water and SiC Grinding Paper of Grit P 1200 followed by Grit P 2500 until the tephra was exposed at the surface. The stubs were polished using TEXMET 1000 cloths with 9 and 3μm diamond polishing compound (diamond paste and metadi fluid), followed by MASTERTEX cloths with 1 and 0.25μm diamond polishing compound until the exposed tephra surfaces were smooth and flat. Prior to microprobe analysis, a thin layer of carbon was applied to the blocks under vacuum in a carbon coater.

Analyses of Lake Amatitlan samples were carried out on the Cameca SU30 scanning electron microprobe at the RLAHA, Oxford University, and the Medicinal Trail samples carried out on the JEOL JXA 8800R scanning electron microprobe at Begbroke Science Park, Oxford University. Tephra shards were first located under backscattered imagery. At the RLAHA, nine major element oxides were measured sequentially with WDA using stoichiometric quantitative analysis with 1 WD spectrometer, 15KeV accelerating voltage, 10nA electron beam current, a beam size of 10μm, and a counting time of 10s for the measurement of each element. At Begbroke, 4 WD spectrometers were used, each with two analysing crystals. Counter dead time was corrected for and ZAF correction was also applied for the effects of atomic number (Z), x-ray absorption (A) and secondary fluorescence (F), following Sweatman and Long (1969).

In this study, the microprobe beam was not de-focused to 8μm to reduce heating and

sodium mobilisation. Sodium measurements were, however, undertaken as the first in each series to prevent misidentification resulting from sodium mobilisation.

The microprobe was calibrated using the Lipari CB obsidian secondary standard (following the protocol suggested by Hunt and Hill 1996 and verified by the UK tephrochronology community) at the RLAHA and Begbroke and NIST 612 at Begbroke. Since most samples in this study had low major element totals, some totals below 95% were included (contrary to Dugmore *et al*. 1995) but are considered provisional values only.

6.2.4. Correlating tephras analysed in this study:

6.2.4.1. The Amatitlan reference core:

Samples from the Amatitlan core containing glass were subjected to WDA (fig. 6.2.4.1-1.). Although the integrity of the sequence is unknown, it is thought that the tephra accumulations represent a series of highland Guatemalan eruptions.

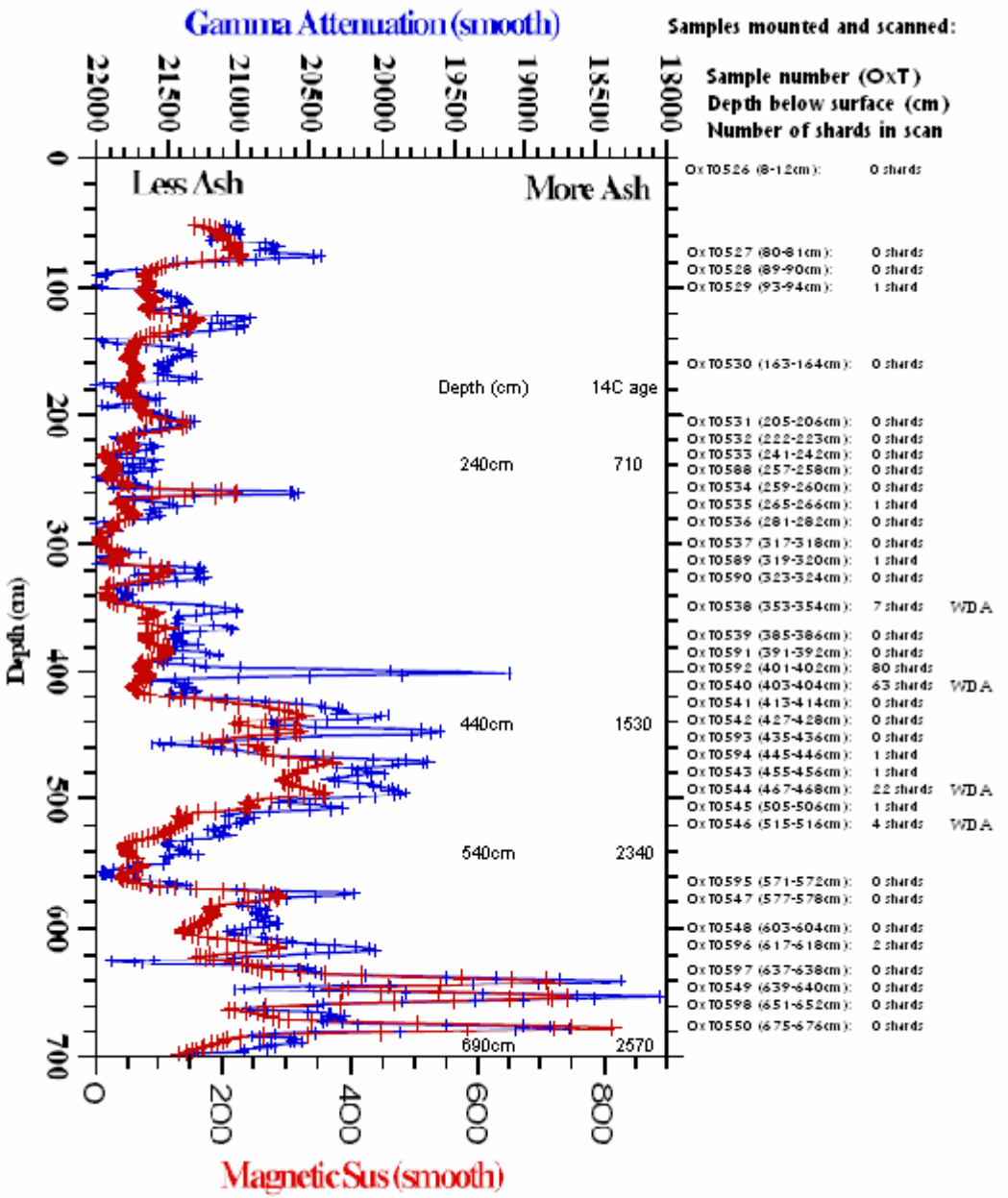

Figure 6.2.4.1-1. Amatitlan magnetic susceptibility, gamma attenuation and radiocarbon data (provided by Curtis) to the left; samples mounted in resin and scanned for tephra at the RLAHA indicated on the right. Samples marked 'WDA' were probed. Radiocarbon dates appear to be uncalibrated and lack error bars; they should therefore be viewed with caution

Assessing the integrity of data prior to interpretation:

Data with major element totals below 95% or above 100% are usually discarded (Dugmore *et al*. 1995). There are some instances, however, where data with low totals are reliable; for example the presence of water (incorporated at the time of magma

eruption and glass formation) results in low totals without significantly affecting major element compositions. Given the small sample numbers in this study and the arbitrariness of the 95% cutoff, it was hoped that data with low totals could provisionally be included in data interpretation.

Major element totals (%) were plotted against SiO_2 to assess the reliability of data with low totals:

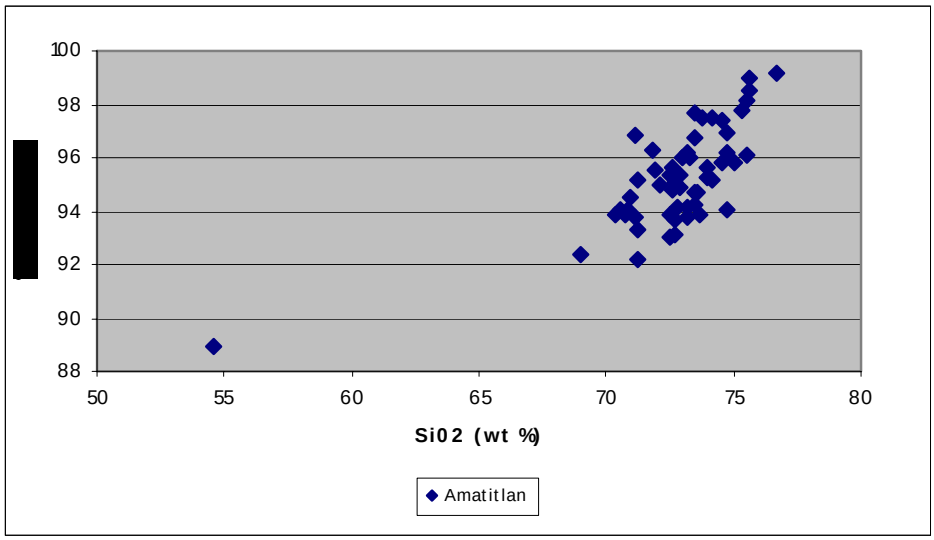

Figure 6.2.4.1-2. Percent total vs SiO_2 for Amatitlan data; a single anomaly identified

A single anomalous point (88.955% total) was identified and discarded from further plots. However, the linear relationship between % total and SiO_2 suggest that the remainder of the data is satisfactory, and that a 95% cutoff would result in the loss of seemingly good data.

Discriminating between eruptions using major element geochemistry:

Plots of total alkali (Na_2O + K_2O) against SiO_2 (TAS plots) usually provide a good means of discriminating between tephras. A TAS plot was first produced for standards

(Lipari 1 and NIST 612) analysed in this study to assess the reliability and comparability of the two probes (at the RLAHA and Begbroke):

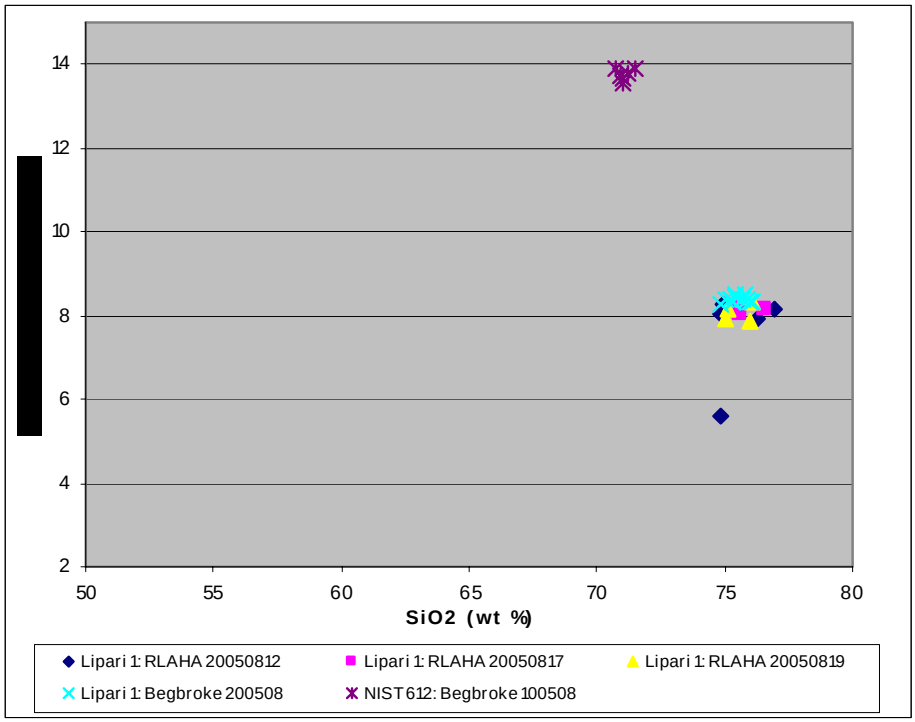

Figure 6.2.4.1-3. TAS plot of Lipari 1 and NIST 612 standards (excluding first few points per run and points with focus errors)

The same scale was used above as for subsequent data plots (see figs. 6.2.4.1-4.a-c.). Geochemical data from the two probes appears to be comparable based on Lipari 1 standards, although there is one anomalous point (hit #12 20050812; see appendix B.).

Since it is unconventional to include data with low totals, another attempt was made to assess the reliability of data prior to data interpretation. To this end, TAS plots were produced using all data including totals below 95% (fig. 6.2.4.1-4.a.), excluding totals below 95% (fig. 6.2.4.1-4.b.) and including totals below 95% with the exception of the single anomalous point (fig. 6.2.4.1-4.c.):

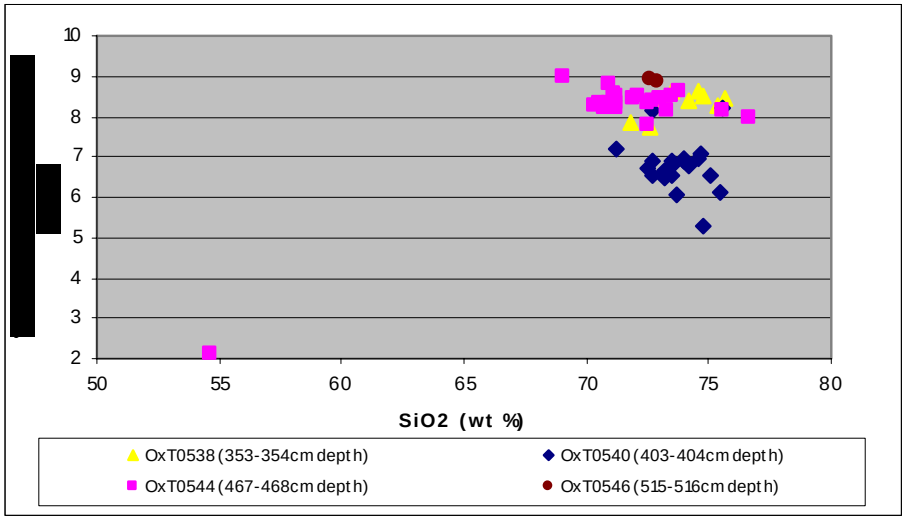

Figure 6.2.4.1-4.a. TAS plots of Amatitlan data (including totals below 95%)

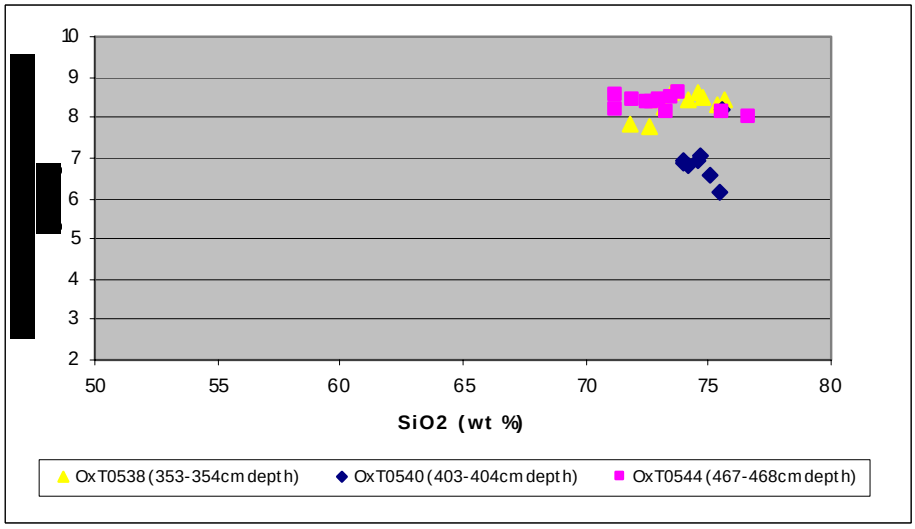

Figure 6.2.4.1-4.b. TAS plots of Amatitlan data (excluding totals below 95%)

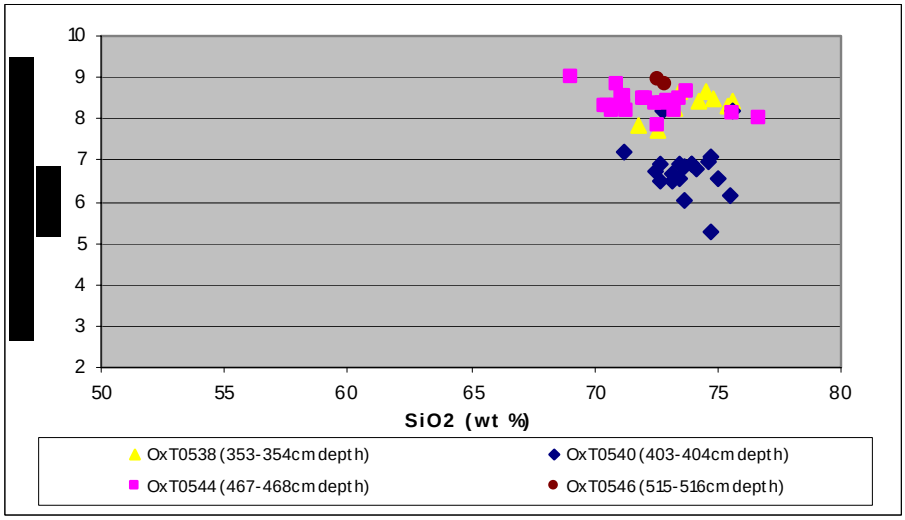

Figure 6.2.4.1-4.c. TAS plots of Amatitlan data (including totals below 95% except anomaly)

The sample with 88.955% total (54.601 SiO_2) was clearly anomalous, whilst all other data with totals below 95% served to increase sample size without distorting the picture. It was therefore decided that subsequent plots would include all data except the sample with an anomalously low total (88.955%).

In TAS plots, tephras from sample OxT0540 are clearly distinct from the other three samples. The two tephras from sample OxT0546 also appear at the periphery, but this could be an artefact of small sample size. OxT0538 and OxT0544 tephras overlap considerably despite the presence of an intervening tephra layer (OxT0540) and vertical separation that exceeds a metre. Although OxT0538 and OxT0544 tephras are indistinguishable on the basis of TAS plots, they can be separated in this instance on stratigraphic grounds.

A series of other plots were produced to assess whether tephras from the four samples (and especially OxT0538 and OxT0544) could be clearly distinguished from one another:

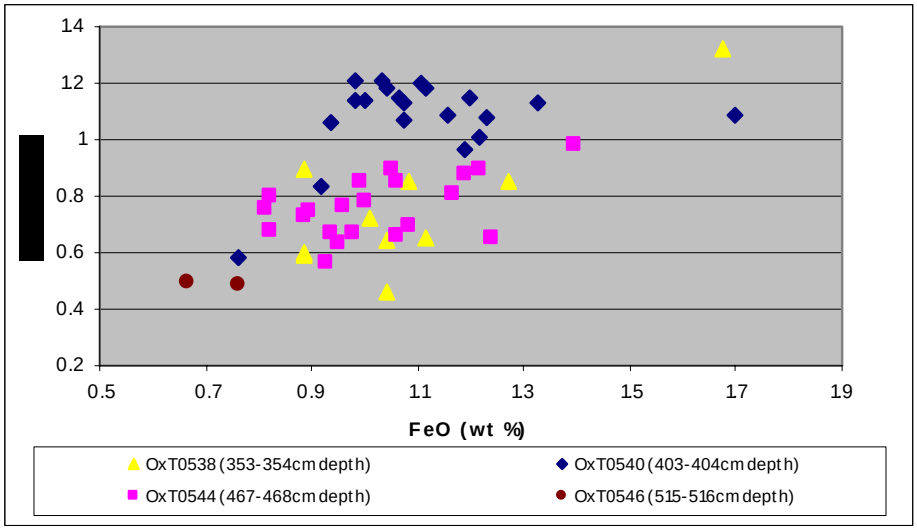

Figure 6.2.4.1-5. CaO vs FeO for Amatitlan data (including totals below 95% except anomaly)

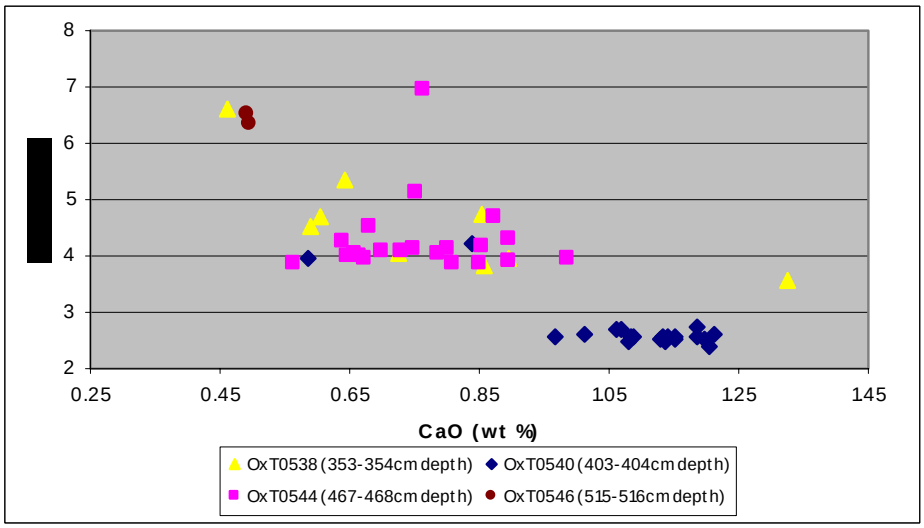

Figure 6.2.4.1-6. K_2O vs CaO for Amatitlan data (including totals below 95% except anomaly)

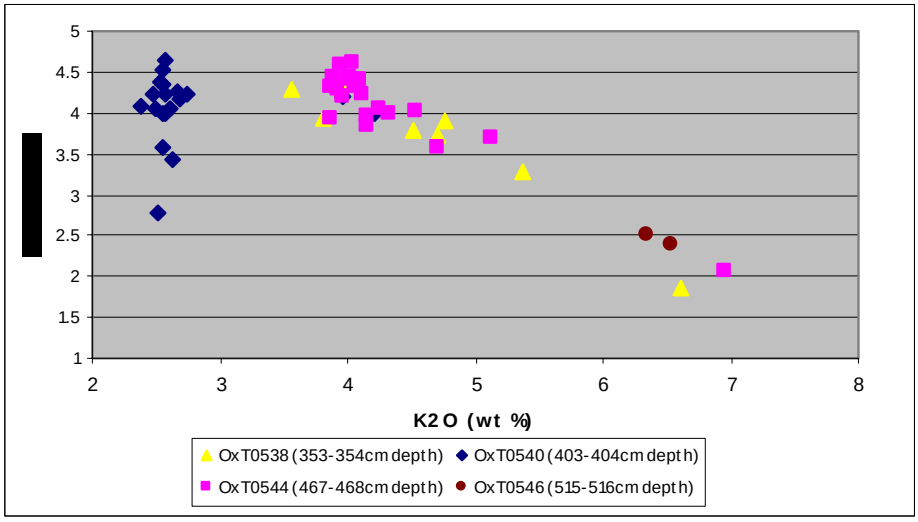

Figure 6.2.4.1-7. Na_2O vs K_2O for Amatitlan data (including totals below 95% except anomaly)

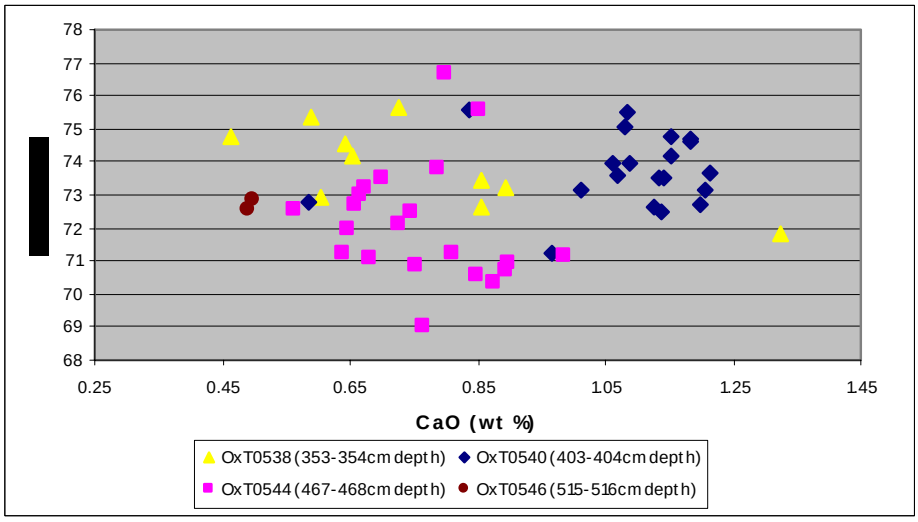

Figure 6.2.4.1-8. SiO_2 vs CaO for Amatitlan data (including totals below 95% except anomaly)

All plots succeed in distinguishing OxT0540 tephras from the remaining three samples. The two OxT0546 tephras have very similar major element chemical compositions to one another and constantly appear at the periphery of OxT0538 and OxT0544 tephra plots. A larger sample size would indicate whether OxT0546 tephras are distinct from OxT0538 and OxT0544 tephras, but this cannot be confidently ascertained here. None of the plots succeed in separating OxT0538 and OxT0544, with the possible exception of the plots of SiO_2 against CaO. It will certainly be a difficult task to assign dates to

archaeological sequences if distal microtephras have comparable geochemical compositions to tephras of OxT0538 or OxT0544; indeed, these may be just two of many eruptions with similar geochemical compositions.

Clearly there are several factors that limit the use of the Amatitlan sequence as a reference chronology and geochemical database. Firstly, the core was initially sampled for diatom analysis rather than tephrochronological analysis (Ford pers. comm.). 1cm sub-samples were sieved using 250μm mesh and anything below 250μm was discarded (Curtis pers. comm.). Unfortunately this extraction protocol is likely to have resulted in a greater representation of volcanic minerals rather than glass particles. Furthermore, heavy liquid density separation was not carried out on these samples to separate glass from minerals; this is recommended for future analyses, as it will result in greater efficiency when scanning mounted slides prior to WDA. Due to time constraints, only 35 samples (each representing 1cm depth from the 701cm Amatitlan core) were mounted in resin and scanned for glass shards; these samples were chosen based on magnetic susceptibility peaks and physical appearance of particles (see fig. 6.2.4.1-1. earlier). Ideally, the entire sequence would be systematically mounted and scanned if the core is to be used as an exhaustive database with tephras representing multiple eruption events. Since the Amatitlan caldera is known to have produced a complex tephra sequence (Rose *et al*. 1981:205), it may nevertheless be difficult to establish a reliable chronology of eruptions and database of tephra chemical compositions using the Amatitlan core.

6.2.4.2. Correlating distal microtephras from archaeological samples with tephras of known composition throughout Central America and Mexico:

Only one sample (representing the top 4cm of the Medicinal Trail archaeological sequence) yielded enough tephras of adequate size (each with 10μm of flat non-vesicular surface) for WDA analysis (appendix B). Unfortunately comparison between the various Belizean samples was therefore impossible, and the start of a lowland Maya tephrochronology and tephrostratigraphy could not be established.

The Medicinal Trail tephras were plotted against reference data on glass shards from the TVB, CVA and the Amatitlan and Ilopango calderas. Unfortunately the reference database is not exhaustive, with over-representation of the TVB (despite it being furthest from the lowland Maya area), under-representation of the CVA, and non-representation of the TVC and CAVA. The decision to only include data resulting from WDA of single glass shards resulted in the exclusion of a large amount of data on bulk samples and mineral fractions. The newly generated Amatitlan data play a small part in a much bigger reference database. All reference data represent single shards except the Salvadorean and Honduran samples which are mean averages (hence the single standard deviation shown where possible).

Assessing integrity of data prior to data interpretation:

As with the Amatitlan samples, % totals were plotted against SiO_2 to assess whether data with low totals should be discarded from data interpretation:

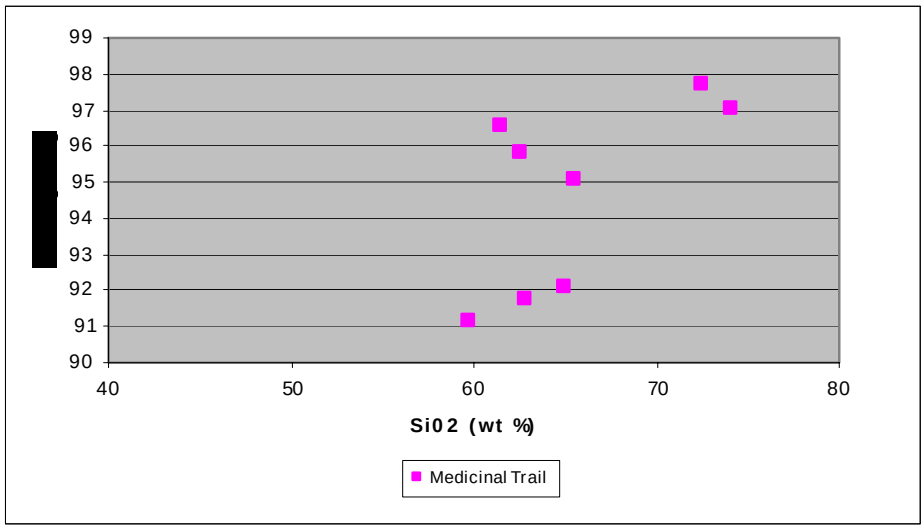

Figure 6.2.4.2-1.a. Percent total vs SiO_2 for Medicinal Trail data

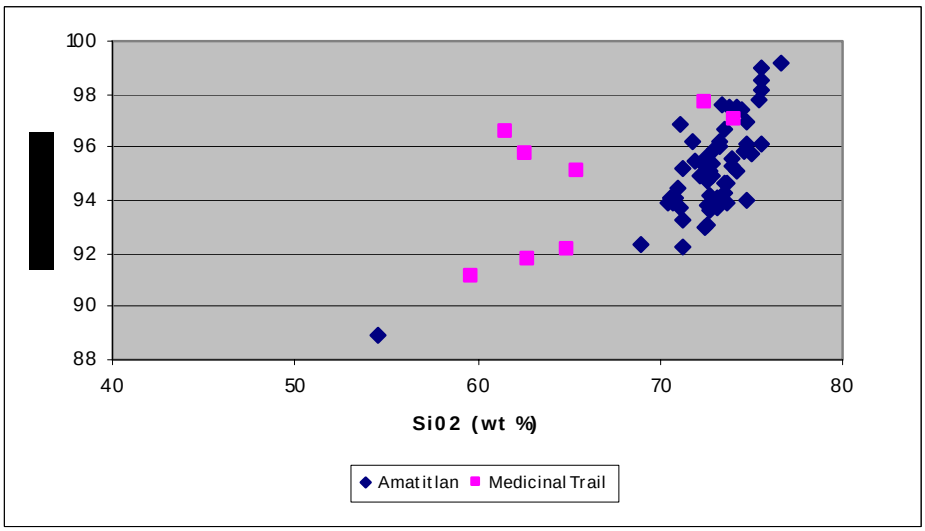

Figure 6.2.4.2-1.b. Percent total vs SiO_2 for Medicinal Trail and Amatitlan data (identifies a single anomaly for Amatitlan but less systematic for Medicinal Trail)

It was unclear from the above plots whether low totals indicated unreliable data. Medicinal Trail samples are certainly less uniform in their ratio of % total against SiO_2 than were Amatitlan data. All samples have been included in subsequent plots but should be viewed with caution.

Discriminating between eruptions using major element geochemistry:

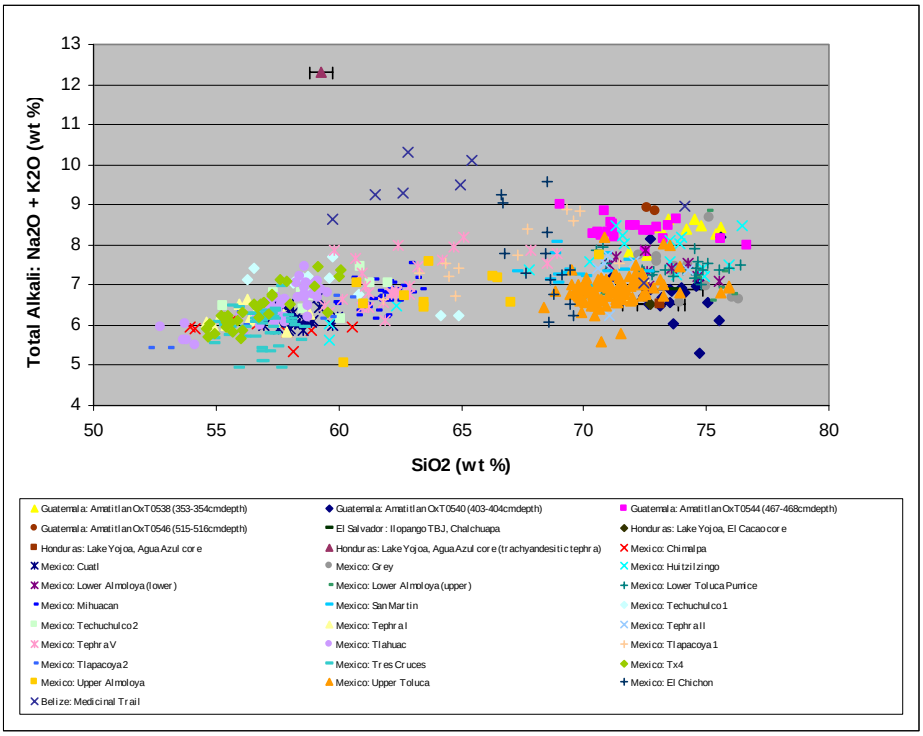

Figure 6.2.4.2-2. TAS plots of Central American tephra data (excluding totals below 95% for published; including totals below 95% for new data except anomaly).
(Data from *Tephrabase* and Mehringer *et al.* 2005)

The Amatitlan tephras have a high SiO_2 content (i.e. they are rhyolitic) but overlap with some TVB tephras, which cover the full SiO_2 range (i.e. rhyolitic, andesitic and basaltic). Interestingly, tephras from the Medicinal Trail site do not appear to resemble any of the reference database samples and stand out as having high total alkali ratios with intermediate SiO_2 content. In other words, they cannot be correlated with the El Chichón tephra, the Amatitlan tephra, or the TVB tephras. The other plots (figs. 6.2.4.2-4 through to 6.2.4.2-7) also show the Medicinal Trail tephras as distinct from the reference database. This would suggest that a) tephras from the Medicinal Trail site are chemically altered or b) the reference database is inadequate. If the tephras were chemically altered, we would generally expect a lower rather than higher total alkali ratio. Tephras can, however, alter to produce similar chemical compositions as the above archaeological samples if subjected to extremely alkaline conditions (pH>9). In

such cases, SiO_2 leaches out of the glass matrix, whilst alkalis can sometimes linger (Pollard pers. comm.). Although the lowland Maya area is highly calcareous, it nevertheless seems unlikely that terrestrial soil deposits should have pH values that exceed 9. If, on the other hand, the difference in chemical compositions between Medicinal Trail microtephra and reference data results from an incomplete reference database, it is possible that microtephras at the Medicinal Trail site originated from the andesitic cones of the CAVA (volcanic front; see fig. 6.2.4.2-3). These were not represented in the reference database, since most geochemical data on CAVA tephras were produced from bulk samples. Additionally, it may be necessary to look at tephra compositions outside Central America and Mexico, since the stark difference in tephra compositions hints that microtephras analysed in this study may have originated from an entirely different volcanic system. In all cases, the geochemical data produced for this study negates the hypothesis that microtephras identified in samples from Belizean sites resulted from the 1982 eruption of El Chichón, since it is unlikely that differences in laboratory preparation and probe procedures can account for such a difference in geochemical compositions.

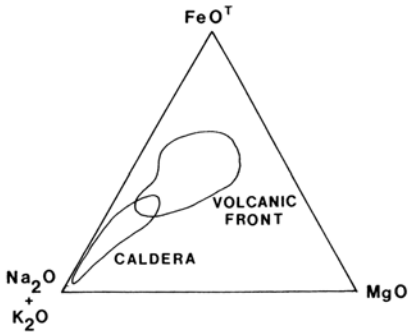

Figure 6.2.4.2-3. Alkali-Iron-Magnesium (AFI) plot showing generalised fields of composition for caldera and volcanic front rocks. NB data is likely to have been generated from bulk analyses (Rose et al. 1981:199)

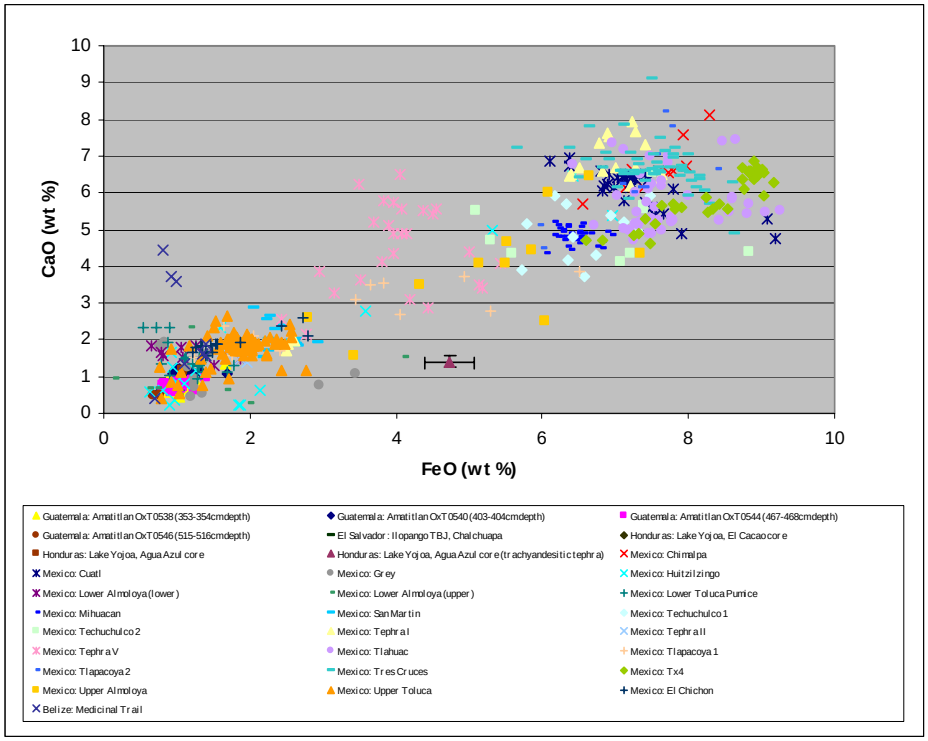

Figure 6.2.4.2-4. CaO vs FeO of Central American tephra data (excluding totals below 95% for published; including totals below 95% for new data except anomaly)
(Data from *Tephrabase* and Mehringer *et al.* 2005)

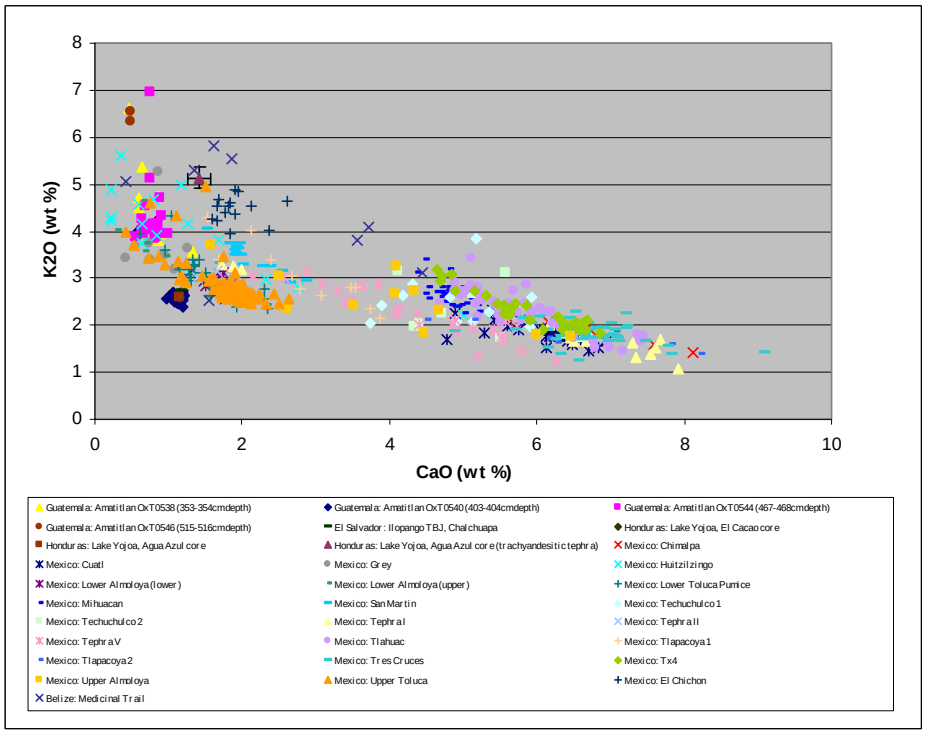

Figure 6.2.4.2-5. K_2O vs CaO of Central American tephra data (excluding totals below 95% for published; including totals below 95% for new data except anomaly)
(Data from *Tephrabase* and Mehringer *et al.* 2005)

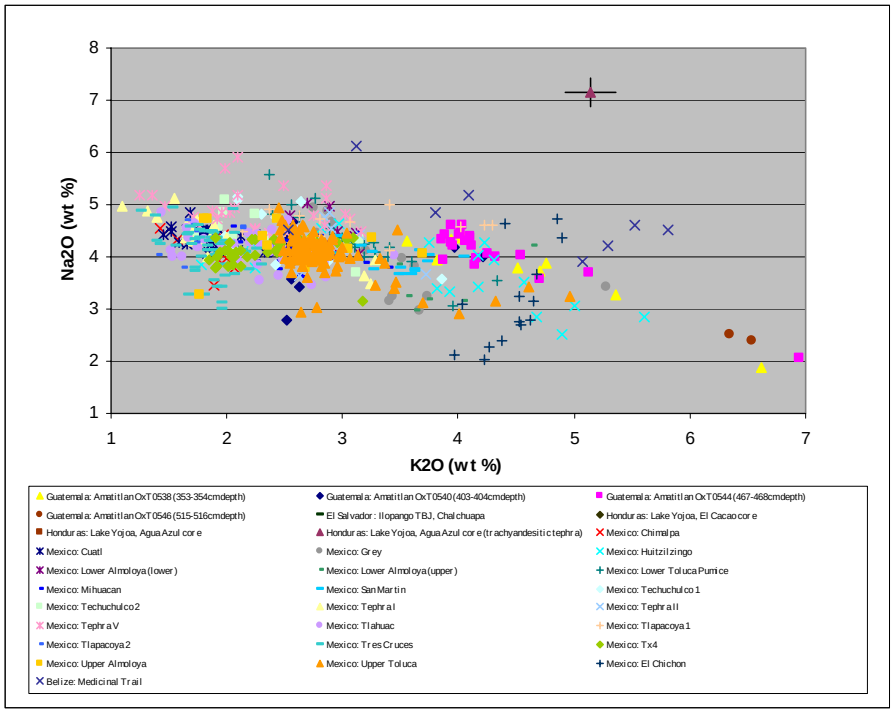

Figure 6.2.4.2-6. Na_2O vs K_2O of Central American tephra data (excluding totals below 95% for published; including totals below 95% for new data except anomaly)
(Data from *Tephrabase* and Mehringer *et al.* 2005)

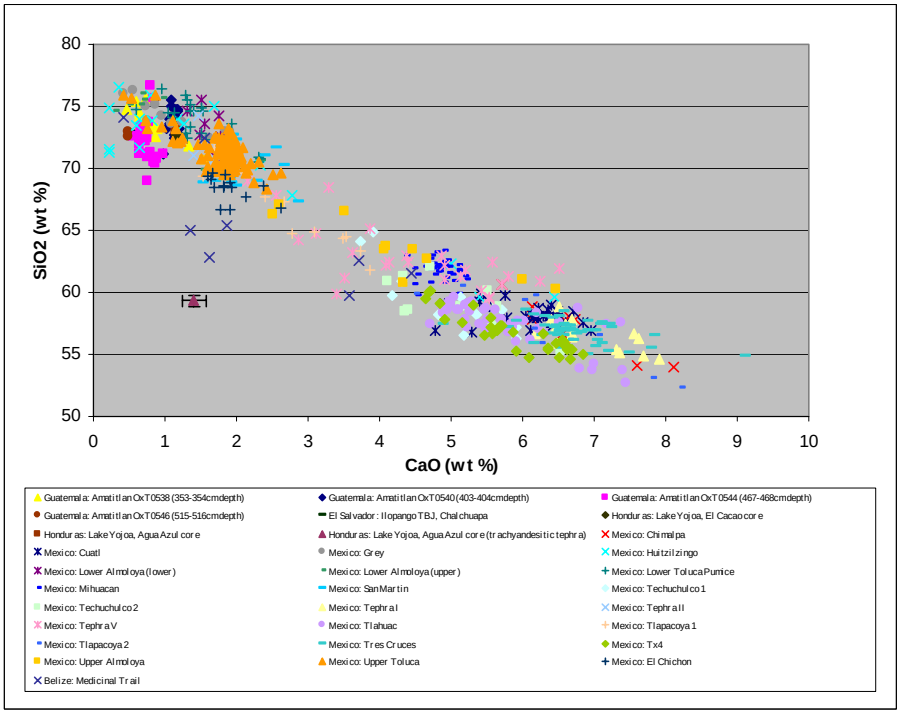

Figure 6.2.4.2-7. SiO_2 vs CaO of Central American tephra data (excluding totals below 95% for published; including totals below 95% for new data except anomaly)
(Data from *Tephrabase* and Mehringer *et al.* 2005)

6.2.5. Limitations of WDA:

Tephrochronology relies heavily on the ability of microprobes to produce precise and accurate geochemical data, so that newly generated data can be compared against existing data. An inter-laboratory comparison programme conducted in 1991-1992 suggested, however, that a number of laboratories generate geochemical data that is inadequate for distinguishing between tephras and may in some cases lead to faulty correlation (Hunt and Hill 1996). Complicating factors include the phenomena of sodium mobilisation and sodium gain, as well instrumental problems and differences in correction, standardisation and analytical procedures (*ibid.*). Consequently, the Lipari obsidian has been widely implemented as a secondary standard to monitor the precision and reproducibility of microprobe analyses of tephra.

There are other sources of error. A recent study has suggested that reducing microprobe beam size (to analyse thin glass walls and/or to reduce sodium mobilisation) can distort geochemical data and create analytical differences that generate inappropriate tephrochronological fingerprints (Hunt and Hill 2001). The presence of small crystalline inclusions in tephra can also distort geochemical fingerprints, such that anomalously elevated alumina values must be viewed with caution (Hunt and Hill 2001:114).

Finally, problems can arise with statistical analysis of geochemical data. Electron microprobe analysis of tephra shards generates large amounts of geochemical data that are expected to fall into distinctive groups (associated with each eruptive centre or eruption). Since geochemical differences can be small, rigorous statistical methods of

assessment (e.g. standard deviation, similarity coefficients and cluster analysis) must be used rather than relying solely on simple graphical methods (Westgate and Gorton 1981:89-90). Unfortunately there is an inherent statistical problem associated with microtephra analysis. Shards analysed from distal deposits are often few in number (exacerbated still further by sample loss during grinding and polishing of sample stubs) and do not always result in statistically significant datasets. Indeed, low shard recovery has prevented successful geochemical analysis of tephras at Sluggan Bog, N. Ireland (Lowe *et al*. 2004), Sweden (Bergman *et al*. 2004), Scotland (Turney *et al*. 1997), and elsewhere. Likewise, the small tephra counts in several of the Belizean samples analysed for this study precluded statistically dependable geochemical analysis. Pilcher (2002:2) suggests that most scholars analyse somewhere between 10 and 20 individual tephra fragments; anything below this raises the question of repeatability.

6.3. CHEMICAL STABILITY AND ALTERATION OF TEPHRA:

As discussed in chapter 4, the geochemical composition of glass shards must remain unaltered by laboratory procedures and/or natural processes if reliable correlation of tephra layers is to take place. Volcanic glass is, however, thermodynamically unstable (with a poorly ordered internal structure of loosely linked SiO_4 tetrahedra) and is consequently prone to chemical degradation in the post-depositional environment (Fisher and Schminke 1984:312).

Whilst breakdown of glass in the absence of water is extremely slow, contact between glass and hot aqueous solutions greatly accelerates both hydration and dissolution rates (Fisher and Schminke 1984:329). The predominant mechanism of aqueous attack in

mildly basic to acidic environments (pH <9) is ionic exchange between hydronium ions (H_3O^+) from solution and non-framework cations from the 'terminal structure' of alkali ions (i.e. those associated with non-bridging oxygen sites) at the glass surface (Pollard and Heron 1996). This leads to the formation of a leached surface gel layer enriched in network forming cations, which eventually undergoes hydrolysis (Wolff-Boenisch 2004:4844). It appears that the durability of vitreous material depends on the degree to which this inert Si gel layer, typically ca 20μm in thickness, forms on the surface of the glass shard (Blockley *et al*. 2005). The durability of glass can also be affected by organic compounds, which control the release and transport of solutes by complexing Al and Fe and causing low pH values (Antweiler and Drever 1983 in Fisher and Schminke 1984:313).

In more basic media (pH >9), the main process of tephra alteration is network dissolution. This involves hydroxyl ions in solution disrupting the siloxane bonds in the glass surface, ultimately leading to glass dissolution (Pollard *et al*. 2004). The resulting non-bridging oxygen terminals can dissociate other water molecules producing excess hydroxyls (*ibid.*). In some cases these hydroxyls accumulate in the corrosion layer and increase the pH, accelerating network dissolution and stripping cations. Once the local pH has exceeded 9, the Si network begins to break up and silicon is removed into solution as $Si(OH)_4$, leading ultimately to the complete dissolution of the glass Si network (*ibid.*). At conditions where dissolution rates are controlled by the detachment of atoms from surfaces, these rates are believed to be proportional to the aqueous solution-surface interfacial area (Wolff-Boenisch *et al*. 2004:4851).

In practice, both processes (cationic leaching from the matrix and complete destruction

of the silica network) occur together at different rates, controlled by local pH, glass surface area, temperature, bacteria, inhibitory-catalytic ion effects, aqueous transport, the degree of disequilibrium on natural glass dissolution kinetics, and glass composition (Pollard *et al*. 2004). If environment is held constant, the stability of vitreous material appears to be primarily a function of the chemical composition of glass, with the proportions of Si and Al determining molecular structure and durability (Blockley *et al*. 2005:2).

Hay (1963 in Fisher and Schminke 1984:330) recognised three overlapping stages of transition of silicic glasses: a) formation of clay (commonly montmorillonite) represented by the outer leached skin of shards or the more intensely altered fractures in perlite; b) partial to complete dissolution of glass shards; and c) precipitation of authigenic minerals, especially zeolite, in the new cavities and original pore space. A succession of alteration stages in glass of intermediate alkaline composition is shown in fig. 6.3-1.:

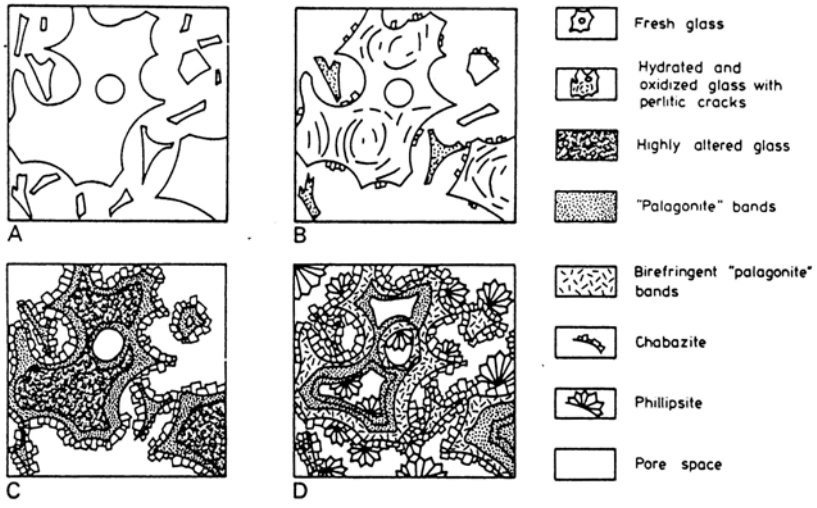

Figure 6.3-1. Sequence of three alteration stages (B to D) of tephritic phonolitic glass from the Pliocene Roque Nublo Formation, Gran Canaria (Fisher and Schminke 1984:330)

6.3.1. Theoretical stability modelling of Central American and Mexican tephras:

Theoretical stability calculations were undertaken on tephra from Central America and Mexico to assess the degree to which tephra analysed in this study was inherently prone to chemical degradation. The underlying assumption is that chemical composition should reflect the relative rate of chemical alteration or complete dissolution of tephras if burial environment is held constant. Following Pollard *et al*. (2003), several methods were used:

1. Numerous studies indicate that glass dissolution rates increase with decreasing Si content, and that corrosion resistance is therefore highest for rhyolitic glass (Wolff-Boenisch 2004:4854). Consequently, theoretical stability was calculated using the Si:O molar ratio, which is related to the number of non-bridging oxygens in the network structure. This assumes that silicon is the major network former in glass, and that the numerical ratio of silicon to oxygen atoms is therefore a measure of the stability of the network.

2. Using the Si:O ratio and an equation given by White and Minser (1984), the number of non-bridging oxygens (NBO) per silicon tetrahedral was calculated. The equation used here is based on the molar composition of the glass, where the oxide formula represents the mole fraction of each oxide:

$$NBO_{WM} = \frac{2(Na_2O + K_2O + CaO + MgO + FeO - Al_2O_3 - Fe_2O_3)}{(SiO_2 + 2(Al_2O_3) + 2(Fe_2O_3))}$$

It is therefore considered the most appropriate for calculating NBO for tephra (Pollard *et al*. 2003).

3. The potential for cationic exchange to occur in aqueous conditions (and hence the thermodynamic instability of glass) can be determined using Gibb's free energy of hydration (ΔGhyd). The change in free energy (combining the enthalpy and entropy of a system) during a reaction (ΔG) determines the spontaneity and direction of that reaction (Pollard *et al*. 2004). The value of ΔGhyd can be calculated as the sum of the hydration free energy (stabilities) of the major oxides weighted by their mole fraction in the glass (Paul 1982 in Pollard *et al*. 2003:386-7). It is worth noting that this calculation assumes alteration of tephra has occurred in a wet post-depositional environment.

The calculated values of Si:O, ΔGhyd and NBO provide a series of relative stability models (Pollard *et al*. 2003):

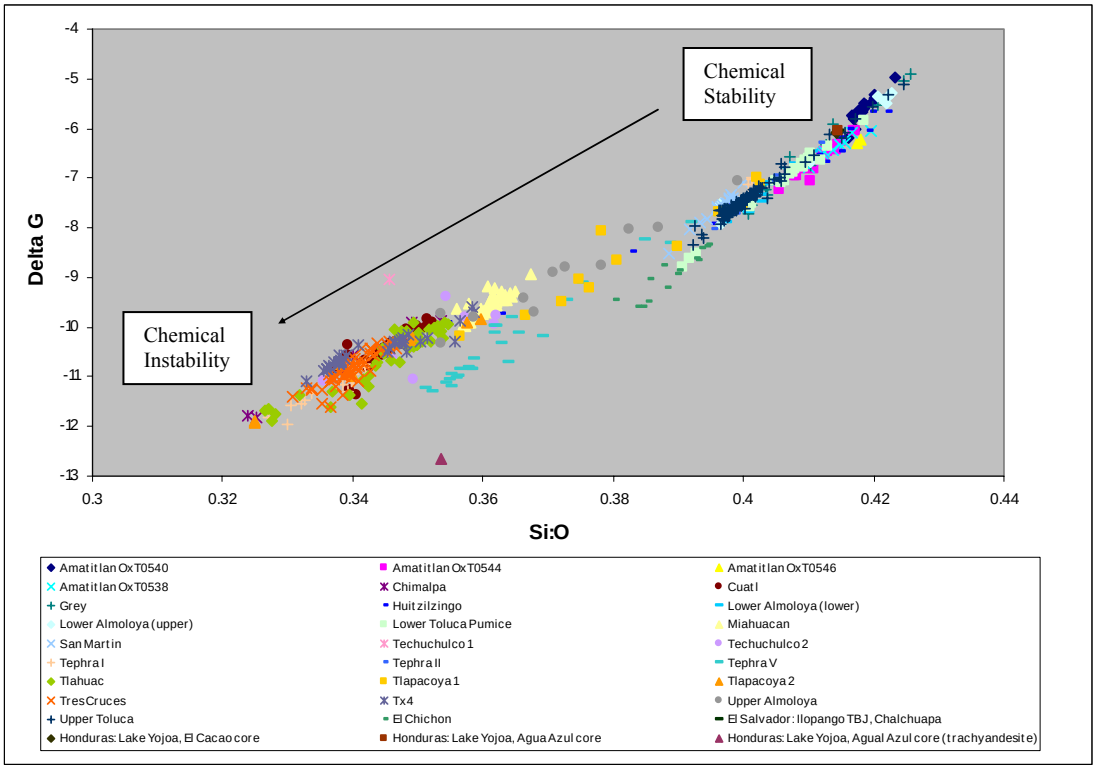

Figure 6.3.1-1. Delta G (ΔGhyd) vs Si:O ratio for Central American and Mexican data (Data from *Tephrabase* and Mehringer *et al.* 2005)

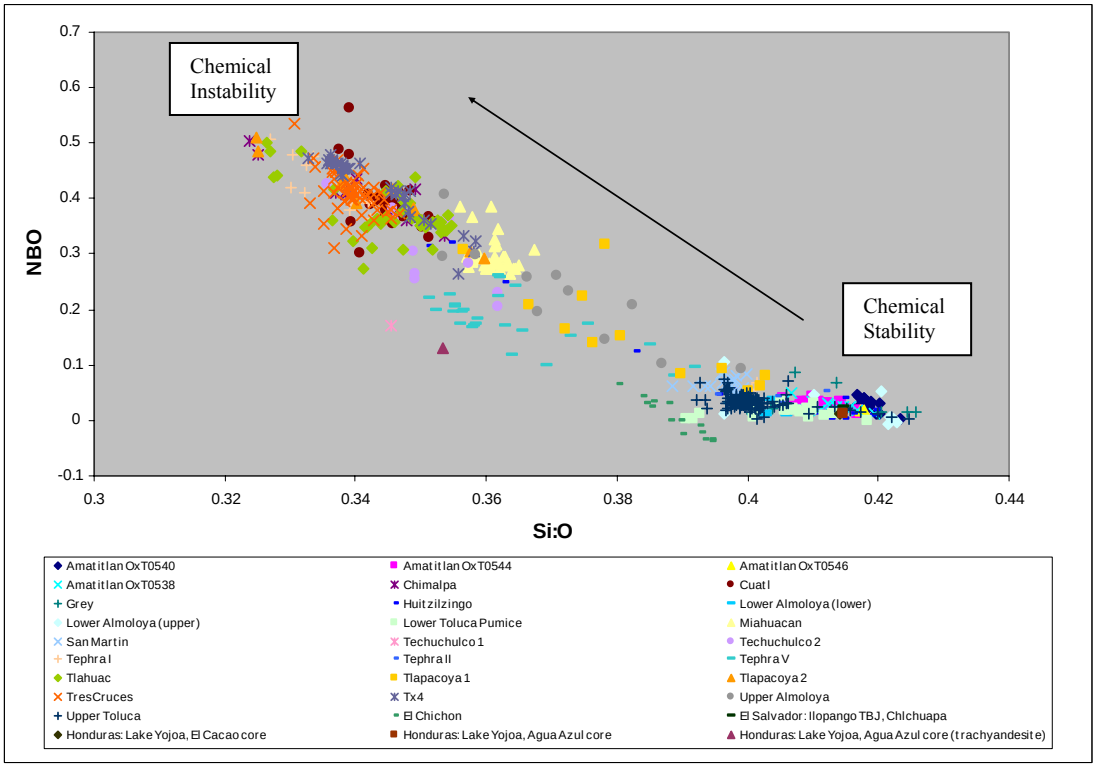

Figure 6.3.1-2. NBO (calculated using the White and Minser method) vs Si:O ratio for Central American and Mexican data (Data from *Tephrabase* and Mehringer *et al.* 2005)

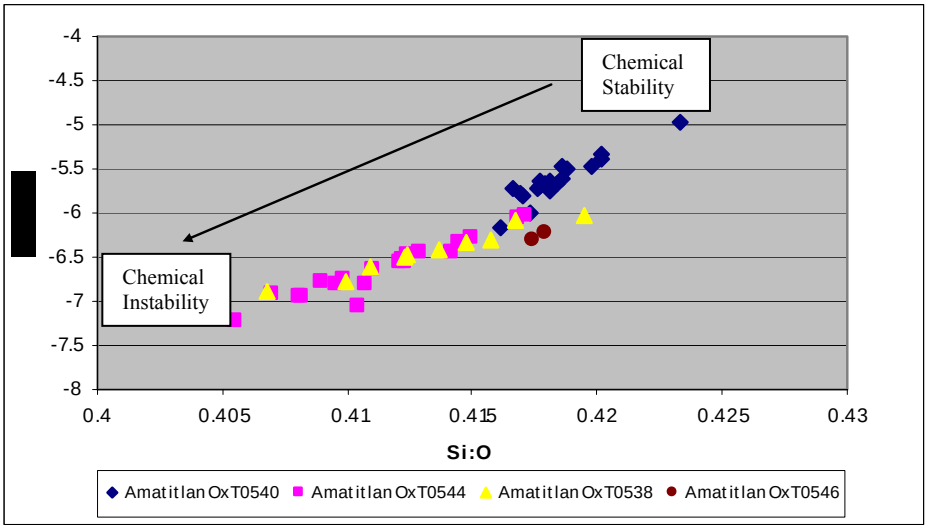

Figure 6.3.1-3. Delta G (ΔGhyd) vs Si:O ratio for Amatitlan data

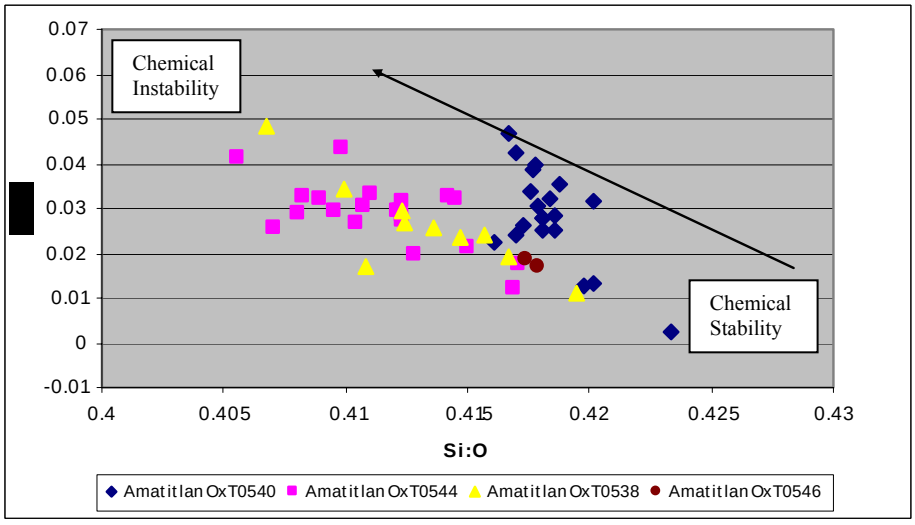

Figure 6.3.1-4. NBO (calculated using the White and Minser method) vs Si:O ratio for Amatitlan data

As with Pollard *et al*'s study (2003), there was a substantial correlation between the different indicators of chemical stability for tephra; samples with lower stability on one measure also showed low stability on all other indicators. The chemical stability calculations undertaken here indicate that Central American and Mexican tephras span a stability range similar to that of Icelandic tephras, with some tephras (e.g. Amatitlan OxT0540) exceeding the most stable of Icelandic tephras (see Pollard *et al*. 2003). The Amatitlan tephras all have high SiO_2 content and are consequently very stable; the TVB tephras range from highly stable to highly unstable (i.e. rhyolitic to basaltic); and the El

Chichon tephras are of intermediate to high stability. Within the Amatitlan samples, OxTO540 tephras are most stable.

Although we may expect the most stable tephras to dominate the archaeological record, even these are prone to alteration in harsh chemical environments. The lack of microtephra in samples from lowland Belize could result from vigorous chemical weathering as a result of humid tropical climate and high pH associated with carbonate limestone bedrock. Soil alkalinity is generally associated with soils that have high calcium and sodium content (Eden 1964:50). Since calcium is more readily removed from the soil exchange complex, the proportion of exchangeable sodium is augmented, leading to a decrease in soil permeability, accentuated salt accumulation, and runoff of the top layer of soil. Even in highland contexts, tephra degradation can occur; kaolinite (a degradation product of volcanic glass) was identified using backscatter imagery and EDA among Amatitlan OxT0544 tephras. Consequently, the likelihood of chemical degradation in lowland tropical soils is considerable. Since vesicular microtephras have large surface-to-volume ratios, they are also more prone to chemical degradation than are large proximal tephras.

6.3.2. Limitations of theoretical stability models:

The above indicators of chemical stability are directly derived from the major element compositions of tephra, and can therefore be undertaken on any geochemical datasets. This reliance on major element compositions is, however, problematic, since it ignores the possibility that some tephras degrade in the post-depositional environment prior to geochemical analysis and stability modelling. It should also be noted that the calculated

values of Si:O, ΔGhyd and NBO do not provide exact models because a) kinetic stability is not accounted for, and b) a number of empirical assumptions are made in the calculations (e.g. redox state of Fe and Mn ions, Pollard *et al*. 2003).

Wolff-Boenisch *et al*. (2004) use stability models to estimate lifetimes of tephras with different chemical compositions. They conclude that, with increasing Si content, estimated lifetimes increase exponentially and estimated nutrient release rates decrease; a 1mm basaltic glass sphere is thought to survive for 500 years at pH 4 and 25°C, whilst a 1mm rhyolitic glass sphere survives for 4500 years. Their estimated lifetimes do not, however, consider the effects of temperature or pH changes over time in the post-depositional environment, and consequently appear to disagree with true lifetimes in natural environments (*ibid.*).

To summarise, some tephras are inherently less stable than others in any given post-depositional environment. Samples with high Si:O ratios are generally stable, whilst samples with very low Si:O ratios have a high potential for solubility. Although eruption mechanics often limit the extent to which basaltic tephra shards are distributed, the difficulty in finding distal basaltic tephras may also result from their lower chemical stability and tendency to disintegrate. Although processes of geochemical alteration also affect proximal tephras, alteration of distal microtephras are likely to be more exaggerated as a result of high surface-to-volume ratios of microtephra particles. Humid and tropical conditions with high or low pH also encourage glass alteration, and may lead to misidentification, unrecognisable geochemistries, or even complete disappearance of tephras. From a glass durability perspective, however, dry soil deposits from temperate archaeological sites may be more likely to contain unaltered

tephra than aqueous lake and peat deposits.

6.4. SUMMARY:

Tephra beds in areas close to volcanic source vents are often identified and correlated using multiple criteria, including colour, bed thickness, grain size, degree of weathering, lithic content, mineralogical assemblage, sedimentary structures, distribution, and stratigraphic context (Westgate and Gorton 1981:77). However, major element compositions are often the only available means of identifying and correlating distal microtephras embedded in non-volcanic sedimentary sequences (*ibid.*). This form of correlation based on geochemical data alone raises problems, because a) not all eruptions produce tephras that have distinct chemical compositions, b) tephra is prone to alteration in some post-depositional environments, and c) errors can arise during microprobe analysis. Furthermore, there is limited value in determining major element chemistries of glass shards unless a robust reference database containing type material has been established; without this, it is impossible to relate chemical compositions of shards to eruptions of known relative or absolute date.

7. DISCUSSION

The preceding chapters suggest a bleak outlook for microtephrochronology at archaeological sites. Indeed, attention has been drawn to several critical limitations, including the inadequacy of current laboratory procedures, complications resulting from site formation processes, and problems associated with geochemical analysis. Clearly, these limitations must be at the forefront of research when attempting to establish a reliable framework for future microtephrochronological analysis. This chapter discusses methods of improving microtephrochronology as a geoarchaeological dating technique, and also suggests alternative archaeological applications of microtephra analysis.

7.1. IMPROVING LABORATORY PROCEDURES:

Limitations of current microtephra extraction and identification protocols have been outlined in chapter 4. In short, attempts to extract and identify microtephras from Belizean sites illustrated a) the unsuitability of current laboratory procedures and b) the grave consequences of inappropriate knowledge when identifying tephra. In the former case, standard sampling strategies (e.g. scans of 10cm depth sub-samples followed by 1cm depth sub-samples) were shown to be highly inappropriate for archaeological soil sequences, despite their apparent suitability for palaeoenvironmental lake and peat deposits. These inadequacies can, however, be addressed; laboratory protocols can be tailored in such a way that they are suitable for archaeological soil sequences. In practical terms, this might involve replacing initial scans of 10cm depth sub-samples with 5cm depth sub-samples, or ensuring that the quantity of sample processed is

proportional to the number of centimetres (height) represented in a sub-sample. This might resolve the current tendency for tephras to be under-represented in 10cm depth sub-samples compared to sub-samples representing less depth (e.g. 1cm). Another modification might involve discarding 1cm sub-samples since they provide a misleading level of precision for deposits that are inherently prone to reworking. In any case, archaeologists must recognise that microtephrochronology is still in its infancy, and considerable methodological improvements must be made prior to successful application. The necessary methodological changes should not, however, be difficult to implement.

7.2. ADDITIONAL METHODS OF GEOCHEMICAL ANALYSIS:

As discussed in chapter 6, there are several fundamental limitations resulting from the reliance on major element geochemistries to characterise and correlate tephra layers. Although trace element compositions are thought to facilitate tephra differentiation more satisfactorily than major element compositions alone, it had previously not been possible to apply traditional techniques of trace element determination (e.g. XRF and NAA) to single glass shards due to low trace element concentrations. The recent application of laser ablation inductively coupled mass spectrometry (LA-ICP-MS) to proximal single glass shards (e.g. Pearce *et al*. 1999; Pearce *et al*. 2002) does, however, raise the possibility that trace element compositions of microtephras can be determined in the near future. Secondary ion mass spectrometry (SIMS) may also be a suitable technique for determining trace element compositions. This would certainly lend greater credence to microtephrochronology in areas where major element compositions of individual eruptions are not unique.

Although it may soon be possible to analyse trace element compositions of microtephras, there are currently several limitations with LA-ICP-MS for this purpose. Firstly, standard microtephra laboratory procedures involve extraction of shards ranging in size from 25 to 80μm, whilst Pearce *et al*. (2002) analyse shards greater than 150μm using LA-ICP-MS. The authors do, however, suggest the possibility of applying LA-ICP-MS to shards as small as 40μm, in which case some microtephras may be analysable. Secondly, the potential for contaminant materials to be included in LA-ICP-MS analyses is greater than for WD microprobe analysis, since the ICP-MS laser beam often penetrates below the glassy surface of a shard into small inclusions or phenocryst phases (*ibid.*:549). This problem is likely to be accentuated with small microtephras. Finally, the value of trace element analysis is limited in any given instance unless it has been routinely adopted by all tephrochronologists and microtephrochronologists. Hence we return to the problem of inadequate reference chronologies and geochemical data, which currently hinders correlation of tephra layers and may account in part for the inability to relate tephras analysed in this study to their source. Nevertheless, recent technological advances (e.g. the development and refinement of LA-ICP-MS and SIMS) present opportunities for improved characterisation and correlation of microtephra layers.

7.3. EXPLORING THE SUITABILITY OF DIFFERENT SITE-TYPES AND CONDITIONS:

Since laboratory procedures and geochemical characterisation of tephras have the potential for improvement, the fundamental limitation of microtephrochronology lies

with site formation processes and the tendency for soil reworking (chapter 5). In other words, efforts must be made to find archaeological sequences where reworking is a) minimal or b) can be identified and accounted for. Dating these sequences is, however, of little value unless specific archaeological questions are targeted and addressed.

7.3.1. Open-air sites: waterlogged, peat and soil deposits:

The unsuitability of soil deposits for microtephrochronology has already been discussed in chapter 5. Waterlogged and peat deposits, on the other hand, have been given little attention in this study, despite their greater suitability for microtephra analysis. Indeed, much of the pioneering palaeoenvironmental work on microtephrochronology was undertaken on peat deposits (e.g. Turney *et al*. 1997; Hall and Piclher 2002) due to their slow accumulation and lack of sediment-mixing organisms. However, since very few human settlements occur in peat, the archaeological application of microtephrochronology is limited. Some exceptions include the Somerset Levels in England and the Magdalenian site of Schussenquelle in south-west Germany, both of which show evidence of past human/hominin settlement (Dimbleby 1985:37-39). Furthermore, bogs and peats appear to have held ritual significance in many past societies, functioning as sanctuaries or sites for ritual offerings (e.g. Taylor 2002:163). Consequently, it may be possible to use microtephrochronology to assign dates to peat sequences containing archaeological artefacts, and hence date some past human activities. However, the acidic nature of peat deposits has a tendency to alter the chemical composition of tephras, hindering geochemical characterisation and correlation (e.g. Pollard *et al*. 2004).

7.3.2. Sheltered sites: caves and rockshelters:

Palaeolithic archaeologists and palaeontologists seldom investigate open-air sites, since evidence of early hominin activity is frequently concentrated in caves and rockshelters. These naturally sheltered sites also provide a wealth of information on the activities of more recent archaeological societies worldwide (e.g. Hole and Heizer 1965). Thus, it seems necessary to explore the applicability of microtephrochronology to cave and rockshelter deposits.

Caves are formed by groundwater solution and can run underground for hundreds of kilometres. By contrast, rockshelters are formed by mechanical weathering processes and often do not penetrate far into solid rock (Dimbleby 1985:125). Cave and rockshelter deposits can differ from one another as a result of these differences in origin and structure; caves accumulate solution residues, whilst rockshelters accumulate substantial deposits derived from mechanical weathering of roofs and walls, as well as dust and other airborne detritus blown in from outside (*ibid.*). In reality, this distinction is less clear-cut, and cave deposits often contain substantial fallen rock debris, whilst their entrances contain airborne detritus similar to those at rockshelter sites.

Once again, pollen movement and reworking provides a useful analogy for microtephra dispersal and disturbance. Van Campo and Leroi-Gourhan (1956 in Dimbleby 1985) used exposed slides covered with glycerine jelly to explore ways in which modern pollen reached different parts of a cave system. They observed that pollen could normally only be traced up to about 10 metres from the cave entrance, but greater

distances if the cave had a through draught or collapsed roof, or if pollen was brought into caves by flowing water or seepage. Although they suggest that pollen analysis of cave sequences should not be dismissed, the complications are clearly apparent. Furthermore, some areas of caves accumulate deposits rapidly, whilst other areas essentially lack stratified deposits (pers. obs.). In all cases, the frequency of pollen is very low, hindering the reliability of subsequent analyses. These factors would, no doubt, prevent the successful application of microtephrochronology to cave deposits, though rockshelters and cave entrances may be more viable locales.

7.3.3. Social organisation and human activity: hunter-gatherers and urban societies:

Some attempts have been made in the preceding paragraphs to identify types of deposit suitable for microtephrochronology. Since we are concerned with the study of archaeological sites, it also seems necessary to consider the variety of imprints which different types of society (e.g. hunter-gatherer and urban societies) will leave in archaeological deposits. Simply put, hunter-gatherers with transitory settlements may leave few overt marks in the archaeological record, whilst large urban societies may radically alter their landscape and leave behind monumental buildings and considerable evidence of human activity. In the former case, animal bones or stone tools may be neatly covered by an ash fall and remain undisturbed by future human activity, whilst in the latter case building construction may involve considerable cultural modification and disturbance of deposits containing evidence of past human activity. Consequently, microtephrochronology may be far more appropriate for the study of hunter-gatherer societies rather than large urban centres, unless construction history and the integrity of

archaeological sequences can be confidently elucidated at the latter. This is, of course, an over-simplification.

7.3.4. Micromorphological analysis:

Micromorphology is defined as 'the branch of soil science that is concerned with the description, interpretation and, to an increasing extent, the measurement of components, features and fabrics in soils at a microscopic level' (Bullock *et al*. 1985). The micromorphological analysis of intact sequences of deposits in resin-impregnated thin sections allows high-resolution contextual analysis of taphonomy and depositional relationships between sediments, artefacts and biological remains (Matthews *et al*. 1997:281). Consequently, close collaboration between microtephrochronology and micromorphology may resolve some of the current and fundamental limitations of microtephrochronology and enable analysis of a greater range of deposits, including reworked soils. Indeed, in many ways the archaeological application of microtephrochronology *cannot* be considered reliable unless parallel micromorphological studies are carried out. In order to collect intact sediment or soil sequences which facilitate both micromorphological and microtephrochronological analysis, it seems sensible to use a 'kubiena box' (fig. 7.3.4-1.) rather than half-drainpipes. This would also enable the microtephrochronologist to sample multiple adjacent sections (within the area of the box) if variation in lateral deposition was deemed problematic.

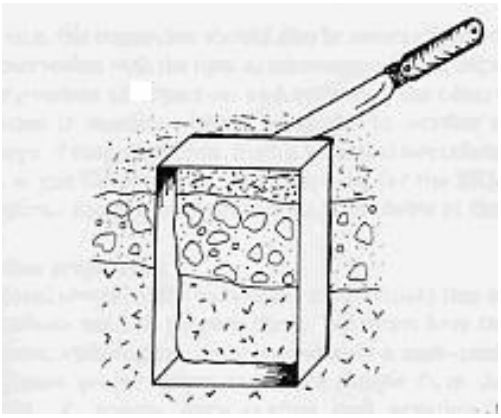

Figure 7.3.4-1. Tin 'kubiena box' used by micromorphologists to collect intact samples from vertical profiles (Courty *et al.* 1989:43)

7.4. ALTERNATIVE ARCHAEOLOGICAL APPLICATIONS:

7.4.1. Refining ceramic typologies:

Despite the current inadequacies of microtephrochronology as a dating and correlation technique, microtephras may nevertheless contribute to archaeological dating, albeit with cruder resolution. Although microtephras are prone to reworking in archaeological soil sequences, they are sometimes preserved intact as ceramic temper (e.g. Arnold 1985, Ford and Rose 1995 and Shephard 1956 for Classic Maya ceramics; Druc 2000 for contemporary Mexican ceramics; and Mallory-Greenough *et al*. 1998 for New Kingdom Egyptian ceramics). The Amatitlan data produced for this thesis will be used by Ford and Spera in an attempt to tie tephra from Late Classic Maya ceramics to known eruptions. Since tephra chemical compositions alter upon firing (Dugmore *et al*. 1992), successful correlation of tephras requires experimental firing of clay at different temperatures to predict the degree and nature of chemical alteration so that original chemical compositions can be determined. If this is achievable, tephras in ceramics have the potential to refine current dating methods based on ceramic typologies by providing additional *terminus post quem* dates for specific ceramic pieces. Unfortunately several problems associated with microtephrochronology nevertheless remain. Firstly, it will be difficult to relate tephras to specific eruptions if chemical compositions of tephras do not change with each eruption; this limitation will be accentuated due to uncertainties resulting from clay firing. Secondly, the problems of stratigraphic integrity also apply, since features of interest are assigned dates based on association with ceramics of known type.

7.4.2. Resolving taphonomic issues:

Despite the suggestions made in preceding paragraphs, it is possible that microtephrochronology will never become a reliable and widespread archaeological dating tool. Microtephras at archaeological sites do, however, have the potential for a very different application, acting as aids to understanding post-depositional processes. Indeed, there has been some recognition in the palaeoenvironmental community that vertical spread of tephras within a deposit may act as a guide to the behaviour of other microparticles such as pollen (e.g. Hall and Pilcher 2002:229; Pilcher 2002:2). Since most tephra fall from a single eruption occurs within a year, the vertical spread of tephras with identical geochemical compositions can be used as an indicator of the extent of reworking and the integrity of the stratigraphic profile. This is perhaps one of the most valuable insights that microtephra analysis can provide, and yet the potential for such analysis has been scarcely explored. One possible and important application relates to the submission of single grains or charcoal fragments for accelerator mass spectrometry (AMS) radiocarbon dating as a means of assigning dates to artefacts or features in the same archaeological stratum. The reliability of associating single grains or charcoal with artefacts or features of interest is considerably increased if the integrity of the stratigraphic profile has been shown. Likewise, the use of association to assign dates can be avoided if an archaeological sequence is shown to have undergone extreme reworking.

Microtephra analysis as a tool for assessing site formation processes would essentially involve the same procedures of analysis as microtephrochronology, without the pretence of being a dating technique. In other words, samples will need extracting,

identifying and geochemical analysis, as outlined in chapters 4 and 6. The methodological problems associated with tephra extraction and identification do, however, still hold true, and must be addressed prior to successful application of this new technique. Likewise, the use of tephra as a tool for assessing taphonomic processes may be inapplicable in tropical areas where tephra is chemically altered and degraded. However, since little emphasis is placed on geochemical correlation, and since each site can be viewed in isolation, the more fundamental problems associated with microtephrochronology can be averted. Thus, microtephra analysis may be far more profitable if emphasis is placed on its use as a tool for assessing taphonomic processes rather than as a reliable means of assigning dates to archaeological strata.

8. CONCLUSION

The correlation of isochronous microtephra horizons (resulting from explosive eruptions) is commonly known as microtephrochronology. At first glance, the widespread inclusion of microtephras in a range of deposits (e.g. distal ice cores, soils, peat, lake and marine sediments) offers the potential to link and date palaeoenvironmental and archaeological sites over great distances. In reality, however, microtephrochronology is fraught with problems, and has not yet reached the point where it can be successfully applied to archaeology. This study highlighted the main problem areas of microtephrochronology, suggested possible improvements, and introduced two alternative archaeological applications for microtephra analysis.

Soil and sediment sequences from several lowland Maya archaeological sites (Lamanai, Medicinal Trail and Yalbac) and one lowland Maya lake site (Lamanai Lake) were subjected to current microtephra extraction and identification procedures. With some exceptions (e.g. Medicinal Trail and Lamanai Lake), very few microtephras were identified in cores analysed for this study. Where present, they were generally concentrated in the top 20cm of sequences and were near-absent at greater depths. This distribution and low frequency of microtephras was attributed to a) unsuitable laboratory extraction and identification protocols, b) reworking of microtephras in the post-depositional environment, and c) degradation of microtephras in lowland Maya tropical soils. Each of these problem areas were discussed in chapters 4, 5 and 6 respectively.

The first major limitation discussed in this study relates to the inadequacy of current

microtephra extraction and identification procedures. Since acid and alkali 'cleaning' extraction phases cause alteration of the geochemical signature of shards, emphasis is increasingly being placed on heavy liquid density flotation (Blockley *et al*. 2005). The use of universal density flotation protocols is, however, unjustified, since tephra densities vary with type of volcanic material, particle size and vesicularity (Turney 1998). Furthermore, current procedures of density flotation suffer from the inadvertent dilution of heavy liquid. Identification of tephra particles can also be problematic, since mineral inclusions in glass affect the behaviour of microtephras under cross-polarised light, whilst the behaviour of the Becke Line (also used to distinguish tephra from other materials) varies with mounting media and time (e.g. Euparol, p. 41). The most problematic criterion for identifying microtephras is, however, physical appearance, since tephras comprise an extremely diverse range of morphologies and colours. All these factors affect microtephra recovery, which is further complicated by the inconsistent lateral deposition of microtephra within a single core or sediment sequence (e.g. Lane 2004). To some degree these problems can, however, be overcome.

The second major limitation discussed in this study relates to tephra dispersal and reworking. Hall and Pilcher (2002:225) emphasise the need to study processes which transport tephra to distal sites, since the abundance of tephras found at proximal and distal deposits do not appear in simple relationships. The incomplete blanketing of tephra hinders successful recovery and highlights the need for multiple cores to be sampled from any given site. Of even greater consequence is the possibility that some tephras circulate in the atmosphere for thousands of years before final deposition (e.g the Mazama ash in the Columbia Basin; Davis 2005), rendering them unreliable chronological markers. Following deposition, many tephras at terrestrial sites are also

subjected to reworking processes, including soil-forming processes, creep, frost activity, bioturbation, earthworm activity and reworking by wind and running water (Westgate and Gorton 1981:91). The likelihood of reworking and soil erosion is considerably higher in continually leached tropical soils than in less aggressive temperate soils (Eden 1964:7-8). At archaeological sites, past and present human activities (e.g. building construction and cleaning) may also lead to tephra redeposition. These various factors affect the reliability of assigning dates to deposits using microtephrochronology, but can be partially overcome (at least insofar as reworking can be identified) through collaboration with micromorphologists.

The third major limitation discussed in this study results from the fact that WD analysis of individual glass shards usually provides the only means for characterising and correlating microtephra layers. Some tephras are inseparable using major element geochemistry, and consequently require separation based on stratigraphic grounds (Hall and Pilcher 2002:228). Although this is possible for visible tephra layers, it is considerably harder for distal deposits where very few microtephra shards represent each eruption. Furthermore, there is an inherent statistical problem with microtephrochronology, since small sample size leads to statistically insignificant datasets. In particular, glass layers of variable composition or multiple origin require large numbers of single shard analyses for adequate identification (Hall and Pilcher 2002:228), but this is often impossible to achieve for distal microtephra deposits.

There are additional problems with the reliance on major element compositions to characterise microtephras. An inter-laboratory comparison programme by Hunt and Hill (1996) suggests that a number of laboratories generate geochemical data that is

inadequate for distinguishing between tephras and may lead to erroneous correlations. Sodium mobilisation, sodium gain, instrumental problems, microprobe beam size and differences in correction, standardisation and analytical procedures can all distort geochemical data (Hunt and Hill 2001). Furthermore, volcanic glass is thermodynamically unstable and prone to chemical degradation in the post-depositional environment (Fisher and Schminke 1984:312). This can affect chemical compositions and prevent correct correlation (e.g. see Medicinal Trail samples analysed for this study, p. 75-78). Chemical stability modelling on tephras from Mexico and Central America did, however, indicate that not all tephras in the study area are inherently prone to chemical degradation.

This study has highlighted problems of microtephrochronology and provided some suggestions. These suggestions include discarding 1cm sub-samples for tephra extraction and identification, considering the use of LA-ICP-MS and SIMS to determine trace element compositions of single microtephra shards, and collaborating with micromorphologists to identify and account for post-depositional processes. Peat deposits were considered suitable locales for microtephra analysis due to slow accumulation and less likelihood of reworking. However, the scarcity of archaeological sites in peat deposits and the low pH of peats (and subsequent potential for chemical alteration of microtephras) limit the archaeological application of microtephrochronology to peat. Deep cave interiors were considered unsuitable for microtephra analysis since few tephras are transported more than 10m beyond cave entrances. Some suggestion was also made that microtephrochronology may have more use for dating hunter-gatherer activities than large urban centres, unless construction history and the integrity of archaeological sequences can be reliably determined at the

latter.

This study has introduced the possibility of two alternative archaeological applications for microtephra analysis. One involves the analysis of microtephras in ceramics to refine current dating methods based on ceramic typologies, and the other involves the use of microtephra distribution in archaeological sequences to determine the integrity of the stratigraphic profile. This latter application holds great potential in archaeological studies and should be actively explored and developed. Indeed, it may be more profitable, at least for the moment, to focus attention on the use of microtephras as a tool for assessing taphonomic disturbance rather than as reliable geochronological markers. If, however, continued efforts are to be expended on developing microtephrochronology as a geoarchaeological dating tool, attempts must be made to consider the suitability of sites, methodologies, and reference databases (including eruption histories and reference tephra geochemistries) prior to archaeological application.

Appendix A: Tephra counts

A.1. Archaeological sites, Belize:

Site	Project	Depth below surface (cm)	Sample number	Shard count
Lamanai Unit 1	P020	4-14 cm	OxT0437	4
Lamanai Unit 1	P020	14-24 cm	OxT0438	0
Lamanai Unit 1	P020	24-29 cm	OxT0439	0

Site	Project	Depth below surface (cm)	Sample number	Shard count
Lamanai Unit 2	P020	10-20 cm	OxT0440	0
Lamanai Unit 2	P020	20-30 cm	OxT0441	0
Lamanai Unit 2	P020	30-35 cm	OxT0442	0

Site	Project	Depth below surface (cm)	Sample number	Shard count
Yalbac	P021	0-10 cm	OxT0496	0
Yalbac	P021	10-20 cm	OxT0497	0
Yalbac	P021	20-30 cm	OxT0498	0
Yalbac	P021	30-40 cm	OxT0499	0
Yalbac	P021	40-50 cm	OxT0500	0
Yalbac	P021	50-60 cm	OxT0501	0

Site	Project	Depth below surface (cm)	Sample number	Shard count
Medicinal Trail	P019	0-10 cm	OxT0855	16
Medicinal Trail	P019	10-20 cm	OxT0856	18
Medicinal Trail	P019	20-30 cm	OxT0857	0
Medicinal Trail	P019	30-40 cm	OxT0858	2
Medicinal Trail	P019	40-50 cm	OxT0859	0
Medicinal Trail	P019	50-60 cm	OxT0860	0
Medicinal Trail	P019	60-70 cm	OxT0861	0
Medicinal Trail	P019	70-72 cm	OxT0862	0

Site	Project	Depth below surface (cm)	Sample number	Shard count
Medicinal Trail	P019	0-4 cm	OxT0607	350
Medicinal Trail	P019	4-8 cm	OxT0608	140
Medicinal Trail	P019	8-12 cm	OxT0609	25
Medicinal Trail	P019	12-16cm	OxT0610	52
Medicinal Trail	P019	16-20 cm	OxT0611	13

A.2. Lamanai Lake, Belize:

Site and core number	Project	Depth below surface of core (cm)	Total depth below surface (cm)	Sample number	Shard count
Lamanai Lake 2-1	P023	0-10 cm	0-10 cm	OxT0455	37
Lamanai Lake 2-1	P023	10-20 cm	10-20 cm	OxT0456	1
Lamanai Lake 2-1	P023	20-30 cm	20-30 cm	OxT0457	0
Lamanai Lake 2-1	P023	30-43 cm	30-43 cm	OxT0458	0
Lamanai Lake 2-2	P023	5-10 cm	55-60 cm	OxT0459	0
Lamanai Lake 2-2	P023	10-20 cm	60-70 cm	OxT0460	1
Lamanai Lake 2-2	P023	20-30 cm	70-80 cm	OxT0461	1
Lamanai Lake 2-2	P023	30-40 cm	80-90 cm	OxT0462	0
Lamanai Lake 2-2	P023	40-50 cm	90-100 cm	OxT0463	1
Lamanai Lake 2-2	P023	50-60 cm	100-110 cm	OxT0464	0
Lamanai Lake 2-2	P023	60-70 cm	110-120 cm	OxT0465	0
Lamanai Lake 2-2	P023	70-80 cm	120-130 cm	OxT0466	0
Lamanai Lake 2-2	P023	80-90 cm	130-140 cm	OxT0467	0
Lamanai Lake 2-3	P023	14-20 cm	154-160 cm	OxT0468	0
Lamanai Lake 2-3	P023	20-30 cm	160-170 cm	OxT0469	0
Lamanai Lake 2-3	P023	30-40 cm	170-180 cm	OxT0470	0
Lamanai Lake 2-3	P023	40-50 cm	180-190 cm	OxT0471	1
Lamanai Lake 2-3	P023	50-60 cm	190-200 cm	OxT0472	0
Lamanai Lake 2-3	P023	60-70 cm	200-210 cm	OxT0473	0
Lamanai Lake 2-3	P023	70-80 cm	210-220 cm	OxT0474	0
Lamanai Lake 2-3	P023	80-90 cm	220-230 cm	OxT0475	0
Lamanai Lake 2-3	P023	90-99 cm	230-239 cm	OxT0476	0
Lamanai Lake 2-4	P023	3-10 cm	243-250 cm	OxT0477	0
Lamanai Lake 2-4	P023	10-20 cm	250-260 cm	OxT0478	0
Lamanai Lake 2-4	P023	20-30 cm	260-270 cm	OxT0479	0
Lamanai Lake 2-4	P023	30-40 cm	270-280 cm	OxT0480	0
Lamanai Lake 2-4	P023	40-50 cm	280-290 cm	OxT0481	0
Lamanai Lake 2-4	P023	50-60 cm	290-300 cm	OxT0482	0
Lamanai Lake 2-4	P023	60-70 cm	300-310 cm	OxT0483	0
Lamanai Lake 2-4	P023	70-80 cm	310-320 cm	OxT0484	0
Lamanai Lake 2-4	P023	80-90 cm	320-330 cm	OxT0485	0
Lamanai Lake 2-4	P023	90-97.5 cm	330-337.5 cm	OxT0486	0

A.3. Lake Amatitlan, Guatemala:

Site	Project	Depth below surface (cm)	Sample number	Shard count
Lake Amatitlan	P022	8-12 cm	OxT0526	0
Lake Amatitlan	P022	80-81 cm	OxT0527	0
Lake Amatitlan	P022	89-90 cm	OxT0528	0
Lake Amatitlan	P022	93-94 cm	OxT0529	1
Lake Amatitlan	P022	163-164 cm	OxT0530	0
Lake Amatitlan	P022	205-206 cm	OxT0531	0
Lake Amatitlan	P022	222-223 cm	OxT0532	0
Lake Amatitlan	P022	241-242 cm	OxT0533	2 basaltic?
Lake Amatitlan	P022	257-258 cm	OxT0588	0
Lake Amatitlan	P022	259-260 cm	OxT0534	0
Lake Amatitlan	P022	265-266 cm	OxT0535	1
Lake Amatitlan	P022	281-282 cm	OxT0536	0
Lake Amatitlan	P022	317-318 cm	OxT0537	0
Lake Amatitlan	P022	319-320 cm	OxT0589	1
Lake Amatitlan	P022	323-324 cm	OxT0590	0
Lake Amatitlan	P022	353-354 cm	OxT0538	7
Lake Amatitlan	P022	385-386 cm	OxT0539	0
Lake Amatitlan	P022	391-392 cm	OxT0591	0
Lake Amatitlan	P022	401-402 cm	OxT0592	80
Lake Amatitlan	P022	403-404 cm	OxT0540	63
Lake Amatitlan	P022	413-414 cm	OxT0541	0
Lake Amatitlan	P022	427-428 cm	OxT0542	0
Lake Amatitlan	P022	435-436 cm	OxT0593	0
Lake Amatitlan	P022	445-446 cm	OxT0594	1
Lake Amatitlan	P022	455-456 cm	OxT0543	1
Lake Amatitlan	P022	467-468 cm	OxT0544	22
Lake Amatitlan	P022	505-506 cm	OxT0545	1
Lake Amatitlan	P022	515-516 cm	OxT0546	4
Lake Amatitlan	P022	571-572 cm	OxT0595	0
Lake Amatitlan	P022	577-578 cm	OxT0547	0
Lake Amatitlan	P022	603-604 cm	OxT0548	0
Lake Amatitlan	P022	617-618 cm	OxT0596	2
Lake Amatitlan	P022	637-638 cm	OxT0597	0
Lake Amatitlan	P022	639-640 cm	OxT0549	0
Lake Amatitlan	P022	651-652 cm	OxT0598	0
Lake Amatitlan	P022	675-676 cm	OxT0550	0

Appendix B: WDA electron microprobe data

B.1. Data with totals greater than 90% (included in data interpretation):

Site	Project	Sample	Hit	Na2O	SiO2	MgO	Al2O3	K2O	CaO	TiO2	MnO	FeO	Total	Date	Time	Lab.
Amatitlan	P022	OxT0540	#3	4.065	75.042	0.255	11.376	2.493	1.079	0.148	0.084	1.23	95.773	20050812	16:13	RLAHA
Amatitlan	P022	OxT0540	#4	4.349	73.959	0.209	11.68	2.55	1.087	0	0.053	1.698	95.585	20050812	16:13	RLAHA
Amatitlan	P022	OxT0540	#10	4.521	74.71	0.179	11.743	2.554	1.184	0.148	0.084	1.042	96.165	20050812	16:13	RLAHA
Amatitlan	P022	OxT0540	#12	3.572	75.506	0.189	11.728	2.56	1.083	0.26	0.084	1.157	96.139	20050812	16:13	RLAHA
Amatitlan	P022	OxT0540	#16	4.223	74.152	0.186	11.378	2.568	1.152	0.26	0.021	1.198	95.137	20050812	16:13	RLAHA
Amatitlan	P022	OxT0540	#17	4.215	74.59	0.177	11.656	2.743	1.184	0.112	0.031	1.115	95.823	20050812	16:13	RLAHA
Amatitlan	P022	OxT0540	#18	4.255	73.972	0.206	11.871	2.674	1.063	0.242	0.074	0.938	95.296	20050812	16:13	RLAHA
Amatitlan	P022	OxT0540	#23	3.997	75.56	0.065	12.408	4.208	0.838	0.055	0.137	0.916	98.183	20050812	16:13	RLAHA
Amatitlan	P022	OxT0540	#1	4.193	72.746	0.085	11.62	3.97	0.586	0.205	0.01	0.76	**94.178**	20050812	16:13	RLAHA
Amatitlan	P022	OxT0540	#5	4.065	73.157	0.174	11.471	2.615	1.013	0.13	0.274	1.218	**94.118**	20050812	16:13	RLAHA
Amatitlan	P022	OxT0540	#6	4.334	73.491	0.201	11.491	2.555	1.133	0.112	0.031	1.324	**94.672**	20050812	16:13	RLAHA
Amatitlan	P022	OxT0540	#7	4.363	72.71	0.184	11.244	2.539	1.198	0.242	0.074	1.105	**93.658**	20050812	16:13	RLAHA
Amatitlan	P022	OxT0540	#8	3.431	73.658	0.191	11.611	2.62	1.213	0.13	0.031	0.98	**93.864**	20050812	16:13	RLAHA
Amatitlan	P022	OxT0540	#9	2.778	74.753	0.224	11.295	2.514	1.152	0.205	0.043	1.064	**94.026**	20050812	16:13	RLAHA
Amatitlan	P022	OxT0540	#13	3.981	73.491	0.259	11.629	2.571	1.142	0.185	0	1.001	**94.258**	20050812	16:13	RLAHA
Amatitlan	P022	OxT0540	#14	3.982	72.65	0.151	11.416	2.543	1.128	0.167	0.01	1.073	**93.12**	20050812	16:13	RLAHA
Amatitlan	P022	OxT0540	#15	4.238	72.475	0.179	11.541	2.473	1.138	0	0	0.98	**93.023**	20050812	16:13	RLAHA
Amatitlan	P022	OxT0540	#19	4.165	73.613	0.229	11.548	2.691	1.07	0.224	0.043	1.073	**94.656**	20050812	16:13	RLAHA
Amatitlan	P022	OxT0540	#20	4.094	73.142	0.176	11.337	2.379	1.205	0.315	0.043	1.032	**93.723**	20050812	16:13	RLAHA
Amatitlan	P022	OxT0540	#21	4.652	71.204	0.181	10.979	2.568	0.967	0.334	0.158	1.187	**92.23**	20050812	16:13	RLAHA

Site	Project	Sample	Hit	Na2O	SiO2	MgO	Al2O3	K2O	CaO	TiO2	MnO	FeO	Total	Date	Time	Lab.
Amatitlan	P022	OxT0544	#25	4.607	73.773	0.174	12.725	4.031	0.786	0.242	0.127	1	97.465	20050812	16:13	RLAHA
Amatitlan	P022	OxT0544	#31	4.309	72.731	0.083	12.034	4.055	0.658	0.148	0.031	1.061	95.11	20050812	16:13	RLAHA
Amatitlan	P022	OxT0544	#35	3.839	76.657	0.046	12.614	4.149	0.8	0.167	0.063	0.823	99.159	20050812	16:13	RLAHA
Amatitlan	P022	OxT0544	#2	3.975	75.605	0.111	12.653	4.159	0.853	0.093	0.074	0.991	98.515	20050812	18:10	RLAHA
Amatitlan	P022	OxT0544	#4	4.594	71.168	0.235	13.143	3.935	0.985	0.13	0.231	1.396	96.816	20050812	18:10	RLAHA
Amatitlan	P022	OxT0544	#5	4.394	73.482	0.133	12.604	4.098	0.7	0.224	0	1.085	96.719	20050812	18:10	RLAHA
Amatitlan	P022	OxT0544	#6	4.206	73.243	0.114	12.567	3.958	0.673	0.224	0.106	0.938	96.028	20050812	18:10	RLAHA
Amatitlan	P022	OxT0544	#8	4.322	71.264	0.189	13.003	3.859	0.809	0.445	0.147	1.167	95.206	20050812	18:10	RLAHA
Amatitlan	P022	OxT0544	#9	4.42	72.967	0.124	12.419	4.008	0.666	0.279	0.106	0.979	95.968	20050812	18:10	RLAHA
Amatitlan	P022	OxT0544	#10	4.227	72.464	0.149	12.419	4.121	0.747	0.167	0.127	0.897	95.318	20050812	18:10	RLAHA
Amatitlan	P022	OxT0544	#11	4.444	71.946	0.139	12.778	4.021	0.648	0.224	0.074	1.24	95.514	20050812	18:10	RLAHA
Amatitlan	P022	OxT0544	#24	4.018	71.114	0.153	12.019	4.536	0.679	0.335	0.063	0.822	**93.739**	20050812	16:13	RLAHA
Amatitlan	P022	OxT0544	#26	4.378	72.122	0.098	12.302	4.104	0.728	0.26	0.074	0.885	**94.95**	20050812	16:13	RLAHA
Amatitlan	P022	OxT0544	#27	4.007	70.952	0.191	12.523	4.318	0.897	0.354	0.178	1.051	**94.471**	20050812	16:13	RLAHA
Amatitlan	P022	OxT0544	#28	3.948	72.539	0.028	11.803	3.864	0.562	0.148	0.031	0.928	**93.852**	20050812	16:13	RLAHA
Amatitlan	P022	OxT0544	#29	3.703	70.875	0.149	12.33	5.125	0.753	0.224	0.116	0.812	**94.086**	20050812	16:13	RLAHA
Amatitlan	P022	OxT0544	#30	4.286	70.74	0.315	12.296	3.932	0.895	0.13	0.084	1.217	**93.895**	20050812	16:13	RLAHA
Amatitlan	P022	OxT0544	#32	4.425	70.554	0.123	12.744	3.884	0.849	0.242	0.19	1.061	**94.072**	20050812	16:13	RLAHA
Amatitlan	P022	OxT0544	#33	4.063	71.202	0.177	11.86	4.251	0.639	0.055	0.084	0.948	**93.279**	20050812	16:13	RLAHA
Amatitlan	P022	OxT0544	#3	2.062	69.022	0.166	12.174	6.952	0.763	0.148	0.116	0.957	**92.36**	20050812	18:10	RLAHA
Amatitlan	P022	OxT0544	#12	3.576	70.376	0.303	12.644	4.704	0.874	0.26	0.074	1.187	**93.898**	20050812	18:10	RLAHA

Site	Project	Sample	Hit	Na2O	SiO2	MgO	Al2O3	K2O	CaO	TiO2	MnO	FeO	Total	Date	Time	Lab.
Amatitlan	P022	OxT0546	#13	2.405	72.569	0.04	11.73	6.536	0.49	0.112	0.116	0.76	**94.757**	20050817		RLAHA
Amatitlan	P022	OxT0546	#14	2.511	72.885	0.056	11.73	6.341	0.497	0.112	0.084	0.666	**94.883**	20050818		RLAHA

Site	Project	Sample	Hit	Na2O	SiO2	MgO	Al2O3	K2O	CaO	TiO2	MnO	FeO	Total	Date	Time	Lab.
Amatitlan	P022	OxT0538	#9	4.413	75.619	0.159	12.801	4.039	0.725	0.075	0.137	1.011	98.979	20050819		RLAHA
Amatitlan	P022	OxT0538	#10	3.271	74.535	0.086	12.243	5.366	0.641	0.148	0.084	1.042	97.418	20050819		RLAHA
Amatitlan	P022	OxT0538	#11	4.371	74.203	0.151	12.687	4.04	0.655	0.279	0	1.115	97.502	20050819		RLAHA
Amatitlan	P022	OxT0538	#12	1.872	74.781	0.06	11.862	6.612	0.462	0.055	0.19	1.042	96.936	20050819		RLAHA
Amatitlan	P022	OxT0538	#13	3.782	75.371	0.118	12.268	4.508	0.59	0.224	0.021	0.886	97.768	20050819		RLAHA
Amatitlan	P022	OxT0538	#14	3.727	72.92	0.121	12.138	4.71	0.603	0.205	0.043	0.886	95.353	20050819		RLAHA
Amatitlan	P022	OxT0538	#15	4.288	71.824	0.29	12.865	3.558	1.324	0.224	0.19	1.676	96.238	20050819		RLAHA
Amatitlan	P022	OxT0538	#16	4.32	73.228	0.184	12.54	3.945	0.895	0.205	0.01	0.886	96.214	20050819		RLAHA
Amatitlan	P022	OxT0538	#18	3.889	73.461	0.214	12.854	4.757	0.855	0.242	0.094	1.271	97.637	20050819		RLAHA
Amatitlan	P022	OxT0538	#20	3.935	72.597	0.186	12.899	3.814	0.856	0.205	0.043	1.085	95.618	20050819		RLAHA

Site	Project	Sample	Hit	Na2O	SiO2	MgO	Al2O3	K2O	CaO	TiO2	MnO	FeO	Total	Date	Time	Lab.
Med. Trail	P019	OxT0607/11	71	3.908	74.136	0.063	12.587	5.07	0.424	0.106	0.009	0.706	97.009	200508		Begbroke
Med. Trail	P019	OxT0607/8	68	4.504	72.459	0.419	14.542	2.537	1.559	0.217	0.079	1.402	97.718	200508		Begbroke
Med. Trail	P019	OxT0607/5	65	4.595	65.442	0.22	15.73	5.528	1.868	0.28	0.048	1.389	95.1	200508		Begbroke
Med. Trail	P019	OxT0607/14	74	5.193	62.613	0.148	18.869	4.09	3.708	0.18	0.054	0.934	95.789	200508		Begbroke
Med. Trail	P019	OxT0607/12	72	6.123	61.494	0.072	20.38	3.116	4.448	0.089	0.012	0.817	96.551	200508		Begbroke
Med. Trail	P019	OxT0607/13	73	4.211	64.956	0.131	14.816	5.29	1.349	0.209	0.054	1.093	**92.109**	200508		Begbroke
Med. Trail	P019	OxT0607/2	62	4.502	62.801	0.207	15.123	5.809	1.613	0.234	0.126	1.351	**91.766**	200508		Begbroke
Med. Trail	P019	OxT0607/7	67	4.834	59.728	0.128	17.855	3.808	3.568	0.15	0.061	0.988	**91.12**	200508		Begbroke

N.B. Samples with totals below 95% are highlighted in **bold**

B.2. Discarded data:

Site	Project	Sample	Hit	Na2O	SiO2	MgO	Al2O3	K2O	CaO	TiO2	MnO	FeO	Total	Date	Time	Lab.	Comments
Amatitlan	P022	andesine	#2	4.361	52.759	0.111	27.922	0.136	12.444	0.093	0.021	0.695	98.542	20050812	16:13	RLAHA	plagioclase feldspar
Amatitlan	P022	OxT0533	#6	3.878	51.407	3.787	12.803	1.323	7.995	2.143	0.276	13.857	97.469	20050817		RLAHA	Groundmass
Amatitlan	P022	OxT0533	#7	1.992	47.385	0.06	31.812	0.076	16.425	0.055	0.074	0.756	98.636	20050817		RLAHA	Groundmass
Amatitlan	P022	OxT0533	#8	3.688	52.526	4.105	12.782	1.277	7.421	1.84	0.072	13.629	97.34	20050817		RLAHA	Ca-plagioclase
Amatitlan	P022	OxT0533	#9	4.179	51.681	3.583	13.443	1.321	7.848	1.536	0.205	12.571	96.367	20050817		RLAHA	Groundmass
Amatitlan	P022	OxT0533	#10	4.838	52.032	3.636	12.893	1.679	7.112	2012	0.114	11.17	95.486	20050817		RLAHA	Groundmass
Amatitlan	P022	OxT0533	#11	3.937	50.35	4.147	13.678	1.207	8.458	1.721	0.247	11.43	95.175	20050817		RLAHA	Groundmass
Amatitlan	P022	OxT0544	#7	1.88	54.601	1.03	27.778	0.214	0.47	0.277	0.158	2.547	**88.955**	20050812	18:10	RLAHA	low total
Amatitlan	P022	OxT0538	#17	6.512	58.069	0.045	25.957	0.359	9.156	0.037	0	0.28	100.415	20050819		RLAHA	plagioclase
Amatitlan	P022	OxT0538	#19	5.978	57.919	0.045	26.894	0.341	10.173	0.093	0	0.583	102.026	20050819		RLAHA	plagioclase
Med. Trail	P019	OxT0607/1	61	2.433	46.928	0.075	18.123	4.569	0.637	0.123	0.291	1.331	**74.51**	200508		Begbroke	low total
Med. Trail	P019	OxT0607/4	64	4.125	58.345	0.248	14.041	4.727	1.582	0.215	0.077	1.175	**84.535**	200508		Begbroke	low total
Med. Trail	P019	OxT0607/6	66	8.551	51.418	0.078	20.31	5.53	0.696	0.151	0.208	1.328	**88.27**	200508		Begbroke	low total
Med. Trail	P019	OxT0607/15	75	4.922	55.097	0.071	20.695	2.101	5.845	0.075	0.035	0.59	**89.431**	200508		Begbroke	low total

N.B. Samples with totals below 95% are highlighted in **bold**

B.3. Standards (Lipari 1 and NIST 612):

Sample	Hit	Na2O	SiO2	MgO	Al2O3	K2O	CaO	TiO2	MnO	FeO	Total	Date	Time	Lab.	Comments
Lipari 1	#11	3.789	76.251	0.061	12.315	4.106	0.841	0.13	0.074	0.844	98.411	20050812	16:13	RLAHA	
Lipari 1	#22	3.028	74.824	0.204	11.488	2.578	1.164	0.224	0.074	0.949	**94.531**	20050812	16:13	RLAHA	
Lipari 1	#34	4.005	76.907	0.124	12.432	4.159	0.82	0.187	0	0.781	99.416	20050812	16:13	RLAHA	
Lipari 1	#1	3.905	74.892	0.108	12.574	4.388	0.841	0.148	0	0.709	97.565	20050812	18:10	RLAHA	
Lipari 1	#13	3.816	70.141	0.134	11.82	3.947	0.819	0.224	0.043	0.762	91.705	20050812	18:10	RLAHA	focus error - ignore
Lipari 1	#14	3.819	74.86	0.099	12.442	4.215	0.879	0.224	0	0.719	97.257	20050812	18:10	RLAHA	
Lipari 1	#1	4.043	75.682	0.118	12.74	4.385	0.898	0	0.063	0.814	98.744	20050817		RLAHA	
Lipari 1	#2	3.995	76.208	0.098	12.604	4.258	0.944	0.13	0.021	0.741	99.001	20050817		RLAHA	
Lipari 1	#3	3.792	76.131	0.116	12.888	4.37	0.793	0.093	0.063	0.699	98.945	20050817		RLAHA	
Lipari 1	#4	3.805	76.537	0.134	12.712	4.368	0.921	0.018	0	0.814	99.31	20050817		RLAHA	
Lipari 1	#5	3.92	75.414	0.138	12.572	4.287	0.876	0.13	0.106	0.731	98.174	20050817		RLAHA	
Lipari 1	#12	3.883	75.598	0.093	12.559	4.128	0.805	0.167	0.19	0.885	98.308	20050817		RLAHA	
Lipari 1	#1	3.712	70.496	0.098	12.585	4.392	0.9	0.057	0	0.741	**92.981**	20050819		RLAHA	
Lipari 1	#2	3.782	75.519	0.104	12.599	4.288	0.874	0.075	0.116	0.668	98.026	20050819		RLAHA	
Lipari 1	#3	3.794	78.063	0.114	12.493	4.247	0.908	0.057	0.137	0.866	100.679	20050819		RLAHA	
Lipari 1	#4	3.879	78.11	0.126	12.661	4.427	0.898	0.187	0.106	0.814	101.208	20050819		RLAHA	
Lipari 1	#5	3.103	46.301	0.101	12.765	4.158	0.915	0.055	0.116	0.749	**68.263**	20050819		RLAHA	
Lipari 1	#6	3.715	74.995	0.123	12.351	4.218	0.883	0.13	0	0.762	97.177	20050819		RLAHA	
Lipari 1	#7	3.56	75.953	0.121	12.499	4.294	0.841	0.317	0.137	0.813	98.535	20050819		RLAHA	
Lipari 1	#8	3.727	75.142	0.113	12.705	4.435	0.795	0.112	0.032	0.762	97.822	20050819		RLAHA	
Lipari 1	#21	3.886	76.043	0.075	12.604	4.434	0.88	0	0.116	0.792	98.831	20050819		RLAHA	
NIST 612/1	1	13.506	71.013	0	2.061	0.023	11.856	0.019	0.076	0.047	98.601	200508		Begbroke	
NIST 612/2	2	13.866	71.465	0.009	2.074	0.023	11.577	0	0	0	99.014	200508		Begbroke	
NIST 612/3	3	13.739	71.168	0.01	2.065	0.023	11.574	0.036	0	0	98.615	200508		Begbroke	
Lipari/1	4	3.784	75.779	0.107	13.042	4.725	0.827	0.113	0.032	0.779	99.188	200508		Begbroke	
Lipari/2	5	3.714	75.845	0.12	13.052	4.644	0.846	0.087	0.135	0.855	99.298	200508		Begbroke	
Lipari/3	6	3.667	76.059	0.115	13.126	4.652	0.826	0.122	0	0.742	99.309	200508		Begbroke	
NIST 612/4	37	13.63	71.04	0.002	2.06	0.025	11.049	0	0	0.022	97.828	200508		Begbroke	
NIST 612/5	38	13.693	70.953	0.004	2.015	0.021	11.263	0.029	0	0.006	97.984	200508		Begbroke	
NIST 612/6	39	13.835	70.704	0.012	2.061	0.047	11.343	0.01	0	0.027	98.039	200508		Begbroke	
Lipari/4	40	3.779	75.868	0.117	13.047	4.588	0.819	0.092	0.047	0.791	99.148	200508		Begbroke	
Lipari/5	41	3.752	75.731	0.119	12.967	4.646	0.815	0.075	0.013	0.835	98.953	200508		Begbroke	
Lipari/6	42	3.688	75.946	0.115	12.97	4.63	0.829	0.089	0.055	0.804	99.126	200508		Begbroke	
Lipari/7	76	3.71	75.231	0.108	12.909	4.656	0.77	0.134	0.072	0.834	98.424	200508		Begbroke	
Lipari/8	77	3.831	75.425	0.114	13	4.658	0.792	0.07	0.051	0.818	98.759	200508		Begbroke	
Lipari/9	78	3.783	75.385	0.08	12.948	4.632	0.82	0.08	0.04	0.843	98.611	200508		Begbroke	
Lipari/10	107	3.731	75.342	0.096	12.898	4.577	0.814	0.109	0.038	0.856	98.461	200508		Begbroke	
Lipari/11	108	3.707	75.323	0.116	12.936	4.642	0.846	0.095	0.003	0.828	98.496	200508		Begbroke	
Lipari/12	109	3.678	75.028	0.122	12.855	4.711	0.789	0.112	0.056	0.824	98.175	200508		Begbroke	
Lipari/13	110	3.73	74.878	0.102	13.04	4.565	0.882	0.101	0.066	0.898	98.262	200508		Begbroke	

N.B. Samples with totals below 95% are highlighted in **bold**

Appendix C: EDA electron microprobe data

C.1. Images: Lamanai Unit 1: OxT0437 (4-14cm below surface):

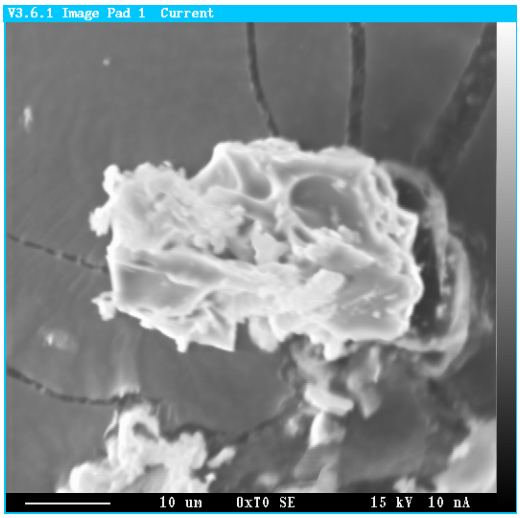

x8460 tephra

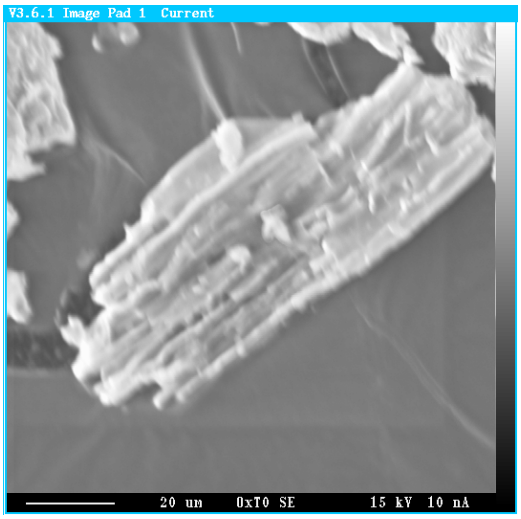

x9777 tephra

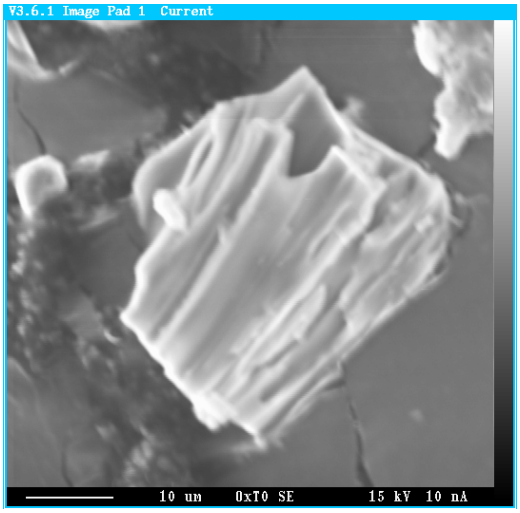

x9079 tephra

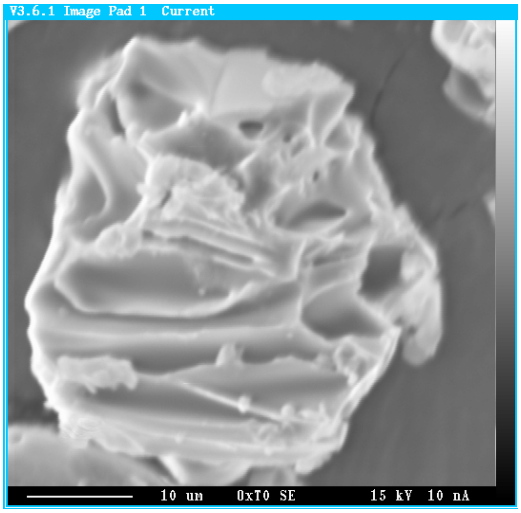

x12605 tephra

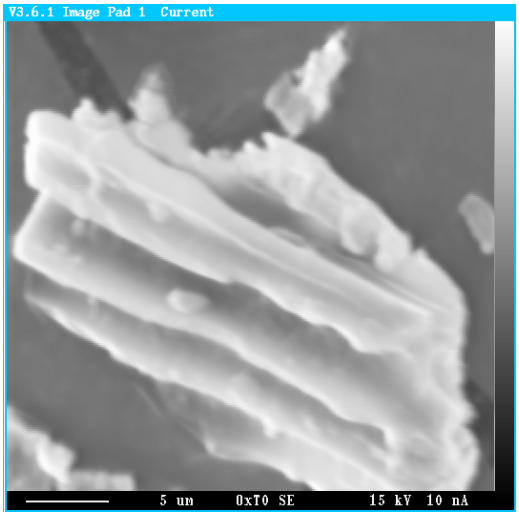

x9153 carbonate

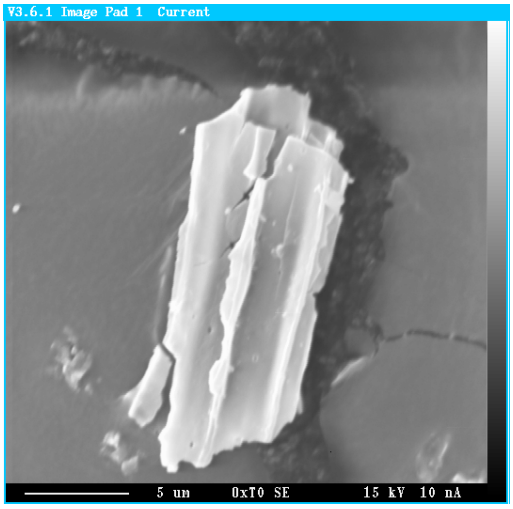

x9967 carbonate

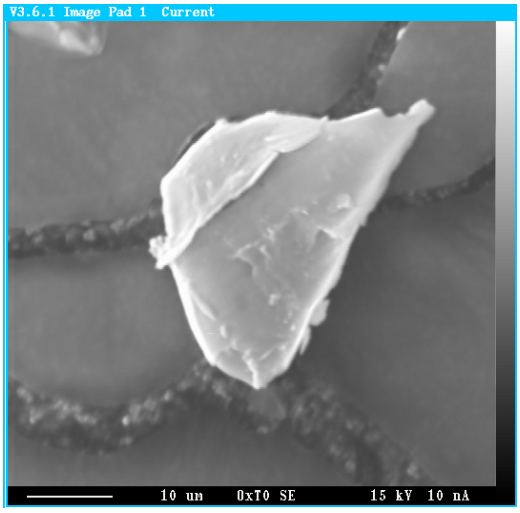

x3758 organics

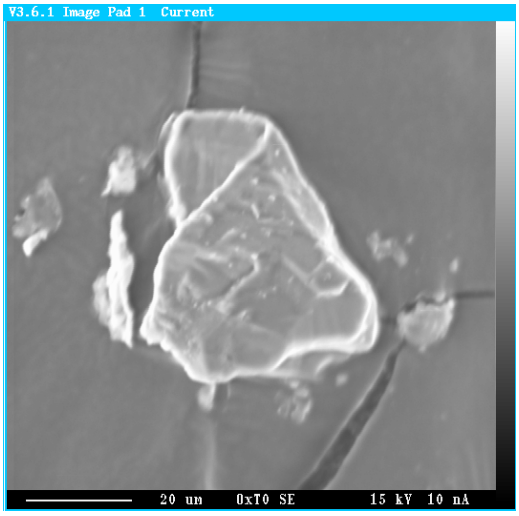

x3086 quartz

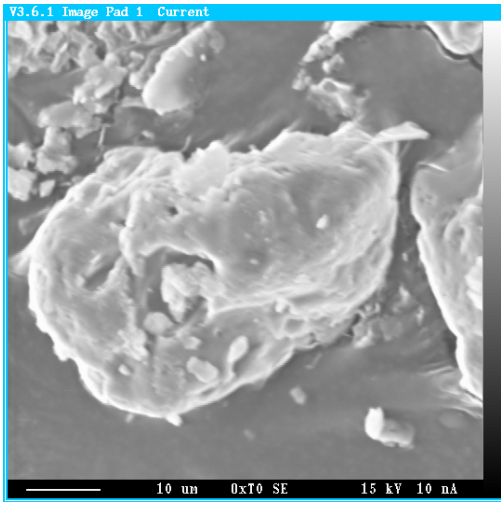

x3621 degraded quartz

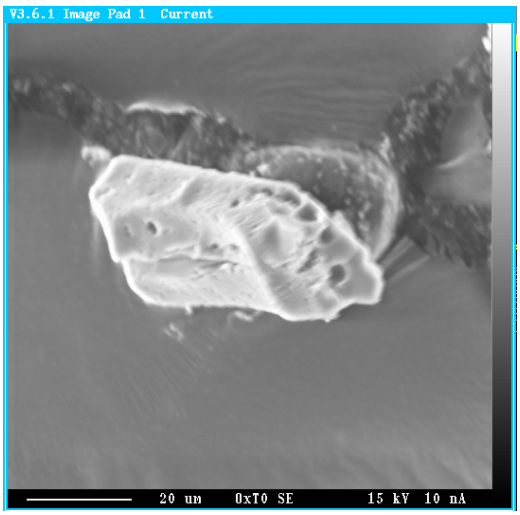

x9093 degraded quartz

C.2. Images: Lake Amatitlan: OxT0533 (241-242cm below surface):

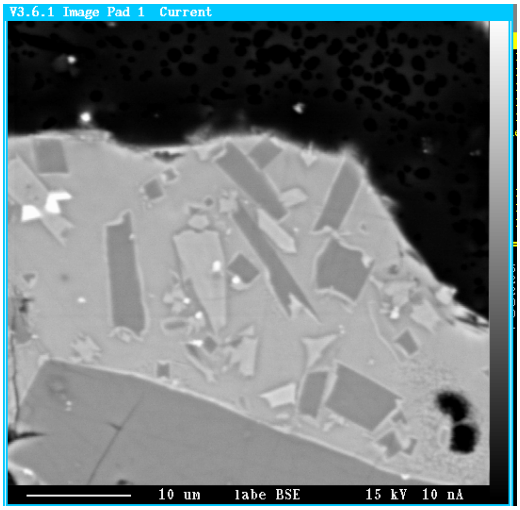

tephra with mineral inclusions

OxT0533 consisted predominantly of crystal lithic tuffs. EDA spectra for OxT0533 tephra indicated the presence of the following mineral inclusions:
calcium plagioclase (in large quantities), an Fe-rich silicate mineral phase (in small quantities) and magnesium olivine.

C.3. EDA spectra: Lamanai Unit 1: OxT0437 (4-14 cm below surface):

EDA spectra on tephra, quartz and organics from OxT0437 are shown on the following pages. This resolved a dispute between laboratory members (regarding microtephras initially believed to be phytoliths) and confirmed the presence of microtephras at Lamanai.

References

Andrade, S. 2005: Temple 3A Looters' Trenches: Construction History. In Lucero, L.J. ed. *Results of the 2004 Valley of Peace Archaeology Project: the temples and ballcourt of Yalbac* (Report submitted to the Institute of Archaeology, Belize).

Arnold, D.E. 1985: *Ceramic Theory and Cultural Process* (Cambridge University Press, Cambridge).

Barker, D.S. 1983: *Igneous Rocks* (Prentice Hall, New Jersey).

Bergman, J., S. Wastegård, S. Hammaelund, D. Wohlfarth and S. Roberts. 2004: Holocene tephra horizons at Kolcka Bog, west-central Sweden: aspects of reproducibility in subarctic peat deposits. *Journal of Quaternary Science* 19(3): 241-249.

Blockley, S.P.E., S.D.F. Pyne-O'Donnell, J.J. Lowe, I.P. Matthews, A. Stone, A.M. Pollard, C.S.M. Turney and E.G. Molyneux. 2005: A new and less destructive laboratory procedure for the physical separation of distal glass tephra shards from sediments. *Quaternary Science Reviews* 24: 1952-1960.

Björck, J. and S. Wastegård. 1999: Climate oscillations and tephrochronology in eastern middle Sweden during the last glacial-interglacial transition. *Journal of Quaternary Science* 14(5): 399-410.

Blong, R.J. 1981: Some effects of tephra falls on buildings. In Self, S. and R.S.J. Sparks eds. *Tephra Studies* (Reidel, London).

Boygle, J. 1999. Variability of tephra in lake and catchment sediments, Svínavatn, Iceland. *Global and Planetary Change* 21: 129-149.

Breen, A.M. 2002. *Holocene Environmental Change: a palaeolimnological study in Belize.* Ph.D. Thesis (Edinburgh University. Edinburgh).

Bullock, P., N. Fedoroff, A. Jongerius, G. Stoops and T. Tursina. 1985: *Handbook for Thin Section Description* (Wayne Research, Wolverhampton).

Carey, S.N. 1997: Influence of convective sedimentation on the formation of widespread tephra fall layers in the deep sea. *Geology* 25: 839-842.

Cas, R.A.F. and J.V. Wright. 1987: *Volcanic Successions Modern and Ancient: a geological approach to process, products and successions* (Allen & Unwin, London).

Courty, M.A., P. Goldberg and R. McPhail. 1989: *Soils and Micromorphology in Archaeology* (Cambridge University Press, Cambridge).

Culbert, T.P. ed. 1973: *The Classic Maya Collapse* (University of New Mexico Press, Albuquerque).

Czamanske, G.K. and S.C. Porter 1965: Titanium dioxide in pyroclastic layers from volcanoes in the Cascade Range. *Science* 150(3699): 1022-1025.

Darwin, C. 1881: *The Formation of Vegetable Mould through the Action of Worms with Observations on their Habits* (John Murray, London).

Davies, S.M., C.S.M. Turney, J.J. Lowe. 2001: Identification and significance of a visible, basalt-rich Vedde Ash layer in a Last Termination sequence on the Isle of Skye, Inner Hebrides, Scotland. *Journal of Quaternary Science* 16: 99-104.

Davis, O.K. 2005. *Volcanic Tephra Studies* (University of Arizona). Available at: http://www.geo.arizona.edu/palynology/geos462/15volctephra.html.

Deevy, E.S., D.S. Rice, P.M. Rice, H.H. Vaughan, M. Brenner and M.S. Flannery. 1979: Mayan urbanism: impact on a tropical karst environment. *Science* 206: 298-306.

Dimbleby, G.W. 1985: *The Palynology of Archaeological Sites* (Academic Press, London).

Druc, I.C. 2000: Ceramic production in San Marcos Acteopan, Puebla, Mexico. *Ancient Mesoamerica* 11: 77-89.

Dugmore, A.J., G.T. Cook, J.S. Shore, A.J. Newton, K.J. Edwards and G. Larsen. 1995: Radiocarbon dating tephra layers in Britain and Iceland. *Radiocarbon* 37: 379-388.

Dugmore, A.J., A.J. Newton, D.E. Sugden and G. Larsen. 1992: Geochemical stability of fine-grained silicic Holocene tephra in Iceland and Scotland. *Journal of Quaternary Science* 7: 173-183.

Eden, T. 1964: *Elements of Tropical Soil Science* (MacMilland & Co, London).

Espíndola, J.M., J.L. Macías, R.I. Tilling and M.F. Sheridan. 2000: Volcanic history of El Chichón volcano (Chiapas, Mexico) during the Holocene, and its impact on human activity. *Buletin of. Volcanology* 62: 90-104.

Fisher, R.V. and H-U. Schminke. 1984: *Pyroclastic Rocks* (Springer-Verlag, Berlin).

Ford, A. and W.I. Rose. 1995: Volcanic ash in ancient Maya ceramics of the limestone lowlands: implications for prehistoric volcanic activity in the Guatemala highlands. *Journal of Volcanology and Geothermal Research* 66: 149-162.

Gifford, J.C. 1976: *Prehistoric Pottery Analysis and the Ceramics of Barton Ramie in the Belize Valley* (Memoirs of the Peabody Museum of Archaeology and Ethnology 18).

Goodhew, P.J., J. Humphreys and R. Beanland. 2001: *Electron Microscopy and Analysis.* 3rd ed. (Taylor and Francis, London and NY).

Hall, A. 1996: *Igneous Petrology* (Longman, London).

Hall, V.A. and J.R. Pilcher. 2002: Late-Quaternary Icelandic tephras in Ireland and Great Britain: detection, characterization and usefulness. *The Holocene* 12(2): 223-230.

Hall, V.A., J.R. Pilcher and F.G. McCormac. 1994: Icelandic volcanic ash and the mid-Holocene Scots pine (*Pinus sylvestris*) decline in the north of Ireland: no correlation. *The Holocene* 4: 79-83.

Hart, W.J.E. and V. Steen-McIntyre. 1980: Tierra Blanca Joven tephra from the AD 260 eruption of Ilopango caldera. In Sheets, P.D. ed. *Archeology and Volcanism in Central America* (University of Texas Press, Austin).

Havinga, A.J. 1968: Some remarks on the interpretation of a pollen diagram of a

podsol profile. *Acta Botanica Neerlandica* 17: 1-4.

Hess, P.C. 1989: *Origins of Igneous Rocks* (Harvard University Press, Massachussetts).

Hole, F. and R.F. Heizer. 1965: *An Introduction to Prehistoric Archaeology* (Holt, Rinehart and Winston, NY).

Hunt, J.B. and P.G. Hill. 1996: An nter-laboratory comparison of the electron probe microanalysis of glass geochemistry. *Quaternary International* 34-36: 229-241.

Hunt, J.B. and P.G. Hill. 2001: Tephrological implications of beam size—sample-size effects in electron microprobe analysis of glass shards. *Journal of Quaternary Science* 16(2): 105-117.

Hyde, D.M. 2005: Report of 2004 excavations at the Medicinal Trail Site, Operation 7. In Valdez, F. ed. *Programme for Belize Archaeological Project: Report of Activities from the 2004 field Season* (Occasional Papers, Number 4. Mesoamerican Archaeological Research Laboratory, University of Texas at Austin).

Keatinge, T.H. 1983: Development of pollen assemblage zones in soil profiles in southeastern England. *Boreas* 12: 1-12.

Lane, C.S. 2004: *Toward a Lateglacial Tephrostratigraphy for the North-West of England: site investigations and methodological recommendations.* M.Sc. Thesis (Royal Holloway, University of London).

Langdon, P.G. and K.E. Barber. 2004: Snapshots in time: precise correlations of peat-based proxy climate records in Scotland using mid-Holocene tephras. *The Holocene* 14(1): 21-33.

Larsen, G. 1981: Tephrochronology by microprobe glass analysis. In Self, S. and R.S.J. Sparks eds. *Tephra Studies* (Reidel, London).

Lowe D.J., R.M. Newnham, B.G. McFadgen and T.F.G. Higham. 2000: Tephras and New Zealand Archaeology. *Journal of Archaeological Science* 27(10): 859-870.

Lowe, J.J., W.Z. Hoek and INTIMATE Group. 2001: Inter-regional correlation of

palaeoclimatic records for the last Glacial-Interglacial transition: a protocol for improved precision recommended by the INTIMATE project group. *Quaternary Science Reviews* 20: 1175-1187.

Lowe, J.J., M.J.C. Walker, E.M. Scott, D.D. Harkness, C.L. Bryant and S.M. Davies. 2004: A coherent high-precision radiocarbon chronology for the Late-Glacial sequence at Sluggan Bog, County Antrim, Northern Ireland. *Journal of Quaternary Science* 19(2): 147-158.

Machida, H. 2003: Quaternary volcanoes and widespread tephras of the world. *Global Environmental Research* 6(2): 3-17.

Macías, J.L., J.L. Arce, J.C. Mora, J.M. Espíndola and R. Saucedo. 2003: A 550-year-old Plinian eruption at El Chichón Volcano, Chiapas, Mexico: explosive volcanism linked to reheating of the magma reservoir. *Journal of Geophysical Research* 108 (3): 1-18.

Mallory-Greenough, L.M., J.D. Greenough and J.V. Owen. 1998: Provenance of temper in a New Kingdom Egyptian pottery sherd: evidence from the petrology and mineralogy of basalt fragments. *Geoarchaeology* 13(4): 391-410.

Matthews, W., C.A.I. French, T. Lawrence, D.F. Cutler and M.K. Jones. 1997: Microstratigraphic traces of site formation processes and human activities. *World Archaeology* 29(2): 281-308.

Mehringer, P.J., A.M. Sarna-Wojcicki, L.K. Wollwage and P. Sheets. 2005: Age and extent of the Ilopango TBJ tephra inferred from a Holocene chronostratigraphic reference section, Lago de Yojoa, Honduras. *Quaternary Research* 63: 199-205.

Morgan, N.A. and F.J. Spera 2001: Glass transition, structural relaxation, and theories of viscosity: a molecular dynamics study of amorphous $CaAl_2Si_2O_8$. *Geochimica et Cosmochimica Acta* 65: 4019-4041.

Newton, A. *Tephrabase* (Institute of Geography, University of Edinburgh). Available at: http://www.geo.ed.ac.uk/tephra/.

Ortega-Gierrero, B. and A.J. Newton. 1998: Geochemical characterization of Late Pleistocene and Holocene tephra layers from the Basin of Mexico, Central Mexico.

Quaternary Research 50: 90-106.

Owen, V.A. 2002: *An Investigation of Classic Maya Cave Mortuary Practices at Barton Creek Cave, Belize.* M.A. Thesis (Colorado State University, Fort Collins).

Pearce, N.J.G., W.J. Eastwood, J.A. Westgate and W.T.Perkins. 2002: Trace-element composition of single glass shards in distal Minoan tephra from SW Turkey. *Journal of the Geological Society* 159: 545-556.

Pearce, N.J.G., J.A. Westgate, W.T. Perkins, W.J. Eastwood and P.Shane. 1999: The application of laser ablation ICP-MS to the analysis of volcanic glass shards from tephra deposits: bulk glass and single shard analysis. *Global and Planetary Change* 21: 151-171.

Pendergast, D.M. 1981: Lamanai, Belize: Summary of Excavation Results, 1974-1980. *Journal of Field Archaeology* 24: 293-313.

Pierce, T.G. 1978: Gut contents of some lumbricid earthworms. *Pedobiologia* 18: 153-157.

Pilcher, J.R. 2002: *The use of tephra in linking stratigraphic sequences between sites and archives* (unpublished manuscript: ESF-HOLIVAR workshop, Finland).

Pilcher, J.R. and V.A. Hall. 1992: Towards a tephrochronology for the Holocene of the north of Ireland. *The Holocene* 2: 255-259.

Pollard, A.M., S.P.E. Blockley and K.R. Ward. 2003: Chemical alteration of tephra in the depositional environment: theoretical stability modelling. *Journal of Quaternary Science* 18(5): 385-394.

Pollard, A.M. and C.P. Heron. 1996: *Archaeological Chemistry* (Royal Society of Chemistry, Cambridge).

Popenoe de Hatch, M., E. Ponciano, T. Barrientos Q., M. Brenner and C. Ortloff. 2002: Climate and technological innovation at Kaminaljuyu, Guatemala. *Ancient Mesoamerica* 13: 103-114.

Potts, P.J., J.F.W. Bowles, S.J.B. Reed and M.R. Cave eds. 1995: *Microprobe*

Techniques in Earth Sciences. The Mineralogical Society Series 6 (Chapman and Hall, London).

Pyne-O'Donnell, S., I. Matthews and N. Branch. 2004: *Identification of micro-tephra shards using light microscopy* (unpublished manuscript).

Reheis M.C., J.L. Slate, C.K. Throckmorton, J.P. McGeehin, A.M. Sarna-Wojcicki and L. Dengler. 1996: Late Quaternary sedimentation on the Leidy Creek fan, Nevada-California: geomorphic responses to climate change. *Basin Research* 8(3): 279-299.

Rose, N.L., P.N.E. Golding, R.W. Battarbee. 1996: Selective concentration and enumeration of tephra shards from lake sediment cores. *Holocene* 6: 243-246.

Rose, W.I., G.A. Hahn, J.W. Drexler, M.L. Malinconico, P.S. Peterson and R.L. Wunderman. 1981: Quaternary tephra of northern Central America. In Self, S. and R.S.J. Sparks eds. *Tephra Studies* (Reidel, London).

Sharer, R.J. 1994: *The Ancient Maya.* 5th ed. (Stanford University Press, Stanford).

Shephard, A.O. 1956: *Ceramics for the Archaeologist* (Braun-Brumfield, Ann Arbor).

Simmons, M.P. and G.F. Brem. 1979: The analysis and distribution of ash-tempered pottery in the lowland Maya area. *American Antiquity* 44(1): 79-91.

Simmons, S.E. and L. Howard. 2003: *Preliminary Report of the 2001-2002 Field Seasons at Lamanai, Belize: The Maya Archaeometallurgy Project and Lamanai Archaeological Project Field School* (UNCW Anthropological Papers 1. Papers of the Maya Archaeometallurgy Project 1).

Smith, D.G.W. and J.A. Westgate. 1969: Electron probe technique for characterising pyroclastic deposits. *Earth and Planetary Science Letters* 5: 313-319.

Steen McIntyre, V. 1981: Tephrochronology and ecological applications. In Self, S. and R.S.J. Sparks eds. *Tephra Studies* (Reidel, London).

Taran, Y., T.P. Fischer, B. Pokrovsky, Y. Sano, M. Aurora Armienta and J.L. Macias. 1998: Geochemistry of the volcano-hydrothermal system of El Chichón Volcano,

Chiapas, Mexico. *Bulletin of Volcanology* 59: 436-449.

Tauber, H. 1967: Investigations of the mode of pollen transfer in forested areas. *Rev. Review of Palaeobotany and Playnology* 3: 277-286.

Taylor, T. 2002: *The Buried Soul: How Humans Invented Death* (Fourth Estate, London and NY).

Turney, C.S.M. 1998: Extraction of rhyolitic component of Vedde microtephra from minerogenic lake sediments. *Journal of Plaeolimnology* 19: 199-206.

Turney, C.S.M., D.D. Harkness and J.J. Lowe 1997: The use of microtephra horizons to correlate Late-glacial lake sediment successions in Scotland. *Journal of Quaternary Science* 12(6): 525-531.

Turney, C.S.M., J.J. Lowe, S.M. Davies, V. Hall, D.J. Lowe, S. Wastegård, W.Z. Hoek, B. Alloway and SCOTAV and INTIMATE members. 2004: Tephrochronology of Last Termination sequences in Europe: a protocol for improved analytical precision and robust correlation procedures (a joint SCOTAV-INTIMATE proposal). *Journal of Quaternary Science* 19(2): 111-120.

Wastegård, S., B. Wohlfarth, D.A. Subetto, T.V. Sapelko. 2000: Extending the known distribution of the Younger Dryas Vedde Ash into northwestern Russia. *Journal of Quaternary Science* 15(6): 581-586.

Westgate, J.A. and M.P. Gorton 1981: Correlation techniques in tephra studies. In Self, S. and R.S.J. Sparks eds. *Tephra Studies* (Reidel, London).

White, W.B. and D.G. Minser. 1984: Raman spectra and structure of natural glasses. *Journal of Non-crystalline Soilds* 67: 45-59.

Wolff-Boenisch, D., S.R. Gislason, E.H. Oelkers and C.V. Putnis. 2004: The dissolution rates of natural glasses as a function of their composition at pH 4 and 10.6, and temperatures from 25 to 74°C. *Geochimica et Cosmochimica Acta* 23: 4843-4858.

Woods, A.E. 2003: *Mountants* (IMVS Division of Pathology, Queen Elizabeth Hospital, Woodville, South Australia). Available at: http://home.primus.com.au/royellis/mts.htm.